ENERGY EFFICIENT COMMUNICATION WITH INTERDEPENDENT SOURCE-CHANNEL CODING FOR WIRELESS SENSOR NETWORKS

A

Thesis Submitted

in Partial Fulfilment of the Requirements

for the Degree of

DOCTOR OF PHILOSOPHY

By

Resmi N C

DEPARTMENT OF ELECTRONICS AND ELECTRICAL ENGINEERING

INDIAN INSTITUTE OF TECHNOLOGY GUWAHATI

GUWAHATI - 781 039, ASSAM, INDIA

May, 2021

Certificate

This is to certify that the thesis entitled "**ENERGY EFFICIENT COMMUNICATION WITH INTERDEPENDENT SOURCE-CHANNEL CODING FOR WIRELESS SENSOR NETWORKS**", submitted by **Resmi N C** (10610210), a research scholar in the *Department of Electronics and Electrical Engineering, Indian Institute of Technology Guwahati*, for the award of the degree of **Doctor of Philosophy**, is a record of an original research work carried out by her under my supervision and guidance. The thesis has fulfilled all requirements as per the regulations of the institute and in my opinion has reached the standard needed for submission. The results embodied in this thesis have not been submitted to any other University or Institute for the award of any degree or diploma.

Dated:

Guwahati.

Dr. Sonali Chouhan

Associate Professor

Dept. of Electronics and Electrical Engg.

Indian Institute of Technology Guwahati

Guwahati - 781 039, Assam, India.

Dedicated to

My Loving Husband and Children,

&

My Beloved Parents, Brother, and In-laws.

Acknowledgements

First and foremost, I feel it as a great privilege to express my deepest and most sincere gratitude to my supervisor Dr. Sonali Chouhan for her excellent guidance throughout my Ph.D. tenure. Her kindness, dedication, and attention to the details have been a great inspiration to me. She has enriched my life in many significant ways. My heartfelt thanks to my supervisor for her unlimited support and patience that she has shown towards me.

I sincerely thank my doctoral committee members: Prof. Sanjay K. Bose, Prof. Prabin K. Bora, and Prof. Roy P. Palathinkal, for sparing time out of their busy schedule to evaluate my progress and enrich this work with their valuable suggestions and feedbacks. I express my deepest gratitude to Dr. Srinivasan Krishnaswamy for providing me with access to his high-performance computing facility. I would also like to thank other faculty members for helping me with my research work in innumerable ways.

I thank Dr. Sanjib Das, Mr. Mukut Baruah, and Mrs. Josephine. S. for offering a helping hand whenever I needed it. I would also like to thank everyone in Communications Lab - II, who made these years enjoyable.

During my Ph.D., I have made wonderful friends at IIT Guwahati. My sincere thanks to my friends and fellow research scholars Dr. Arghya Chakravarthy, Dr. Ezhil Reena Joy, and Dr. Tousif Khan Nizami, for their vital support. These guys made my stay at IIT Guwahati memorable. I will cherish the time spent with them. I want to thank my friend Dr. Sangeetha N.S., a research scholar at the Physics department, from the bottom of my heart for standing as the strongest pillar of support during all the distress. My sincere thanks to Mr. Anoop Balachandran, Dr. Sandeep P., Dr. Yanumula Venkata Karteek, and Mr. Aditya R. Pawar for all their help.

I express my profound appreciation to my husband, Siju, for his unconditional support and understanding. I extend the deepest gratitude to my parents and in-laws for standing by my side not only during this Ph.D. tenure but rather throughout my life. I extend my love to my son Advay and daughter Veda.

Lastly, I extend my sincere thanks to all the staff members of the EEE office and Academic office for helping me out in all sorts of ways during my stay at IITG.

Resmi N C

Abstract

The emergence of Wireless Sensor Networks (WSNs) as one of the dominant technology trends has posed numerous unique challenges to researchers in the past two decades. Their design constraints differ from traditional wireless networks because of their unique characteristics such as small-sized devices, low power, longevity requirement, low cost, random deployment, and a large number of nodes in the network. The limited energy and the requirement of longevity make the need for energy conservation a critical design problem. Literature over time has brought many efficient ways to handle these, like, scheduling the duty cycle in an energy-efficient manner, channel coding to improve bit error rate (BER), and source coding to reduce the amount of data transmitted.

Reliable energy-efficient information transmission is the primary design objective of a WSN, considering its unique energy and resource constraints. Energy efficiency and BER performance are the necessary criteria to be taken into account while designing an optimal error correction scheme for WSNs.

In this thesis, two methodologies for a novel energy-efficient error control scheme are proposed. The methodologies achieve a better BER performance compared to the standard schemes with minimized energy overheads of a typical error control scheme. These include additional bits' transmit energy and encoding/decoding energy. The redundant bits' transmit energy is saved by incorporating compression. Coding energy is minimized by employing simpler operations compared to conventional error control schemes.

The methodology proposed for the new scheme is inclusive of three fundamental convictions for energy efficiency: error correction capability, data compression, and reduced computation. A novel codeword structure is proposed for the same, which combines the source and channel coding methods interdependently, i.e., accomplishing error control without added redundancy, on the contrary, with saving in the number of bits transmitted. The total computation energy is also reduced.

Our second proposed methodology is an enhancement over the first proposal. It further reduces the energy overhead for computation, intensifies the BER performance, and improves the data compression compared to the first proposed methodology.

The methodologies are analyzed with three performance metrics such as BER performance for error control capability, percentage compression for data compression, and total energy consumed per information bit for energy efficiency. For a comprehensive comparison of the energy efficiency of the schemes, both computation energy for the coding operations and communication energy for the data transmission are considered. This proves that saving in communication energy doesn't come with an increase in total energy due to the additional coding operations, which is essential for a highly populated network of low-powered nodes. Both analytical and simulated analyses are performed. The analytical study is performed using the mathematical expressions derived, which helped to validate the simulation results. The validation is further emphasized by deriving the upper and lower bound on the BER performance results. The investigation is performed at two sensor platforms MicaZ and Mica2, under the Additive White Gaussian Noise(AWGN) as well as Rayleigh fading channels.

The efficacy of the proposed methodologies is examined by the quantification of the performance. The first proposed methodology at the Mica2 platform yields a coding gain (CG) of 4.093 dB with a parameter selection of {30, 7, 2, 5}, in AWGN channel at BER of 10^{-5}, as compared to CG of 0.561 dB and 1.485 dB obtained using Hamming (7,4) and RS (31,29), respectively. Further, the standard codes above have redundancy of 75% and 6.9%, respectively, while the proposed code with the above parameters achieves compression of 23.81%. The total energy consumption reduces to 31.61% compared to uncoded, 46.51% compared to Hamming (7,4), and 28.5% compared to RS (31,29). The second proposed methodology for the same characterization in the AWGN channel at the MicaZ platform attains a CG of 4.328 dB. In comparison, Hamming (7,4) obtain a negligible CG and RS (31,29), a CG of 1.068 dB. The compression gained by the scheme is 26.19%. The reduction in total energy consumption is observed to be 42.92%, 63.12%, and 41.95% compared to the uncoded, Hamming (7,4), and RS (31,29), respectively.

The significant achievements observed by the proposed methodologies come with a

tradeoff. By design, the proposed methodologies scramble the transmitted data. In this thesis, we have studied different ways to descramble the data at the receiver for keeping the data in sequence.

Contents

List of Figures xi

List of Tables xvi

List of Acronyms xvii

List of Symbols xx

1 Introduction 1

1.1 An Introduction to Wireless Sensor Networks . . . 2

1.1.1 WSN Features . . . 3

1.1.2 Implementation Challenges . . . 5

1.2 Energy Conservation in WSNs . . . 6

1.3 Reliability in WSNs . . . 8

1.4 Motivation for the Present Work . . . 8

1.5 Problem Formulation . . . 10

1.6 Thesis Contributions . . . 10

1.7 Thesis Organization . . . 11

2 Error Control Schemes in WSNs - A Review 14

2.1 Error Control Schemes in WSNs . . . 15

2.2 Power Control . . . 15

2.3 Automatic Repeat Request (ARQ) . . . 16

2.4 Forward Error Correction (FEC) . . . 17

2.5 Hybrid ARQ . . . 21

2.6 Joint Source-Channel Coding (JSCC) . . . 22

2.7 Summary . . . 23

3 Methodology I **25**

3.1 Introduction . . . 26

3.2 Description of Methodology 1 . . . 26

3.2.1 Encoding . . . 27

3.2.1.1 Definition of Groups . . . 27

3.2.1.2 Alignment . . . 29

3.2.1.3 LABEL Protection . . . 30

3.2.1.4 Concatenation . . . 32

3.2.2 Decoding . . . 32

3.3 Performance Evaluation Framework . . . 33

3.3.1 BER Performance . . . 33

3.3.2 Compression . . . 35

3.3.3 Energy efficiency . . . 35

3.4 Node Energy Model . . . 36

3.4.1 Radio Energy Model . . . 36

3.4.2 Computation Energy Model . . . 38

3.4.3 Total Energy . . . 38

3.5 Simulation Parameters . . . 38

3.6 Results and Discussions . . . 41

3.6.1 Mica2 Platform . . . 41

3.6.1.1 BER Performance and Compression . . . 41

3.6.1.2 Energy Efficiency . . . 45

3.6.2 MicaZ Platform . . . 48

3.6.2.1 BER Performance and Compression . . . 48

3.6.2.2 Energy Efficiency . . . 52

3.6.3 Results for higher error protection for LABEL . . . 54

3.7 Conclusions . . . 55

4 Methodology II **57**

4.1 Introduction . . . 58

4.2 Description of Methodology 2 . . . 58

4.2.1 Encoding . . . 58
4.2.1.1 Group Definition . . . 59
4.2.1.2 Alignment . . . 60
4.2.1.3 Concatenation . . . 61
4.2.2 Decoding . . . 62
4.2.3 Enhancement over Methodology 1 . . . 62
4.3 Performance Evaluation Framework . . . 63
4.3.1 BER Performance . . . 63
4.3.2 Compression . . . 65
4.3.3 Energy Efficiency . . . 65
4.4 Simulation Parameters . . . 65
4.5 Results and Discussions . . . 66
4.5.1 Mica2 Platform . . . 66
4.5.1.1 BER Performance and Compression . . . 66
4.5.1.2 Energy Efficiency . . . 68
4.5.1.3 Comparison with Methodology 1: . . . 71
4.5.2 MicaZ Platform . . . 73
4.5.2.1 BER Performance and Compression . . . 73
4.5.2.2 Energy Efficiency . . . 75
4.5.2.3 Comparison with Methodology 1: . . . 78
4.5.3 Results for Higher d_{min} among Group Members . . . 80
4.5.4 Comparison with Conventional Source plus Channel Encoding Schemes . . . 82
4.6 Conclusions . . . 84

5 Methodology I and II in Rayleigh Channel 85

5.1 Introduction . . . 86
5.2 Performance Evaluation Framework . . . 86
5.2.1 BER Performance . . . 86
5.2.2 Energy Efficiency . . . 87
5.3 Simulation Parameters . . . 87
5.4 Performance Analysis of Methodology 1 in Rayleigh Channel . . . 87

5.4.1 BER Performance and Compression 87
5.4.2 Energy Efficiency 91
5.5 Performance Analysis of Methodology 2 in Rayleigh Channel 93
5.5.1 BER Performance and Compression 93
5.5.2 Energy Efficiency 97
5.6 Performance Comparison of Methodology 1 and 2 in Rayleigh Channel 99
5.7 Conclusions 100

6 Descrambling Methods **101**

6.1 Introduction 102
6.2 Method 1: Delta Encoded Sequencing 102
6.3 Method 2: Successor Label Identification 103
6.4 Method 3: Successor Group Identification 105
6.5 Method 4: Predecessor Group Identification and Successor Group Identification 106
6.6 Conclusions 107

7 Conclusions and Future Work **109**

7.1 Summary of the Present Work 110
7.2 Future Directions of the Research 111

List of Figures

1.1 A wireless sensor network structure. 2

1.2 The architecture of a sensor node. 3

1.3 Thesis organization. 12

2.1 Classification of Error Control Schemes in WSNs. 15

3.1 Grouping examples 28

3.2 Methodology 1: Alignment of the input data as [LABEL: SYMBOL]. 29

3.3 Example input messages 29

3.4 Alignment output as [LABEL: SYMBOL] 30

3.5 Alignment output as [Protected LABEL: SYMBOL] 31

3.6 Concatenation of SYMBOLs with LABEL. 31

3.7 Methodology 1: codeword structure. 32

3.8 The output codeword 32

3.9 BER vs. E_b/N_0 performance of the uncoded, Hamming, RS, and Methodology 1 for $\{S,\ 7,\ 2,\ 5\}$ with $S = 5,\ 10,$ and 30 in Mica2. 42

3.10 Theoretical, simulation, upper bound, and lower bound BER of Methodology 1 for $\{30,\ 7,\ 2,\ 5\}$ in Mica2. 42

3.11 BER vs. E_b/N_0 performance of Methodology 1 for cases contained in $\mathscr{R}_{k_2}$ in Mica2. . 43

3.12 BER vs. E_b/N_0 performance of Methodology 1 for cases encompassed in $\mathscr{R}_{k_m}$ in Mica2. 44

3.13 BER vs. E_b/N_0 performance of Methodology 1 for cases contained in $\mathscr{R}_{k_1}$ in Mica2. . 44

3.14 Comparison of energy expenditure of Methodology 1 with standard codes and uncoded in Mica2. 45

3.15 Comparison of simulated energy expenditure of Methodology 1 with standard codes and uncoded in Mica2. 46

3.16 Effect of varying S in energy expenditure of Methodology 1 in Mica2. 47
3.17 Energy comparison of Methodology 1 for different distances in Mica2. 47
3.18 Energy comparison of Methodology 1 for different path loss exponent in Mica2. 48
3.19 BER vs. E_b/N_0 performance of the uncoded, Hamming, RS, and Methodology 1 for $\{S,\ 7,\ 2,\ 5\}$ with $S = 5,\ 10,$ and 30 in MicaZ. 49
3.20 Theoretical, simulation, upper bound, and lower bound BER of Methodology 1 for $\{10,\ 7,\ 2,\ 5\}$ in MicaZ. 49
3.21 BER vs. E_b/N_0 performance of Methodology 1 for cases contained in $\mathscr{R}_{k_2}$ in MicaZ. . 50
3.22 BER vs. E_b/N_0 performance of Methodology 1 for cases encompassed in $\mathscr{R}_{k_m}$ in MicaZ. 51
3.23 BER vs. E_b/N_0 performance of Methodology 1 for cases contained in $\mathscr{R}_{k_1}$ in MicaZ. . 51
3.24 Comparison of energy expenditure of Methodology 1 with standard codes and uncoded in MicaZ. 52
3.25 Effect of varying S in energy expenditure of Methodology 1 in MicaZ. 53
3.26 Energy comparison of Methodology 1 for different distances in MicaZ. 53
3.27 Energy comparison of Methodology 1 for different pathloss exponent in MicaZ. 54
3.28 BER performance comparison of Methodology 1 for LABEL protected for 1-bit and 2-bit error-correction. 55
3.29 Energy consumption comparison of Methodology 1 for LABEL protected for 1-bit and 2-bit error-correction. 55

4.1 Methodology 2: Alignment of the input data as [LABEL: SYMBOL]. 60
4.2 Alignment output as [LABEL: SYMBOL] 61
4.3 Methodology 2: codeword structure. 61
4.4 The output codeword 61
4.5 BER vs. E_b/N_0 performance of the uncoded, Hamming, RS, and M2 $\{S,\ 7,\ 2,\ 5\}$ with $S = 5,\ 10,$ and 30 in Mica2. 66
4.6 BER vs. E_b/N_0 performance of Methodology 2 for cases in $\mathscr{R}_S$ in Mica2. 67
4.7 Theoretical, simulated, upper bound, and lower bound BER of M2 $\{30,\ 8,\ 2,\ 6\}$ in Mica2. 68
4.8 Comparison of energy expenditure of Methodology 2 with standard codes and uncoded in Mica2. 69

4.9 Comparison of simulated energy expenditure of Methodology 2 with standard codes and uncoded in Mica2. 69
4.10 Effect of varying S in energy expenditure of Methodology 2 in Mica2. 70
4.11 Energy comparison of Methodology 2 for different distances in Mica2. 71
4.12 Energy comparison of Methodology 2 for different pathloss exponent in Mica2. 71
4.13 BER vs. E_b/N_0 performance comparison of the Methodology 1 with Methodology 2 in Mica2. 72
4.14 Energy comparison of Methodology 2 and Methodology 1 in Mica2. 73
4.15 BER vs. E_b/N_0 performance of the Methodology 2 for $\mathscr{R}_{k_m k_1 k_2}$, uncoded, Hamming, and RS in MicaZ. 74
4.16 BER vs. E_b/N_0 performance of the Methodology 2 for the instances of $\mathscr{R}_S$ in MicaZ. . 74
4.17 Theoretical, simulated, upper bound, and lower bound BER of M2 {30, 8, 1, 7} in AWGN channel and MicaZ platform. 75
4.18 Comparison of energy consumption of the Methodology 2 with standard codes and uncoded in MicaZ, Radio energy computed theoretically. 76
4.19 Comparison of energy expenditure of the Methodology 2 with standard codes and uncoded in MicaZ. 76
4.20 Effect of varying S in energy expenditure in MicaZ. 77
4.21 Comparison of energy expenditure with varying distances in MicaZ. 78
4.22 Comparison of energy expenditure with varying path loss exponent in MicaZ. 78
4.23 BER vs. E_b/N_0 performance comparison of Methodology 1 and 2 in MicaZ platform and AWGN channel. 79
4.24 Energy comparison of Methodology 1 and 2 in the MicaZ platform and AWGN channel. 79
4.25 BER vs. E_b/N_0 performance of the Methodology 2 with $d_{min} = 5$, uncoded, and RS in MicaZ. 80
4.26 BER vs. E_b/N_0 performance comparison of the Methodology 2 with $d_{min} = 3$ and $d_{min} = 5$ in Mica2. 81
4.27 Energy performance of the Methodology 2 with $d_{min} = 5$ compared with uncoded and RS (31, 27) in MicaZ. 81

4.28 Energy comparison 2-bit and 1-bit error correction per block schemes of Methodology 2 in Mica2 82
4.29 Comparison of energy consumption of the Methodology 2 with conventional source and channel codes combined and uncoded, Radio energy computed theoretically. 83
4.30 Comparison of energy expenditure of the Methodology 2 with conventional source and channel codes combined and uncoded. 83

5.1 BER vs. E_b/N_0 performance of the uncoded, Hamming, RS, and M1 $\{S,\ 7,\ 2,\ 5\}$ with $S = 5,\ 10,$ and 30 in Mica2 platform and Rayleigh fading channel. 88
5.2 Theoretical, simulation, upper bound, and lower bound BER of M1 $\{30,\ 7,\ 2,\ 5\}$ in Mica2 platform and Rayleigh fading channel. 88
5.3 BER vs. E_b/N_0 performance of Methodology 1 for cases contained in $\mathscr{R}_{k_2}$ in Mica2 platform and Rayleigh fading channel. 89
5.4 BER vs. E_b/N_0 performance of Methodology 1 for cases encompassed in $\mathscr{R}_{k_m}$ in Mica2 platform and Rayleigh fading channel. 90
5.5 BER vs. E_b/N_0 performance of Methodology 1 for cases contained in $\mathscr{R}_{k_1}$ in Mica2 platform and Rayleigh fading channel. 90
5.6 Comparison of energy expenditure of Methodology 1 with standard codes and uncoded in Mica2 platform and Rayleigh fading channel. 91
5.7 Effect of varying S in energy expenditure of Methodology 1 in Mica2 platform and Rayleigh fading channel. 92
5.8 Energy comparison of Methodology 1 for different distances in Mica2 platform and Rayleigh fading channel. 92
5.9 Energy comparison of Methodology 1 for different pathloss exponent in Mica2 platform and Rayleigh fading channel. 93
5.10 BER vs. E_b/N_0 performance of the uncoded, Hamming, RS, and M2 $\{S,\ 7,\ 2,\ 5\}$ with $S = 5,\ 10,$ and 30 in Mica2 platform and Rayleigh fading channel. 94
5.11 BER vs. E_b/N_0 performance of Methodology 2 for cases contained in $\mathscr{R}_{k_2}$ in Mica2 platform and Rayleigh fading channel. 95
5.12 BER vs. E_b/N_0 performance of Methodology 2 for cases encompassed in $\mathscr{R}_{k_m}$ in Mica2 platform and Rayleigh fading channel. 95

5.13 BER vs. E_b/N_0 performance of Methodology 2 for cases contained in $\mathscr{R}_{k_1}$ in Mica2 platform and Rayleigh fading channel. 96
5.14 Theoretical, simulated, upper bound, and lower bound BER of M2 {10, 8, 2, 6} in Mica2 platform and Rayleigh fading channel. 96
5.15 Comparison of energy expenditure of Methodology 2 with standard codes and uncoded in Mica2 platform and Rayleigh fading channel. 97
5.16 Effect of varying S in energy expenditure of Methodology 2 in Mica2 platform and Rayleigh fading channel. 98
5.17 Energy comparison of Methodology 2 for different distances in Mica2 platform and Rayleigh fading channel. 98
5.18 Energy comparison of Methodology 2 for different pathloss exponent in Mica2 platform and Rayleigh fading channel. 99
5.19 BER vs. E_b/N_0 performance comparison of Methodology 1 and 2 in Mica2 platform and Rayleigh channel. 99
5.20 Energy consumption comparison of Methodology 1 and 2 in Mica2 platform and Rayleigh channel. 100

6.1 Structure of the codeword with delta coded sequence numbers. 103
6.2 BER vs. E_b/N_0 performance of M2 {5, 6, 1, 5} with added sequence bits. 103
6.3 Structure of the codeword with Successor LABEL Identification. 104
6.4 BER vs. E_b/N_0 performance of M2 for {30, 6, 1, 5} with added Successor LABEL Identification. 104
6.5 BER vs. E_b/N_0 performance of M2 for various S in {S, 7, 2, 5} with added Successor LABEL Identification. 105
6.6 Structure of the codeword with Successor Group Identification. 105
6.7 BER vs. E_b/N_0 performance of M2 for {30, 7, 2, 5} with added Successor Group Identification. 106
6.8 Structure of the codeword with PGI and SGI. 106
6.9 BER vs. E_b/N_0 performance of M2 with PGI and SGI. 107

List of Tables

3.1 Code Parameters 39
3.2 Channel Parameters - with Mica2 platform 40
3.3 Channel Parameters - with MicaZ platform 40

4.1 Latency Estimate 77

List of Acronyms

AWGN	Additive White Gaussian Noise
ARQ	Automatic Repeat Request
BER	Bit Error Rate
BCH	Bose-Chaudhuri-Hocquenghem
CG	Coding Gain
ECC	Error Control Codes
ERFC	Complementary Error Function
FEC	Forward Error Correction
HARQ	Hybrid ARQ
JSCC	Joint Source-Channel Coding
LDPC	Low-Density Parity-Check
M1	Methodology 1

M2	Methodology 2
NCBFSK	Noncoherent Binary Frequency-Shift Keying
NF	Receiver Noise Figure
OQPSK	Offset Quadrature Phase-Shift Keying
PA	Power Amplifier
PGI	Predecessor Group Identification
QoS	Quality-of-Service
RS	Reed-Solomon
RLE	Run-Length Encoding
SNR	Signal to Noise Ratio
SLI	Successor Label Identification
SGI	Successor Group Identification
WSN	Wireless Sensor Network

List of Symbols

N	Codeword length of conventional codes in bits/symbols
K	Input block length of conventional codes in bits/symbols
t	Number of bits/symbols that can be corrected per codeword
d_{min}	Minimum Hamming distance
R	Code rate
K	Constraint length of convolutional codes
E_b/N_0	Average signal to noise ratio per bit
P_b	Probability of error
k_m	Input block length of the proposed schemes in bits
k_2	SYMBOL length in bits
k_1	$k_m - k_2$
$A(k_2, d_{min})$	Maximum possible number of codewords for a code of length k_2 and minimum distance d_{min}

S	Number of SYMBOLs in a codeword
p	Channel transition probability
P_M	Block error probability
P_{bit}	Bit error probability
P_{LABEL}	Error probability of LABEL in Methodology 1
P_{SYMBOL}	Error probability of SYMBOL in Methodology 1
P_e	Error probability of the proposed codeword in Methodology 1
E_{radio}	Radio energy per bit
P_{ON}	Power consumed in the ON state of the node
P_{SP}	Power consumed in the SLEEP state of the node
P_{TR}	Power consumed in the TRANSIENT state of the node
T_{ON}	Duration spent in the ON state of the node
T_{SP}	Duration spent in the SLEEP state of the node
T_{TR}	Duration spent in the TRANSIENT state of the node
P_{trans}	Power consumed for signal transmission

P_{ckt}	Power consumed by the transceiver circuitry
P_{PA}	Power consumed by the Power amplifier
L	Number of bits transmitted
λ	Transmit signal wavelength
d	Distance between the transmitter and receiver
n	Pathloss exponent
P_r	Received power
G_r	Receiver antenna gain
G_t	Transmitter antenna gain
b	Number of bits transmitted by each modulation symbol
B	Channel bandwidth
N_0	Noise power density for an AWGN channel
η	Drain efficiency of the Power amplifier
α	A function of η
E_{enc}	Encoding energy per information bit

E_{dec}	Decoding energy per information bit
f_c	Centre radio carrier frequency
k	Boltzmann's constant
T	Reference receiver temperature in degrees Kelvin
P_{DB}	Block error probability of one data-block in Methodology 2
P_{DBNE}	Block error probability of a data-block with no error correction applied in Methodology 2
P_{WGD}	Probability of a wrong group determination in Methodology 2
P_{DBUE}	Probability of an uncorrectable error in a data-block provided the group determination is correct in Methodology 2
P_{AUE}	Probability of all possible uncorrectable errors in a codeword provided the group determination is correct in Methodology 2
$P_{CWberUP}$	Block error probability (upper bit error probability) of the entire codeword
$P_{CWberLOW}$	Lower bit error probability of the entire codeword
T_c	Time duration spent for data collection
T_a	Time duration spent for running algorithm of encoding/decoding

1

Introduction

Contents

1.1	An Introduction to Wireless Sensor Networks	2
1.2	Energy Conservation in WSNs	6
1.3	Reliability in WSNs	8
1.4	Motivation for the Present Work	8
1.5	Problem Formulation	10
1.6	Thesis Contributions	10
1.7	Thesis Organization	11

1.1 An Introduction to Wireless Sensor Networks

Wireless Sensor Network (WSN) is one of the key technologies of the twenty-first century. A WSN is a set of connected nodes deployed for observing a physical phenomenon and is widely used in a variety of applications [1]. A few examples include temperature, light, sound, and humidity monitoring. The monitored readings are transmitted over a wireless channel to be used by an application [2]. Data collection, monitoring, surveillance, and medical telemetry are a few of the typical applications of WSNs. The WSNs can work not only for sensing applications but also for control and activation purposes.

A largely deployed sensor nodes form a highly distributed network of small, lightweight sensor nodes. The number of sensor nodes may vary from a few to several hundreds or even thousands, where each node is connected to one (or sometimes several) sensors. The interconnected sensor nodes allow for multihop communication to the sink node. The sink node is connected to either the end-user or through the internet to the user. A typical wireless sensor network is shown in Fig. 1.1.

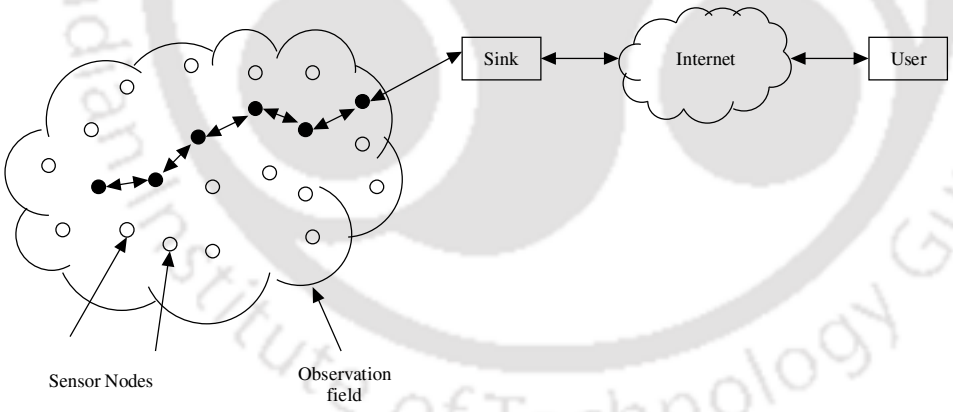

Figure 1.1: A wireless sensor network structure.

The typical node architecture is shown in Fig. 1.2. The architecture of a sensor node comprises of sensing, computing, and communication units so that the system as a whole can instrument, observe, and react to events and phenomena in the observed environment [3].

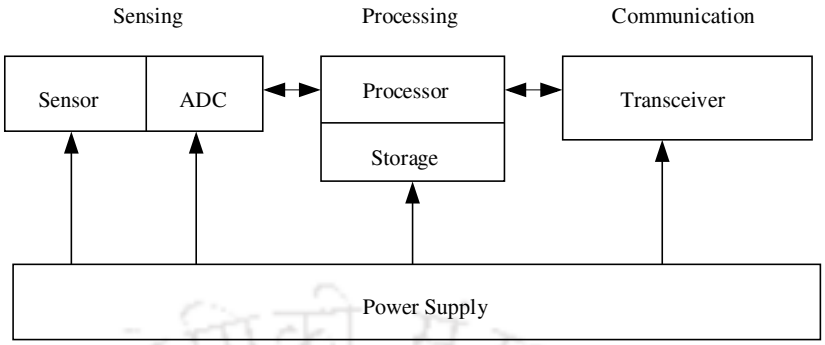

Figure 1.2: The architecture of a sensor node.

The tiny sensor nodes have sensors, microprocessors, and radio transceivers. The sensors perform the sensing task. Microprocessors carry out the data processing tasks. And the radio transceivers are responsible for all the inter-node and node-to-sink communications. The communications are usually wireless over a short distance.

1.1.1 WSN Features

The design constraints of WSNs are very different from other traditional wireless networks, such as cellular networks and Mobile Ad-hoc Networks, because of their unique features. A few of the distinctive characteristics of sensor networks are listed below [1, 3, 4, 5, 6].

- ***Tiny Nodes:*** With the development in micro-electronic-mechanical systems and wireless communication technologies, sensor nodes are made very cheap and small. However, we can find sensor nodes in various orders of magnitude in size, from nanoscopic-scale devices to macroscopic-scale devices.

- ***Dense Node Deployment:*** The tiny sensor nodes are usually deployed in large numbers in the observation field. They are usually deployed densely. There can be several hundred or thousand sensor nodes in the field of interest.

- ***Random Node Deployment:*** Generally, sensor networks are deployed in remote and secluded locations, and hence random node deployment has to be chosen often.

- ***Battery-Powered Nodes and Limited Battery Life:*** Sensor nodes are powered by a small battery. Most of the time, these batteries can not be recharged or replaced as the observation fields are usually remote, harsh, or dangerous. The battery lifetime of nodes is also hence limited. However, there are sensor nodes with energy harvesting capabilities as well.

- ***Energy, Computation, and Storage Constraints:*** Since the sensor nodes are tiny and battery-powered with no recharging/replacing facilities, the energy, processing, and storage units also face constraints. The energy, computation, and storage capabilities of a sensor node are very limited compared to conventional wireless nodes.

- ***Application Specific:*** Unlike traditional networks, each sensor network is designed for a specific application. Hence, the design requirements are also highly dependent on the application in hand, and a general design is not appropriate.

- ***Self-Configurable:*** As the sensor nodes are deployed randomly and are in hostile environments, the network has to be self-configured after deployment.

- ***Prone to Damages:*** The harsh and dangerous sensor field can cause physical harm or failure to sensor nodes.

- ***Frequent Topology Change:*** Due to frequent node damage, failure, energy depletion, node addition, and fading channels, the topology of the network may change frequently. Hence, the nodes have to self configure and adjust to the circumstances often.

- ***Correlated Input Data:*** As the sensor nodes are densely deployed in a field towards a common goal, the data sensed by the neighboring nodes are highly correlated. Hence the data redundancy will be very high.

- ***Need for In-network/Local Processing:*** The energy cost of data transmission is directly proportional to the amount of data. Therefore, it sometimes calls for local processing of information before transmitting to the sink.

- ***Many-to-One Flows:*** As can be observed from Fig. 1.1, the nodes sense the data from the field and communicate to the sink node. A large number of sensor nodes sense and process data and send it to the sink. Hence a many-to-one traffic pattern can be observed in typical sensor networks.

- ***No Global Addressing:*** The network has a large number of sensor nodes with minimal storage capacity. Hence maintaining the address information of all the nodes in the field is highly impossible. Thus, a global node addressing is not employed.

1.1.2 Implementation Challenges

The implementation of WSNs pose some unique challenges compared to conventional wireless networks [3, 4, 7, 8, 9].

- ***Reliability:*** Most of the applications require a robust information transmission. The wireless channels are usually noisy, error-prone, time-varying, and fading. For the applications to perform correctly, the data must be reliably transmitted through these channels.

- ***Need for Low-power Operations:*** The most crucial challenge of a WSN to have as low power consumption as possible. This is because sensor nodes have limited power supply and are deployed in locations where recharging/replacing batteries is not feasible. An energy-depleted node may affect network connectivity, force the network to change topology, or even make the whole network unusable. The low-power operations include low-power communication, low-power on-node computing, and low-power sensing sessions.

- ***Limited Hardware Resources:*** Sensor nodes, tiny in size and low cost, have limited processing and memory capacities. Hence, the computational capability is also limited. Along with limited energy constraints, limited hardware constraints also have to be taken care of during network design.

- ***Adaptability:*** The low-power nodes may fail, new nodes may join, or nodes may change their place with time in sensor networks. Sensor networks must be adaptive to such changes always.

- ***Self-Configurability:*** The sensor networks must be able to self configure during the random deployment phase. They must also be able to self reconfigure during the operation phase, a topology change, or node failure.

- ***QoS Assurance:*** Sensor networks are highly application-specific. WSNs find their use in a wide variety of applications [3, 10, 11, 12, 13]. Broadly these can be listed as environmental monitoring, health monitoring, military applications, traffic monitoring, disaster management, structural health monitoring, surveillance, industrial monitoring, and home/office automation. There cannot be any general design guidelines, unlike other networks. The quality-of-service (QoS) requirements of each application may be quite different in terms of bit error rate (BER),

delivery latency, and packet loss. For example, the BER performance required for various applications depends on the reliability they demand. Ensuring reliability is significant in medical monitoring, emergency applications like disaster management, and military applications compared to other applications. It can be stated in general that query-driven and event-driven applications demand high reliability than continuous monitoring applications [14, 15]. Also, the safety applications, like fire alarming, are delay-sensitive. However, applications like data collection are delay tolerant, but cannot tolerate packet loss. Hence WSN design should contemplate application-specific QoS requirements.

- ***Scalability:*** The WSN should be scalable to different orders of sensor nodes.
- ***Efficient use of Bandwidth:*** The bandwidth is a limited resource for WSNs. Hence the design should consider utilizing the channel as efficiently as possible.
- ***Security:*** Often, sensor networks are employed in strategic locations, and the information collected by the sensor network has to be secured from unauthorized access or malicious attacks.

1.2 Energy Conservation in WSNs

WSNs attempt to achieve energy efficiency in many ways. A few examples include in-network and in-node data processing, low duty cycle operation, short-range multihop communication, transmit power control, and perceptive sensor placement [3, 16, 17, 18, 19].

In-network and in-node processing of data lessen the quantity of data transmitted and the time required for transmission. The communication energy spent on transmitting data reduces as the amount of data and the time of operation reduces. This, in turn, reduces the total energy consumption. The reduction of the amount of data transmitted is achieved by numerous data aggregation and compression techniques. This local data processing is possible because of the density of the network and the inherent redundancy in the data collected. An in-node compression technique is proposed in [20] suitable for resource constraint sensor nodes. This method makes use of the correlation present in the node's consecutively collected samples. The in-network data processing consists of two techniques, namely, data compression and data aggregation. The in-network data compression [21, 22, 23, 24], on the other hand, work in a distributed fashion in the network, which exploits the redundancy in the sensed data arisen due to the density of the network. Data aggregation combines the data from

different sensors related to the same event and reduces the number of transmissions or the transmitted packet length. The trade-off for this achievement is the need for coordination among nodes, making the scheme complex [25, 26, 27].

The duty cycle can be adjusted in an energy-efficient manner since the major part of energy consumption is the node's radio consumption. Energy is saved by reducing the duty cycle, which reduces the active transmission/reception time and increases the sleep time because the power consumption in sleeping mode is negligible to the power consumption in active mode [28, 29]. There are numerous medium access control protocols with a low duty cycle designed to achieve this, particularly for WSNs [30]. A broad classification of these is based on the approach used to regulate access to the shared wireless medium. Reservation based schemes allot slots to every node in each time frame [31, 32, 33]. Contention-based schemes, on the other hand, allot slots only to the nodes intend to transmit/receive [34, 35, 36] and hybrid schemes combine the strength of both the above approaches while neutralizing their weaknesses [37, 38, 39].

Instead of each node transmitting a long way to sink in a single hop, making a path through intermediate nodes to the sink reduces that node's energy consumption. This saves the node from draining out of energy fast and making the coverage area of the node unreachable. A short-range multihop communication towards the sink makes use of a small amount of energy from each node on the way [2].

Similarly, transmit power control also helps reduce energy consumption [5]. As the nodes need to transmit a very short distance to the neighboring node, a minimal amount of transmit power is sufficient to achieve communication to sink even if the data collecting node is distant from the sink.

Perceptive sensor placement for effective coverage also plays a key role in managing energy consumption. The random deployment of sensor nodes may seem like a hindrance to this. However, several algorithms exist to use a subset of nodes at a time for efficient area coverage when a higher density of sensor nodes are randomly deployed. A high density of nodes means having nodes greater than the optimum number needed to perform the area monitoring. An energy-efficient coverage solution is to have disjoint sets of nodes, where each set can perform the monitoring task discretely, and other sets of nodes can go to low-energy sleeping mode [40, 41]. Distributed and localized methods exist that schedule the nodes' operation with adjustable sensing range [42] or fixed sensing range [42] or fixed sensing range [43]. Another approach is to make use of a minimum number of working nodes

for adequate coverage and connectivity [44, 45, 46].

1.3 Reliability in WSNs

Reliable data transmission is the first and foremost goal of any communication system. From the classic paper [47], the communication fraternity stimulated the research in information theory and coding theory. With Hamming's milestone work in [48], communication engineers developed a fairly large number of error control schemes for a variety of applications. Now there exists a wide range of schemes with various error detecting/correcting capabilities and implementation complexities so that an appropriate scheme can be selected for the application in hand.

However, unlike conventional networks, WSNs have distinct features like low energy requirement and the collaborative nature of sensors. Hence selection of a befitting error control scheme should be carefully scrutinized to be energy-efficient too. The prime goal of the error control schemes is to facilitate reliable communication over the channel. A wireless channel can have more adverse effects on communication than wired channels due to fading, interference, time variance, and loss of bit synchronization. The result is to have channel errors that cause the information exchanged unreliably. The chances of errors in WSNs are still higher as the sensor nodes are forced to use low-power techniques for communication, and multiple sensors are transmitting simultaneously in a limited area. Accordingly, the use of error control schemes is essential in WSNs along with the constraint of low energy consumption.

The error control can be achieved in WSNs in various ways such as transmit power control, automatic repeat request, forward error correction, and hybrid automatic repeat request. A new variant exploiting the redundancy in collected data was also introduced for WSNs named as a joint source-channel coding scheme. The detailed account of the literature for reliable data transmission in WSN is presented in Chapter 2.

1.4 Motivation for the Present Work

The wireless networks are more prone to errors due to fading, interference, shadowing, and time variance compared to their wired counterparts. The main focus of any communication system is to have reliable information exchange. Hence resisting the effects of channel errors is essential for any system, and there are various methods developed over time for achieving this. A communication

engineer can select the appropriate scheme depending on the application's required QoS and tolerable latency.

In the case of WSNs, this selection of an error control scheme comes to be more demanding compared to other conventional networks. The primary reason is the need for low energy operations in order to extend the battery lifetime. Hence, along with the considered parameters like error-correcting capability and delay tolerance, one needs to examine the energy efficiency of the schemes also before selecting a suitable scheme. The energy consumed for error correction operations and energy expended for transceiver operations also have to be appraised.

As a result of this, a WSN designer can not effortlessly pick an error control scheme looking at its error correction capability alone. The very close placement of sensor nodes makes computation energy comparable to radio energy [49]. Hence, the saving in radio energy achieved by the error control scheme should be higher enough to outshine the increase in computation energy for implementing the error control [50]. Over time many researchers have studied the energy efficiency of various error control schemes to find a suitable scheme for WSNs. In this design space, our motivation is to design a novel method that can be applied to typical WSN applications. The method should be inclusive of the possible ways to reduce total energy consumption and offer error correction capability.

The data compression techniques in conventional wireless networks generally are focused on saving storage and are not concerned about energy efficiency. However, in energy-constrained networks, these techniques may increase the total energy consumption [51]. Data compression schemes consuming less computational energy have been researched in the context of WSN. As explained in Section 1.2, this compression is mainly exploiting the node density of the network and the redundancy in data sensed. Our motivation is to design a scheme which is not dependent on the correlation information, which can also act orthogonally to such compression techniques. The compressive sensing techniques exploiting temporal, spatial, and spatiotemporal sparsity save on computation, storage space, and energy consumption at the sensor nodes [52]. Nevertheless, the processing burden is transferred to the sink nodes. Consequently, the techniques will be suitable only for the networks in which sensor nodes perform only encoding and the sink node perform the decoding. We are driven with the idea of a scheme which can be used in any types of network, including those with sensor nodes perform both encoding and decoding operation. This demands a scheme having not only less encoding load but also less decoding load. In essence, we are motivated to achieve data compression along with error

correction with minimal computation requirements.

1.5 Problem Formulation

Problem 1 Design an energy-efficient methodology of error correction for typical low-powered WSNs. The aim is to design the scheme in such a way so as to achieve better error correction capability compared to standard error correction schemes, at the same time reducing the redundancy occurring in conventional error correction schemes. In addition to the reduction in redundancy, a significant compression in data is also aimed. The accomplishments should come with lesser energy spent on computation.

Problem 2 Design a scheme that further improves the error correction capability while increasing the compression achieved and the computation operations to achieve better energy efficiency compared to the first scheme.

Problem 3 Modify the scheme in order to alleviate the scrambling that occurs in the data as a result of the codeword construction.

1.6 Thesis Contributions

In this thesis, we aim at designing an energy-efficient error correction scheme for typical WSNs. The proposed scheme is inclusive of three basic notions for energy efficiency: error correction capability, reduction in the amount of data transmitted, and reduced computation. Error correction capability helps to reduce the transmit power required for a specific BER. Reduction in the amount of data transmitted, in other words, data compression, reduces the time and energy required for transmission. These two attributes minimize radio energy needed for obtaining the desired QoS, while the third attribute, reduced computation, lessens the computation energy. The total energy comprises radio and computation energy, and a reduction in both reduces the total energy consumption of the node. This thesis contributes two methodologies of such an energy-efficient error control scheme. We name it the 'Energy-Efficient Interdependent Source-Channel Coding technique '. The source coding and channel coding here are interdependent to each other and hence the name.

I. Methodology 1: An Energy-Efficient Interdependent Source-Channel Coding Technique

We propose a novel unconventional technique to achieve reliability and energy efficiency in typical WSN applications. It has the following three features. First, the methodology offers higher error correction capability. Second, it gives an unconventional compression that is interdependent on the channel coding. It is unconventional because, unlike compression schemes in other source coding techniques for WSN, our methodology doesn't require or depend on the correlation information of the neighboring sensor nodes. Third, the computation energy necessary for these operations are surpassed by the saving in radio energy achieved through the source and channel coding. Hence, the overall scheme is energy efficient. The three attributes of the scheme are quantified theoretically and by simulation, and the upper and lower bound on BER performance are derived.

II. Methodology 2: An Enhanced Methodology for Energy-Efficient Interdependent Source-Channel Coding

Next, we present an enhanced methodology for the energy-efficient interdependent source-channel technique. Here, we have the following three enhancements. First, the error correction capability is improved compared to that of Methodology 1. Second, the compression achieved also is improved. Third, the computation energy required to achieve this enhanced feature is less compared to the previous methodology. Similar to the previous methodology, the attributes are quantified, and the performance bounds are derived.

III. Methods to Combat Sequence Disorder, Introduced by the Proposed Schemes

The two methodologies proposed work on efficient grouping and placing of data. This particular structure of the data sequence is the basis of all the achievements, such as error correction capability, data compression, and energy efficiency. The magnificent accomplishments of the methodologies have a trade-off. They may alter the data sequence. Further, the methods to alleviate sequence disorder are discussed.

1.7 Thesis Organization

This thesis is organized into seven chapters. The summary of each chapter is briefly outlined as follows. A structural organization of the thesis is shown in Fig. 1.3.

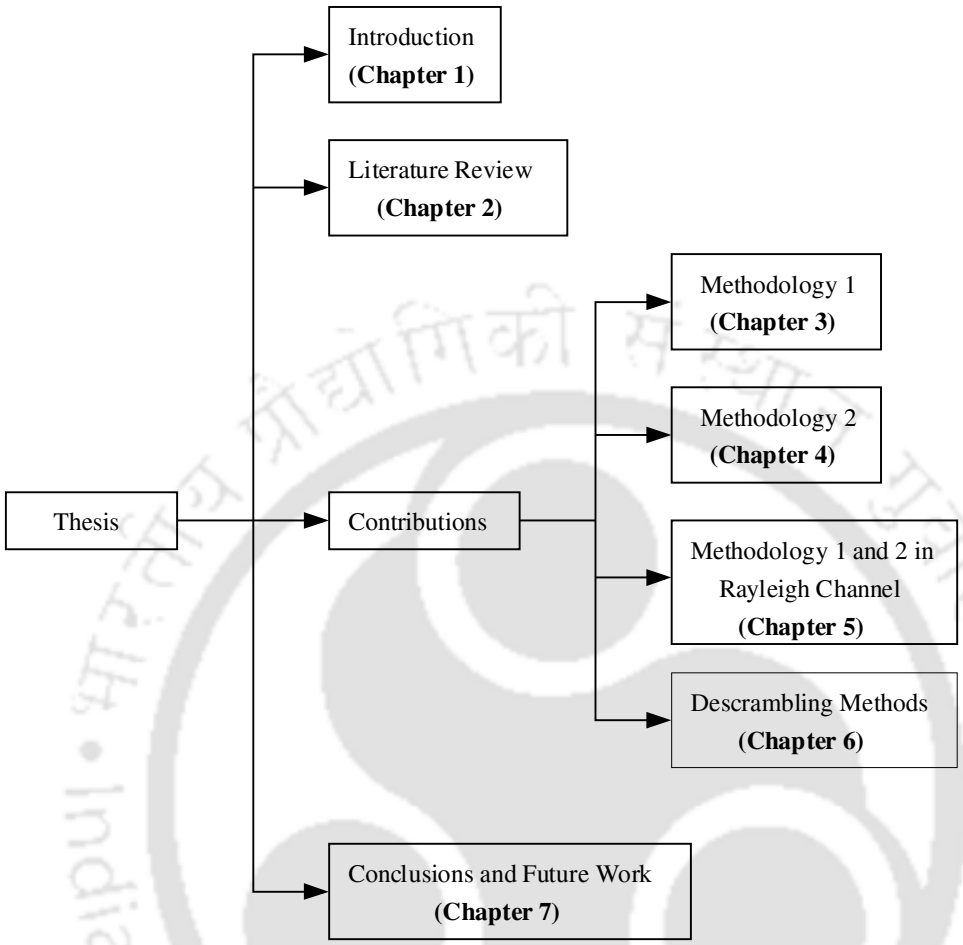

Figure 1.3: Thesis organization.

- **Chapter 1:** An overview of WSNs, their unique features, and implementation challenges are briefed in this chapter. The two primary focuses of WSNs to have energy efficiency and reliability are highlighted. The motivation for the present work is discussed. This chapter also encapsulates the problem formulation, thesis contributions, and a brief outline of the thesis organization.

- **Chapter 2:** This chapter explores the current state-of-the-art literature pertinent to our work. Here, we review the work done in the literature for achieving reliability in WSNs. We also discuss in brief the crux behind existing data compression techniques for WSNs. The joint source-channel coding schemes are also reviewed in this chapter.

- **Chapter 3:** We present our novel scheme for energy-efficient, reliable communication in WSNs in this chapter. The first methodology for the same is detailed, analyzed, and validated. The methodology is studied in various platforms and the Additive White Gaussian Noise (AWGN)

channel model. The results are shown and scrutinized.

- **Chapter 4:** An improved methodology for the same scheme is presented in this chapter. The methodology is studied in detail, like Methodology 1 in the previous chapter. The differences in both methodologies are listed. The results are examined and compared with that of Methodology 1.

- **Chapter 5:** In this chapter, Methodology 1 and 2 are again analyzed and studied in a fading environment. The analysis of the scheme in the Rayleigh fading channel is studied to find its suitability in a more realistic environment.

- **Chapter 6:** The sequence disorder problem that may arise in the proposed scheme is addressed here. Methods to alleviate the effect of this are examined, and results are studied in this chapter.

- **Chapter 7:** This chapter summarizes the work done in the thesis and provides recommendations that may be considered for future research.

2

Error Control Schemes in WSNs - A Review

Contents

2.1	Error Control Schemes in WSNs	15
2.2	Power Control	15
2.3	Automatic Repeat Request (ARQ)	16
2.4	Forward Error Correction (FEC)	17
2.5	Hybrid ARQ	21
2.6	Joint Source-Channel Coding (JSCC)	22
2.7	Summary	23

In the previous chapter, we have given a brief introduction to WSNs and their unique characteristics and design challenges compared to conventional wireless networks. We have also highlighted two key design challenges of the system, which are reliability and energy efficiency. This chapter further reviews some related works from the literature on error control codes (ECC) of WSNs. The review focus on the energy-efficient aspect of each scheme, along with its robustness.

2.1 Error Control Schemes in WSNs

We have discussed in Chapter 1 that the prime concern of a WSN design is energy consumption, as the sensor nodes have severe energy constraints. Hence, the main design goal of error control protocols should be energy efficiency, along with reliability. The communication system of a WSN expends energy in both computation and transmission/reception. Hence, an energy efficiency analysis should consider both these components of energy.

The error control schemes in WSNs are mainly of four types, power control, automatic repeat request (ARQ), forward error correction (FEC), and hybrid ARQ (HARQ). As the sensors are usually densely deployed in the observation field, the data collected from neighboring nodes are highly correlated. This redundancy gave rise to another variant of error control scheme named joint source-channel coding (JSCC). Hence, we have five types of schemes to achieve robustness in WSNs. The classification is illustrated in Fig. 2.1.

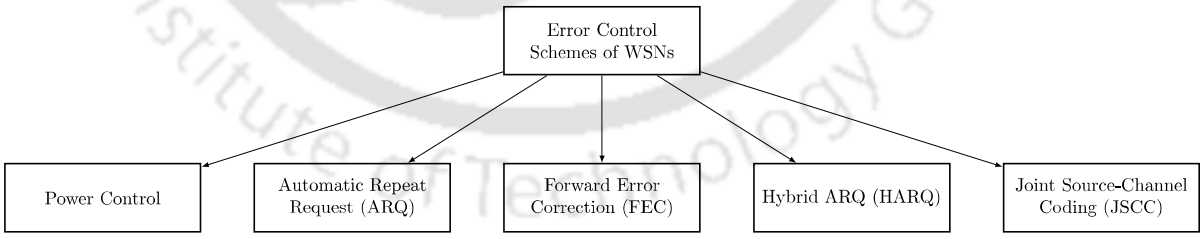

Figure 2.1: Classification of Error Control Schemes in WSNs.

2.2 Power Control

An increase in transmit power improves the average Signal power to Noise power Ratio (SNR), which reduces the error rate of the data transmitted and received. That means, the required bit error rates can be reached by controlling the transmit power in wireless communication systems [4]. However, this is not a good solution for error control because of the following reasons. First, the

increase in the transmit power of one node raises its energy consumption. Secondly, it also increases the neighboring node's interference with the node [53]. Third, per-packet power control also needs complex circuitry and uses memory and other resources. Hence, power control can not be taken as a stand-alone solution for error control in resource-constrained and energy-constrained WSNs. However, power control helps improve energy efficiency due to the saving in transmit energy by implementing forward error control schemes [5, 54]. Withal, transmission power control techniques are utilized to achieve energy efficiency [55, 56].

2.3 Automatic Repeat Request (ARQ)

ARQ schemes help attain reliability by the retransmission of lost and erroneous packets [57]. ARQ runs on an error detection scheme. Along with the data payload, the source node address and a checksum of the payload are transmitted. The checksum of the payload is again calculated at the receiver node and compared with the checksum field entry. If they match, the packet is considered error-free; else otherwise. The report will be sent to the source node with the help of acknowledgments. Either a positive acknowledgment will be sent for each correct packet received or a negative acknowledgment for each erroneous packet. An erroneous packet is retransmitted by the source node. There are three approaches to ARQ, such as stop-and-wait, go-back-N, and selective repeat. The stop-and-wait approach sends a single packet at once and waits for its acknowledgment. On receiving a positive acknowledgment, the next packet will be transmitted. Otherwise, the current packet will be retransmitted [58]. The Go-back-N approach allows the sender to send N packets till an ACK is received. For any number of erroneous packets, all N packets in the row will be retransmitted [59]. In the selective repeat approach, only the erroneous packets are retransmitted [60]. Here stop-and-wait approach has the least memory and resource requirements and is the mainly used ARQ scheme in WSNs.

ARQ is simpler compared to FEC schemes and hence seems to be more suitable for WSNs since complexity adds to energy expenditure. However, the authors in [61, 62, 63, 64, 65] found ARQ energy-inefficient for WSNs, because of the additional communication/resource overhead due to retransmissions and acknowledgments. Also, ARQ requires more memory for storing data at the transmitter until it reaches the destination successfully. The energy consumed for sending acknowledgments and retransmitting packets, and the memory used to save the packets until a positive acknowledgment

is received are huge for a resource and energy-constrained WSN. Also, ARQ increases the latency of communication. However, in fairly good channel conditions, ARQ is the best choice because it doesn't pay in terms of redundant bits and computation for correct packets like FEC. However, in adverse channel conditions, ARQ is highly inefficient and causes high latency. Hence FEC has to be considered.

2.4 Forward Error Correction (FEC)

ARQ schemes call for two-way communications. In systems where two-way communication is not possible and channel conditions are adverse, FEC schemes are used. FEC schemes add some additional bits to the data payload. These redundant bits help correct the errors at the receiver, liberating the system from the need for acknowledgments and additional memory to save transmitted packets until received error-free. However, FEC schemes require transmitting and receiving additional (redundant) bits, and an encoding/decoding procedure needs to be run on each packet. FEC is more common than ARQ, even if the system is able to provide two-way communication [57].

FEC schemes, also called channel codes, are generally of two types; linear block codes and convolutional codes [66]. Block codes work on blocks of K-bits/symbols, known as source words, and map them to blocks of N-bits/symbols, known as codewords. The difference in the number of bits/symbols of two codewords is referred to as the Hamming distance between them. The smallest Hamming distance between any two codewords among all the possible codewords is termed as minimum distance or minimum Hamming distance and is represented as d_{min}. A block code is usually represented as (N,K,t), where t bits/symbols can be corrected per codeword, and $t = \lfloor (N-K)/2 \rfloor$ and is said to have code rate $R = K/N$.

Convolutional codes, on the other hand, don't work on blocks. Sequential K-tuples are mapped to N-tuples in such a way to have distance properties needed for error detection and correction. Convolutional codes are characterized by code rate R and constraint length K. Constraint length gives the number of K-tuples joined to form each N-tuple [66].

The selection of FEC codes must be judicious, especially in the case of WSNs. Each application has a level of error tolerance, and an FEC code is chosen to achieve that level in the given channel conditions. FEC codes correct the errors in the received packet. Hence a communication system with a channel code implemented requires less transmit energy to achieve a specific error rate compared

to a system with no code implemented. This energy difference or precisely the difference between the E_b/N_0 values is called the coding gain (CG) [67]. E_b/N_0 is the average SNR per bit.

The level of error is usually calculated as the probability of error, P_b. if the application can tolerate a higher P_b value, it is better not to use an FEC code. This is because computation energy is small at high P_b, and radio energy is the dominant component of the total energy consumption. As an FEC code has additional redundant bits to transmit and receive, the radio energy increases, and the uncoded scheme becomes better compared to a coding scheme. For instance, in [68] authors have shown that the uncoded system gives better energy efficiency compared to convolutional codes with a code rate of 1/2 and a constraint length of 3 for a P_b greater than 10^{-4} in tracking applications with a high density of nodes and small-sized packets. The inter-node communication is assumed to be in frequency non-selective, slow Rayleigh fading channel with AWGN. Nevertheless, for P_b less than 10^{-5}, coding of data is more energy-efficient than the uncoded counterpart. This conveys that the selection of a coding strategy should be dependent on the quality requirement of the application.

FEC codes achieve error correction at the receiver. This capability can be made use to decrease the transmit power for achieving the required error performance compared to an uncoded scheme. However, this is possible with an increase in computation energy. Computation energy here indicates the energy spent on encoding and decoding FEC schemes at transmitter and receiver, respectively. In addition to that, added redundancy increases the transmitted packet length and, therefore, the increased transmission/reception energy. Hence, an FEC scheme can only be considered energy efficient if the energy saved in the transmission is greater than the additional computation and redundancy transmission energies. And WSNs should work with the minimum feasible energy in order to maximize the lifetime of the sensor nodes while also taking care of network connectivity and availability [18]. In general, energy spent on the transmission is very high compared to the energy spent on computation [69]. But, authors of [70] show that in the case of a dense network, nodes are very close to each other, and the difference between computation energy and transmitting energy cannot be high. But in the case of large distances or short distances with obstructions, FEC is useful. Authors in [71] show that the optimal selection of an error control scheme can save a node's energy up to 60%. An optimal scheme selection has to consider signal, circuit, and computation energy components, distance, path loss exponent, codeword length, error correction capability, and modulation parameters.

There have been a number of researches to find out the optimal FEC scheme for WSNs, though

none is standardized. To find the optimal scheme, both BER performance and energy expenditure have to be considered. It has been observed that stronger codes give better protection but expends more energy. Basically, there are two types of codes i) Block codes and ii) Convolutional codes. Authors of [63] show that medium rate codes are the most energy-efficient in the case of convolutional codes. In contrast, low rate codes give good reliability, but limited energy efficiency and high rate codes give poor reliability and hence poor energy efficiency. But even the best convolutional codes are not energy efficient compared to Bose-Chaudhuri-Hocquenghem (BCH) codes [63]. In [70], authors have observed that to achieve the same CG, convolutional code needs higher redundancy than Reed-Solomon (RS) code. And the implementation of decoders of convolutional code is more complex than those of RS code. The authors in [49] have shown that the convolutional coded channel with a Viterbi decoder expends more energy than the uncoded channel and hence not suitable for WSN.

Therefore, we move our focus to block codes. The authors in [72] compared hamming code, Golay code, Convolutional code, and RS codes and concluded that hamming code is the simplest code but has the lowest performance among all the other observed codes. Authors in [71] have shown that as the codeword length increases, the Hamming code doesn't gain in SNR much, and computation energy also doesn't change much. Many researchers have studied the BCH code for the WSN case. Authors of [63] have compared BCH codes and convolutional codes with the uncoded case. They concluded that four error correcting BCH code is 23% more energy-efficient than the uncoded case and 15% more energy-efficient than the best performed convolutional code. The authors of [49, 61, 62] also have proposed the BCH code to be the most suitable coding technique for WSN.

The authors in [70] compared RS codes with convolutional codes and found that RS codes perform better. Authors in [64] have studied the well-known codes comprehensively for the case of Industrial WSNs based on the standard IEEE 802.15.4. They found that the stronger codes fail to achieve the memory and timing constraints while simpler codes don't give satisfactory performance. Hence they concluded that RS (15, 11) is the most suitable for this specific application. The author in [73] compared different RS codes (RS (15, 11), RS (31, 26), RS (31, 21), RS (31, 16), and RS (31, 11)) for their BER and energy consumption performance and observed RS (31,21) to be the optimal scheme. Y. Qassim and M. E. Magafia modified the RS code algorithm for the applications that can tolerate errors to some degree. This error-tolerant version of RS codes reduced decoding computation by 11% but gave a comparable performance to the original RS codes [74]. The RS codes are further researched,

and an RS code-based adaptive scheme is designed in [75] for WSNs in a 500 kV line-of-sight substation smart grid environment. Various hamming, convolutional, and RS codes with QPSK modulation are compared in [71] with all the energy components of a node, and RS (31, 29) is found to be the optimal code. In [50], authors have expanded the work to find the optimal ECC-modulation pair, as modulation constellation size also affects the node energy expenditure. It has been observed that the error-correcting capability of the code changes with the modulation type and constellation size. An optimal ECC can be found for a fixed modulation scheme, and an optimal modulation scheme can be found for a fixed ECC.

Turbo family of codes provides the best BER performance among block codes. However, owing to significantly higher energy consumption in turbo decoders, the design of a low complexity decoder is an absolute necessity for its use in energy-constrained networks [76]. The authors in [77] also observed that low-density parity-check (LDPC) codes outperform BCH codes. Further, adaptive coding schemes based on LDPC codes are investigated in [78] for clustered WSNs and in [79] for multi-hop WSNs. However, the study in [64] shows that the BER performance of LDPC codes and Turbo codes are significantly higher than Hamming, RS, cyclic, BCH, and repetition codes. Nevertheless, their memory consumption, execution time, and complexity are too high to be considered for power-constrained and resource-constrained Industrial wireless sensor networks.

The relatively recent polar codes introduced in [80], to achieve capacity limits with the use of low-complexity code construction, encoding, and decoding techniques, have also been investigated for its suitability in WSNs scenario [81, 82]. In [81], a power-efficient coding architecture of polar codes for WSN is introduced, in which a few supernodes with higher processing energy are needed for accomplishing decoding. The work in [82] compares the polar codes with Turbo and LDPC codes and shows its efficacy at low communication distances.

There are two types of nodes based on the way of decoding coded data. Type 1 nodes don't attempt to perform decoding. They simply collect the data and transmit the coded data to the sink. Then the nodes need to consider only encoding energy for node energy analysis. In contrast, Type 2 nodes perform the decoding of data at the battery-powered nodes themselves. These nodes have to collect data and make decisions locally. Then the nodes need to consider not only encoding energy but also decoding energy for node energy analysis.

Condensing the literature review on the optimality of FEC codes for WSNs, it has been observed

that many researchers have agreed on RS block codes as a compromise between the BER performance and energy efficiency. In [71], RS codes and Hamming codes with various parameters are compared with all energy components of a node under AWGN channel condition with QPSK modulation. RS (31, 29, 3) is found to be the optimal code when both encoding and decoding operations occur at a node. The authors in [64] have utilized RS code considering its BER performance, memory footprint, and processing time. In view of the wide acceptance of RS codes, they have emerged as a benchmark coding scheme for intended applications in WSN and can be used for performance comparison of other coding schemes.

2.5 Hybrid ARQ

When the channel conditions are right, ARQ schemes are more efficient than FEC codes. This is because in the right channel conditions, there is no need for retransmissions for ARQ, and the transmission and processing of the redundant bits in FEC become fruitless. However, if the channel is adverse, the ARQ scheme incurs retransmissions of the whole packet even if it has a few bits in error, which is an inefficient exercise. And the FEC codes are efficient in such situations as there is no retransmission, and a few bits of errors can be corrected with the help of added redundancy. Hence, the usage of ARQ is recommended in good channel conditions, and the usage of FEC is recommended in adverse channel conditions [61].

HARQ schemes are employed to make use of the merits of both ARQ and FEC schemes. HARQ schemes sent the first packet uncoded or lightly coded so as to check the channel conditions. If the packet is received erroneously, it will be retransmitted with a more robust FEC code. Precisely this is the HARQ-I technique. In the HARQ-II technique, only the redundant bits are retransmitted.

HARQ-I and HARQ-II schemes consisting of ARQ scheme and BCH (128, 78, 7) are analyzed for their energy consumption and latency in [5]. It is reported that the HARQ-II schemes perform better than ARQ, BCH (128, 78, 7), and HARQ-I schemes. The HARQ schemes are also compared with RS (31, 19, 6), and the HARQ-II scheme is observed to be more energy-efficient compared to its component schemes and HARQ-I scheme. However, the end-to-end latency performance of HARQ-II and RS (31, 19, 6) are very close.

The authors in [83] have proposed a HARQ scheme using BCH coding for WSNs with code division multiple access and single-hop data transmission. Results assure that the scheme is better performing

compared to simple ARQ when the node density is high in the region of interest. Cross-layer analysis of FEC, ARQ, HARQ-I, and HARQ-II schemes is performed in [54]. A series of extended BCH codes with a codeword length of 128 and various error correction capabilities and RS codes with three different characterizations are considered for FEC and ARQ with only one retransmission, and BCH codes are considered for HARQ schemes. The results show that HARQ-II schemes are more energy-efficient than HARQ-I, ARQ, BCH, and RS codes for MicaZ nodes. The authors in [84] have addressed the interference in high-density networks to design a better HARQ scheme with network condition estimation. Nevertheless, it is a matter of fact that HARQ schemes also require acknowledgments and retransmissions and hence require the provision for two-way communication.

2.6 Joint Source-Channel Coding (JSCC)

Source coding, also known as data compression, is the process of removing unwanted data from the source without affecting its essence so that the source can be recovered at the receiver by the process decompression. And channel coding is the process of adding redundancy to the data intelligently to combat channel errors. The pioneering work by Shannon in [47] resulted in the separation theorem, proving that the separation of source coding and channel coding doesn't compromise the optimality of the system. Accordingly, most of the communication systems' design strategy is to remove the redundancy in source data (source coding) and then add intelligent redundancy to the data (channel coding) to achieve reliable transmission. This separation theorem geared up many pieces of research in the communication field, and numerous source and channel coding techniques were evolved.

Nevertheless, this theorem holds only in infinite source code dimension and infinite channel code block length. This principle doesn't apply in finite blocklength cases. In addition, the theorem holds for stationary channels and does not hold in time-varying channels [85]. The channel decoder can exploit the redundancy in the source for error correction. This is the basic idea of joint source-channel coding techniques. Hence, instead of separate source and channel encoder-decoder pairs, a JSCC scheme performs the source and channel coding of an information source that has redundancy using a single code [86, 87]. This reduces the complexity of the system. The tradeoff for this complexity reduction is flexibility loss [88]. A jointly coded system can not be easily used in a different channel or source.

Numerous JSCC schemes were proposed in the literature for conventional systems [87, 89, 90].

Nevertheless, these techniques are not specific for WSNs and are generally energy inefficient in the WSN scenario. And those JSCC techniques specific to WSNs, based on different channel codes and distributed source coding technique [22], exploit the redundancy in sensor data due to the correlation resulting from dense deployment of nodes. Researchers have modeled this correlation in various ways resulting in various JSCC techniques [91, 92]. The JSCC scheme based on polar codes for WSNs in [93, 94] also uses a correlation between different sources like other JSCC schemes. The techniques which exploit correlation don't call for correlation information at the encoder. Instead, the burden is transferred to an energy-abundant decoder [95]. Most of the joint decoding techniques are iterative [92]. This calls for correlation information and decoder with ample energy. In networks with Type 2 nodes, the battery-powered nodes will not be capable enough to perform this task. This leaves scope for further research on the design of energy-efficient coding techniques, which relaxes the strict requirement of data correlation and energy abundant nodes for performing complex decoding in JSCC based methodologies.

Researches aiming reliability and power efficiency are carried out further today for next-generation networks such as internet of things (IoT) based WSNs. The work in [96] proposes a fast and power-efficient error control scheme for IoT-based WSNs. Authors in [97] investigate the suitability of the JSCC scheme based on systematic polar codes in next-generation WSNs. The scheme again works on the correlation of sources and provides lossy compression. The work in [98] combines retransmission, compression, and joint channel coding for networks with a periodic monitoring application. The authors in [99] consider an adaptive joint lossy source-channel coding scheme for monitoring applications in multihop WSNs. This work reiterates that channel decoding performed at the base station leads to energy efficiency rather than decoding performed at intermediate nodes, which is beneficial in terms of reliability. These recent projects ensure that the scope of research in this area is still open.

2.7 Summary

From the cited literature, it is evident that the more robust codes which provide high gain have higher decoder complexity. This restricts their use in some particular topologies, especially with a unidirectional transmission, where sensor nodes perform only encoding, and the complex decoding operation is employed at the receiver. JSCC schemes also tend to make use of the decoder to perform complex calculations. A simpler code has to be applied when a node performs both encoding and

decoding, which generally has a better BER performance. Hence, there is enough design space to design schemes with better BER performance and lower decoder complexity. Therefore, in the same spirit, we propose an error control scheme with two methodologies that employs a simple encoder. In furtherance, the decoder complexity is less than the encoder complexity. Hence, the proposed scheme is inferred to be suitable for any topologies for WSNs.

A methodology with simple computations, higher error performance, and significant compression is proposed in the next chapter. The proposed methodology is described in detail and evaluated analytically and by simulation. A comprehensive performance evaluation framework is presented in this regard.

3

Methodology I

Contents

3.1	Introduction	26
3.2	Description of Methodology 1	26
3.3	Performance Evaluation Framework	33
3.4	Node Energy Model	36
3.5	Simulation Parameters	38
3.6	Results and Discussions	41
3.7	Conclusions	55

3.1 Introduction

In this chapter[1], a novel energy-efficient error control scheme for typical WSNs, termed Methodology 1 and abbreviated as M1, is proposed and presented. The methodology minimizes the energy overheads of a typical error control scheme. These include additional bits' transmit energy and encoding/decoding energy while achieving a better BER performance than the conventional ECC schemes. The redundant bits' transmit energy is saved by incorporating compression along with error correction, and coding energy is minimized by employing simpler operations compared to other schemes. A simple encoder and a much simpler decoder make the scheme suitable for any network topology as opposed to most of the FEC and JSCC coding techniques that rely on sink nodes or super nodes with ample energy for decoding. The methodology can be applied to the data from typical applications in WSNs such as temperature-, pressure-monitoring, etc.

As explained in Section 1.2, data compression also contributes to energy efficiency. Usually, a separate source encoder performs data compression by exploiting the redundancy in sensor data obtained due to the dense deployment of the nodes. The proposed methodology achieves lossless data compression implicitly because of the particular structure of the codeword itself. This data compression is interdependent with the error control capability of the system. Hence we name the scheme 'Interdependent Source-Channel Coding'.

The proposed scheme is validated in the context of MicaZ, and Mica2 motes [100]. The BER performance and energy consumption of the presented scheme are studied and compared with standard error control schemes, such as Hamming (7, 4) and RS (31, 29). Quantification of energy consumption corresponding to each of the above schemes is also provided to prove the energy efficiency of the proposed technique.

3.2 Description of Methodology 1

The basic idea of the scheme lies in efficient grouping and placing of the input data. A part of the input data is segregated into groups, where all group members of any group are at a distance

[1]The work reported in this chapter has been in part presented in the following conference:
Resmi N.C. and S. Chouhan, "An Interdependent Source-Channel Coding for Energy Efficient Communication in WSNs," in WPMC, Dec. 2015
and published in the following journal:
Resmi N.C. and S. Chouhan, "A Novel Interdependent Source-Channel Coding Technique for Enhanced Energy Efficiency in Communication over Wireless Sensor Networks," Wireless Pers Commun, Springer, vol. 96, Issue 3, pp. 3727-3743, Oct 2017.

of a minimum Hamming distance d_{min} with each other. Each group has a label termed group label. A codeword is formed by concatenating the data from the same group together, alongside its group label.

3.2.1 Encoding

The encoding algorithm can be explained in four steps, namely the definition of groups, alignment, LABEL protection, and concatenation. The first and third steps are done offline so that the computation required in real-time can be reduced. The encoding algorithm is summarized in Algorithm 3.1 in a nutshell.

Algorithm 3.1 Encoding algorithm

Group definition (offline)
1: Input d_{min}, input message length k_m, SYMBOL length k_2 ($k_2 >= d_{min}$)
2: $k_1 = k_m - k_2$
3: Divide all 2^{k_2} SYMBOLs into groups with minimum distance $d_{min} = 3$
4: Set a group label for each group
Alignment
5: Set least significant k_2 bits of input message as SYMBOL
6: Find the group of SYMBOL and pick its group label
7: Set LABEL with most significant k1 bits of input message and group label
LABEL protection (offline)
8: Encode LABEL with Rectangular code
Concatenation
9: **for** each LABEL **do**
10: codeword=[protected LABEL]
11: **for** each SYMBOL with the selected LABEL **do**
12: codeword=[codeword : SYMBOL]
13: **end for**
14: **end for**

3.2.1.1 Definition of Groups

The input with a length of k_m bits is split into k_1 and k_2 bits, where $k_1 = k_m - k_2$. The least significant bits are termed as SYMBOL. The parameter k_2 is selected in accordance with the required error correction capability per SYMBOL. Here, the required error correction capability is defined per SYMBOL and not per codeword. Each codeword has a much higher error correction capability to a maximum value of the product of the number of SYMBOLs in a codeword and the error correction capability per SYMBOL. Therefore, k_2 is chosen to be equal to or greater than the required d_{min} and less than k_m. Since the SYMBOL length is k_2 bits, there are 2^{k_2} possible SYMBOLs. These

SYMBOLs are divided into groups, with members of a minimum distance restriction of d_{min}.

The number of groups and the number of group members can be defined in multiple ways. For instance, we can have $2^{k_2-k_1}$ groups of 2^{k_1} members, or we can fix the number of groups or number of group members and then calculate the other term accordingly. In any of the cases, the number of group members selected should be in line with the 'main coding theory problem' optimization [101]. A code can correct $t = \lfloor (d_{min} - 1)/2 \rfloor$ bits of errors per codeword if all the codewords in the code satisfy the minimum Hamming distance constraint. To ensure the minimum distance d_{min} within each group, the number of members in each group is restricted by the term $A(k_2, d_{min})$. $A(k_2, d_{min})$ is the maximum possible number of codewords for a code of length k_2 and minimum distance d_{min}, given by the inequality obtained by combining the weak and strong Gilbert-Varshamov bounds,

$$GP2LT\left(\frac{2^{k_2}}{\sum_{i=0}^{d_{min}-2}\binom{k_2-1}{i}}\right) \leq A(k_2, d_{min}) \leq \frac{2^{k_2}}{\sum_{i=0}^{\lfloor (d_{min}-1)/2 \rfloor}\binom{k_2}{i}}, \tag{3.1}$$

where GP2LT indicates the greatest integral power of 2 less than its argument [102]. The number of groups thus formed can be obtained from the equation

$$\text{No. of groups} = 2^{k_2 - \log_2 \text{No. of members per group}}. \tag{3.2}$$

Each group is labeled with a Group Label for group identification. The minimum no. of bits required to represent the groups is $\log_2(No.\ of\ groups)$.

For further understanding, an instance of $k_m = 7$, $k_2 = 5$, and $k_1 = 2$ is taken. If the d_{min} intended within each group is 3, no. of groups and no. of members per group are obtained using (3.1)-(3.2) as 8 and 4, respectively. The Group Label needs $\log_2(8) = 3$ bits for representing each group. Two such groups, $group_A$ and $group_B$ are shown in Fig. 3.1 as samples from the set of 8 groups.

$$group_A = \begin{bmatrix} 0 & 0 & 0 & 0 & 0 \\ 0 & 0 & 1 & 1 & 1 \\ 1 & 1 & 0 & 0 & 1 \\ 1 & 1 & 1 & 1 & 0 \end{bmatrix}, group_B = \begin{bmatrix} 0 & 0 & 0 & 1 & 0 \\ 0 & 0 & 1 & 0 & 1 \\ 1 & 1 & 0 & 1 & 1 \\ 1 & 1 & 1 & 0 & 0 \end{bmatrix}$$

Figure 3.1: Grouping examples

3.2.1.2 Alignment

The grouping in Section 3.2.1.1 shows that each input message of length k_m bits, with its least significant k_2 bits, termed as SYMBOL, belongs to one of the defined groups. The most significant k_1 bits of the input message and the Group Label of the SYMBOL are together named LABEL, requiring a minimum of $k_1 + \log_2(No.\ of\ groups)$ bits. Each k_m bit long input message is aligned in the form of [LABEL: SYMBOL] at this step. This alignment requires $k_1 + \log_2(No.\ of\ groups) + k_2$ number of bits. The alignment part is depicted in Fig. 3.2. Hence, now, the $\log_2(No.\ of\ groups)$ bits used for indicating the group label is redundancy for each input message.

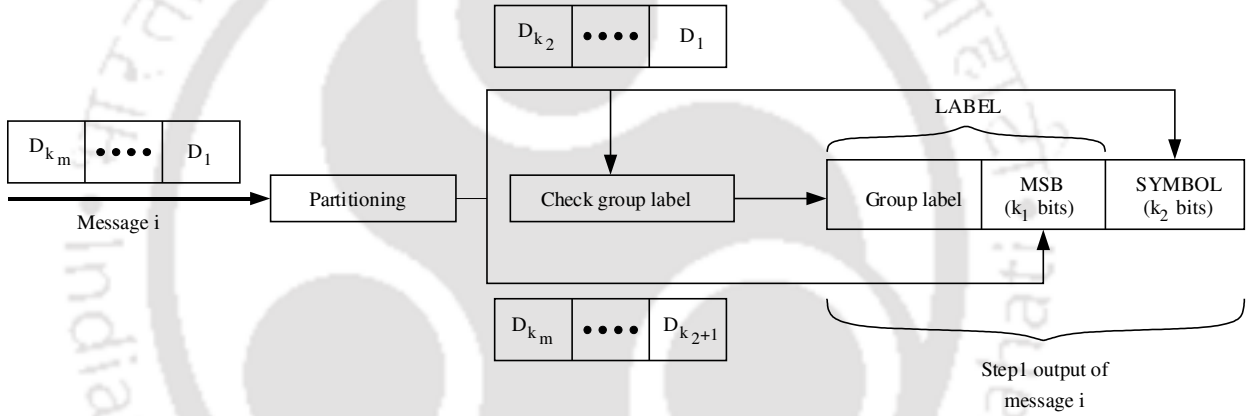

Figure 3.2: Methodology 1: Alignment of the input data as [LABEL: SYMBOL].

Returning to the instance given in Section 3.2.1.1, the input messages are 7 bits long. Consider the five input messages *Input*, for example.

$$\text{Input} = \begin{bmatrix} 1 & 1 & 0 & 0 & 0 & 0 & 0 \\ 1 & 1 & 0 & 0 & 1 & 1 & 1 \\ 1 & 1 & 1 & 1 & 0 & 0 & 1 \\ 1 & 1 & 1 & 1 & 1 & 1 & 0 \\ 1 & 1 & 0 & 0 & 1 & 1 & 1 \end{bmatrix}$$

Figure 3.3: Example input messages

The first input message [1100000] on partitioning has the least significant five bits [00000], the

SYMBOL, fall into $group_A$. If we consider the Group Label of $group_A$ is [000], the most significant two bits of the input message [11] along with the Group Label forms the LABEL=[11000]. The output of the alignment process comes as [1100000000]. The output after alignment is obtained by processing the same way for all the five input messages, as shown in Fig. 3.4. The example messages are judiciously selected for having the same SYMBOL group and LABEL to show the concatenation process also.

$$\text{Alignment step output} = \begin{bmatrix} 1 & 1 & 0 & 0 & 0 & 0 & 0 & 0 & 0 & 0 \\ 1 & 1 & 0 & 0 & 0 & 0 & 0 & 1 & 1 & 1 \\ 1 & 1 & 0 & 0 & 0 & 1 & 1 & 0 & 0 & 1 \\ 1 & 1 & 0 & 0 & 0 & 1 & 1 & 1 & 1 & 0 \\ 1 & 1 & 0 & 0 & 0 & 0 & 0 & 1 & 1 & 1 \end{bmatrix}$$

Figure 3.4: Alignment output as [LABEL: SYMBOL]

3.2.1.3 LABEL Protection

In the codeword, a LABEL is associated with a number of SYMBOLs all from the same group, which has a minimum distance restriction of d_{min}. As a result, there are $(d_{min} - 1)/\ 2$ bits of error correction capability among the SYMBOLs associated with a LABEL. However, for the above to be true, the LABEL and thus, the group should be identified correctly. A suitable code is selected in accordance with the required error correction capability and the length of the LABEL. Herein we use simple rectangular codes for this purpose.

Rectangular codes, also known as product codes, are 2-dimensional parity check based codes [103]. The message bits are arranged into a rectangle of M rows and N columns. Horizontal parity checking is applied to each row, and vertical parity checking is applied to each column. The parity check bits are appended with the message bits to form the codeword. These parity check bits are used at the decoder for error detection and correction. These types of codes can correct any single error pattern because the location of these errors can be identified by the intersection of the row and column whose parity check bits are altered.

The example shown in the previous steps shows that the common LABEL of all the selected input

messages is [11000]. To give 1-bit error protection to this LABEL of 5 bits, we choose the nearest possible simple linear block code: rectangular (11, 6) code. Since our LABEL length is 5, we add one 0-bit to the LABEL and perform rectangular (11, 6) encoding, wherein the notation (n, k) denotes the code length by n and the block length by k, respectively. The result is [01100000011]. But, while transmitting, the first bit is removed since it is known at the receiver. Finally, the rectangular (11, 6) code ends up in a (10, 5) code. Hence the protected LABEL is [1100000011].

$$\text{The output with protected LABEL} = \begin{bmatrix} 1 & 1 & 0 & 0 & 0 & 0 & 0 & 0 & 1 & 1 & 0 & 0 & 0 & 0 & 0 \\ 1 & 1 & 0 & 0 & 0 & 0 & 0 & 0 & 1 & 1 & 0 & 0 & 1 & 1 & 1 \\ 1 & 1 & 0 & 0 & 0 & 0 & 0 & 0 & 1 & 1 & 1 & 1 & 0 & 0 & 1 \\ 1 & 1 & 0 & 0 & 0 & 0 & 0 & 0 & 1 & 1 & 1 & 1 & 1 & 1 & 0 \\ 1 & 1 & 0 & 0 & 0 & 0 & 0 & 0 & 1 & 1 & 0 & 0 & 1 & 1 & 1 \end{bmatrix}$$

Figure 3.5: Alignment output as [Protected LABEL: SYMBOL]

The redundancy per input message is further increased at this stage due to the redundancy bits incurred as a result of LABEL protection. This redundancy is compensated, and compression is achieved at the concatenation stage. At the receiver, the 0-bit is appended again, and decoding is performed. The resulting LABEL will be one-bit error corrected. Hence, the group is identified from the group label part of the LABEL. Once the group is known, each of the SYMBOLs can be corrected against a one-bit error, as there is a minimum Hamming distance restriction of 3 within the group.

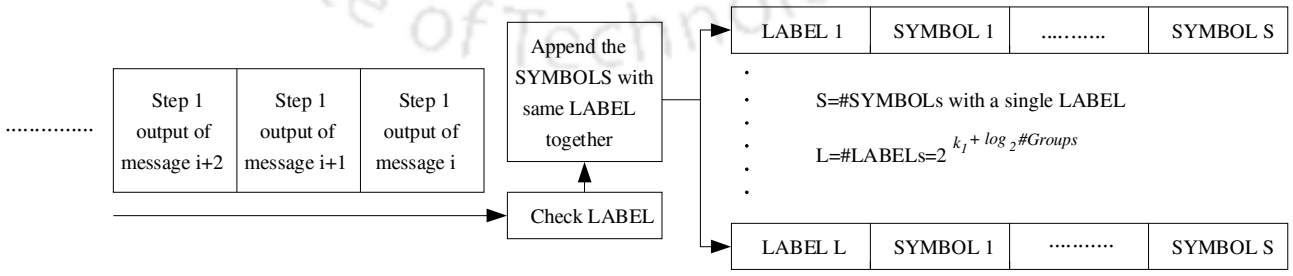

Figure 3.6: Concatenation of SYMBOLs with LABEL.

3.2.1.4 Concatenation

At this stage, all SYMBOLs characterized by the same LABEL are combined, as depicted in Fig. 3.6. S represents the number of such SYMBOLs appended with a LABEL. The corresponding protected LABEL is also appended so that the LABEL appears only once in a codeword rather than appearing alongside each corresponding SYMBOL. This helps in achieving compression and makes our scheme different from general error control codes with redundancy. The protected LABEL and its corresponding SYMBOLs together form a codeword. The codeword structure is diagrammed in Fig. 3.7

Figure 3.7: Methodology 1: codeword structure.

On considering $S = 5$ and as the LABEL for all five input messages are same, the codeword obtained is given in Fig. 3.8. The 35 bits in the input message of the example end up with 35 bits in the output, which means we obtain 1-bit error correction in each SYMBOL, resulting in a maximum of 5-bit error correction per codeword without any redundancy added. Here, it is also inferred that as $S > 5$, we achieve compression along with a maximum of S bits of error protection per codeword.

$$\text{Codeword} = \left[1\,1\,0\,0\,0\,0\,0\,0\,1\,1\,0\,0\,0\,0\,0\,0\,0\,0\,1\,1\,1\,1\,1\,0\,0\,1\,1\,1\,1\,1\,0\,0\,0\,1\,1\,1\right]$$

Figure 3.8: The output codeword

The number of SYMBOLs concatenated with a LABEL is determined by considering the application's delay requirement, required error correction capability, and the amount of compression aimed at. As more SYMBOLs are appended with a LABEL, the amount of compression and error correction capability increases.

3.2.2 Decoding

The decoder is much simpler compared to the encoder. The decoding of the LABEL part, which is rectangular coded, is extremely simple since it is a systematic code. From the LABEL, the group LABEL part is used for identifying the group, and the least significant k_1 bits form a part of the input

message. These k_1 bits are appended with each of the SYMBOLs to recover the input message. The decoding algorithm is summarized in Algorithm 3.2.

Algorithm 3.2 Decoding algorithm

```
for each codeword do
    Decode LABEL
    Check grouplabel from LABEL
    Extract the k1 least significant bits from the LABEL
    for each SYMBOL in codeword do
        Match with the group members for error correction
        Input message=[k1 bits from LABEL: SYMBOL]
    end for
end for
```

Let us take the example-codeword formed in Section 3.2.1. The first 10 bits of the codeword represent the Protected LABEL and is decoded after appending 0-bit again to make it in the rectangular (11,6) format. After checking for errors, the 5-bit LABEL is easily extracted since it is a systematic code. This LABEL identifies the group of the following SYMBOLs in the codeword. Once the group is known, each of the SYMBOLs can be corrected against a 1-bit error, as there is a minimum distance restriction of 3 within the group. These corrected SYMBOLs are each appended with the most significant $k_1 = 2$ bits from the LABEL to retrieve the input messages.

3.3 Performance Evaluation Framework

To study the proposed scheme and compare it with the standard codes, both BER performance and Energy Efficiency need to be considered. The performance is evaluated in the context of Mica2 [104] and MicaZ [105] motes. A code performs better in terms of BER when it has a lower BER curve than those of other codes. And a code can be called energy efficient when the savings achieved in the transmit energy are greater compared to the expended energy for additional parity bit transmission and encoding decoding operations.

3.3.1 BER Performance

BER performance of our scheme and the standard schemes Hamming (7, 4) code and RS (31, 29) are evaluated by rigorous simulations using MATLAB. We choose the AWGN channel model for the analysis in this chapter. MicaZ mote employs CC2420 radio [106], and Mica2 mote employs CC1000 radio [107]. The modulation scheme incorporated with the radio in mica2 is noncoherent binary

frequency-shift keying (NCBFSK), and in MicaZ is offset quadrature phase-shift keying (OQPSK) [5]. The coding gain obtained is used for the comparison of schemes. The SNR per bit for achieving a specific BER is used for the transmission energy calculation as explained in Section 3.4.

BER performance is obtained by both analytical and simulation methods. The block error probability in a binary symmetric channel is [108]

$$P_M \leq \sum_{m=t+1}^{n} \binom{n}{m} p^m (1-p)^{n-m} \tag{3.3}$$

Bit error probability can be calculated using the following expression [109],

$$P_{bit} = \frac{1}{n} \sum_{m=t+1}^{n} (m+t) \binom{n}{m} p^m (1-p)^{n-m}. \tag{3.4}$$

where P_M is the probability of m errors in a block of n bits, known as the block error probability, P_{bit} is the bit error probability, t is the error correction capability, and p defines the channel transition probability. The channel transition probability p of AWGN channel when NCBFSK modulation is employed is given by the mathematical formula [108]

$$p = \frac{1}{2}\exp\left(-\frac{1}{2}R\frac{E_b}{N_0}\right) \tag{3.5}$$

and, when OQPSK modulation is employed is given by [108]

$$p = \frac{1}{2}\mathrm{erfc}\left(R\frac{E_b}{N_0}\right). \tag{3.6}$$

In (3.5) and (3.6), the term R defines the code rate, E_b/N_0 is the per bit signal to noise ratio, and erfc refers to the complementary error function.

Using (3.3) and (3.5) or (3.6), the block error probability of LABEL (P_{LABEL}) and each SYMBOL part (P_{SYMBOL}) can be calculated. Bit error probability of the LABEL and SYMBOL parts can be calculated using (3.4) and (3.5) or (3.6). The error probabilities of both SYMBOL and LABEL are calculated using the above equations. The error probability of the LABEL is based on the linear block code used for LABEL protection. Any simple suitable code can be considered for LABEL protection, depending on the BER requirements. Here, in this work, Rectangular codes have been used for this purpose. Once the LABEL is identified correctly, each SYMBOL has a maximum error correction capability of $t = \lfloor (d_{min} - 1)/2 \rfloor$. If the LABEL is identified incorrectly, the entire codeword

is decoded incorrectly. Hence, the block error probability of the codeword can be calculated by

$$P_e = (1 - P_{\text{LABEL}})P_{\text{SYMBOL}}^{S} + P_{\text{LABEL}} \tag{3.7}$$

where S is the number of SYMBOLs appended with a LABEL. The same expression in (3.7) can be used to calculate the bit error probability of the codeword by substituting the bit error probability of the LABEL and SYMBOL parts calculated using (3.4) and (3.5) or (3.6), in place of P_{LABEL} and P_{SYMBOL}. The upper bound of bit error probability is the block error probability, and the lower bound is the block error probability divided by the number of information bits in the codeword [110]

$$P_{\text{bit-upper bound}} = P_e, \tag{3.8}$$

$$P_{\text{bit-lower bound}} = \frac{P_e}{k_1 + Sk_2}. \tag{3.9}$$

3.3.2 Compression

The conventional error correction schemes incur redundancy as a tradeoff to the error correction or coding gain achieved. An additional compression scheme is employed in order to achieve compression. However, the error correction in this methodology comes with implicit compression without the need for any other compression techniques. The concatenation stage in encoding contributes to this compression. Beyond a certain number of SYMBOLs appended with a protected LABEL, the codeword length is lesser than the total information bits. This minimum number of SYMBOLs in a codeword for achieving compression is not very large. For example, if there are minimum 6 SYMBOLs in a codeword for the case, $k_m = 7$, and $k_1 = 2$, we can achieve compression. As we append more SYMBOLs in a codeword, the compression is increased. Compression can be calculated by taking the ratio of the difference in the number of input and coded bits to the number of input bits.

3.3.3 Energy efficiency

The quantitative analysis of energy efficiency is highly important in optimal FEC selection for energy-constrained WSNs. Intuitively correlating the complexity of a coding scheme with its energy consumption using a proportionality relation may not always be correct. For instance, the Hamming code's encoding and decoding are much simpler compared to those of RS codes. However, a quantitative study of energy components has shown that RS codes are much more energy-efficient than Hamming codes [71, 111]. Hence, we estimate the energy consumption of the codes, both analytically

and experimentally, in this thesis. The metric used to compare the energy efficiency of the proposed scheme with existing standard schemes is the energy consumption per information bit required to achieve a specific value of BER.

Energy consumption per information bit is calculated considering all energy components of a sensor node. If there is no FEC used, the sensor node has to expend energy only for transceiver and sensing units. On the contrary, when an FEC is used, the computation unit also consumes energy for necessary encoding/decoding operations, in addition to the energy spent by the transceiver and sensing units. Sensing unit energy is independent of the usage of FEC and can be neglected in the comparison of FECs. This calls for the modeling of the radio energy and the computation energy units. The radio energy model and the computation energy model used in this work are explained in the next section. We aim to find the difference in transmit-energy saving and the additional energy expenditure of FEC schemes and arrive at a tradeoff between them.

3.4 Node Energy Model

3.4.1 Radio Energy Model

The radio energy model presented in [71] is used in this Thesis in the sense that it is found to be optimal for the comparison of FEC schemes. The radio energy model includes the radio transmit-energy and associated transceiver circuit energy. The required SNR value can be determined from the desired BER of the particular application in use. AWGN channel condition is simulated and the BER vs. E_b/N_0 is obtained. This E_b/N_0, i.e., the average SNR per bit value, helps us calculate the receive/transmit-power and hence the transmit energy. In addition to SNR per bit distance between transmitter and receiver, the frequency of operation, channel bandwidth, modulation scheme used, antenna gains, and packet length plays a role in the radio energy.

Transceiver circuit operates in one of the three states, namely ON, SLEEP, and TRANSIENT. To save energy, the transceiver is kept in ON state only during the transmission or reception. The rest of the time, it goes to SLEEP state. The switching state between ON and SLEEP is termed the TRANSIENT state. Hence, the total energy spent in the radio unit comprises the total energy spent in these three states.

$$E_{radio} = \frac{P_{\mathrm{ON}}T_{\mathrm{ON}} + P_{\mathrm{SP}}T_{\mathrm{SP}} + P_{\mathrm{TR}}T_{\mathrm{TR}}}{L} \tag{3.10}$$

where E_{radio} is the radio energy per bit on transmission of L bits, P_{ON}, P_{SP}, and P_{TR} are the consumed powers and T_{ON}, T_{SP}, and T_{TR} are the duration spent in ON, SLEEP, and TRANSIENT states, respectively. The power consumed in the SLEEP state is meager, and the time duration spent in the TRANSIENT state is also very low. Hence, the energies in the SLEEP and TRANSIENT states can be assumed to be negligible. The considerable contribution in E_{radio} is from the ON state. At the ON state, power is consumed for both signal transmission and associated transceiver circuitry. Thus,

$$E_{radio} = \frac{(P_{trans} + P_{ckt})T_{\mathrm{ON}}}{L} \tag{3.11}$$

where P_{trans} is the power consumed for signal transmission, and P_{ckt} describes the power consumed by the transceiver circuitry.

Power consumed for transmitting L bits can be calculated using [108]

$$P_{trans} = \left(\frac{4\pi}{\lambda}\right)^2 d^n \frac{P_r}{G_r G_t} \tag{3.12}$$

where λ is the transmit signal wavelength, d is the distance between the transmitter and receiver, n is the pathloss exponent, P_r is the received power, G_r and G_t are the receiver and transmitter antenna gains, respectively. The received power in the case of an AWGN channel can be calculated using the expression [108]

$$P_r = \mathrm{SNR}_{perbit} bB \frac{N_0}{2} \mathrm{NF} \tag{3.13}$$

where SNR_{perbit} is the received per bit SNR, b is the number of bits transmitted by each modulation symbol, B is the channel bandwidth, $\frac{N_0}{2}$ is the noise power density for an AWGN channel, and NF is the noise figure of receiver.

The transceiver circuitry components, such as power amplifier (PA), low-pass filters, band-pass filters, digital-to-analog converter, analog-to-digital converter, mixer, frequency synthesizers, intermediate-frequency amplifier, and low-noise amplifier consume power contribute to the total energy consumption. PA is the most power-hungry component. Among all the circuit components, only power consumption by PA is dependent on the transmit power of the signal, and as a consequence, it is directly influenced by the FEC scheme used. Hence, we calculate the energy consumed by PA as a representative of the transceiver circuit energy. Power consumed by PA is related to the transmit power by the expression $P_{\mathrm{PA}} = \alpha P_{trans}$, where α is a function of the drain efficiency of the power

amplifier, given by $\eta = \frac{1}{1+\alpha}$ [112]. Hence, E_{radio} can now be represented as

$$E_{radio} = \frac{(1+\alpha)P_{trans}T_{\text{ON}}}{L}. \tag{3.14}$$

For M-ary frequency shift keying modulation, the transceiver ON time is

$$T_{\text{ON}} = \frac{2^b L}{bB}. \tag{3.15}$$

For M-ary phase shift keying modulation, the transceiver ON time is

$$T_{\text{ON}} = \frac{L}{bB}. \tag{3.16}$$

SNR per bit is dependent on the modulation type and the FEC used and is obtained from the BER performance curve for each of the schemes compared. The radio energy of various sensor nodes can be measured using the simulator AVRORA described in the next section. The energy value obtained from the simulator is averaged out to find the radio energy per information bit.

3.4.2 Computation Energy Model

AVRORA [113], a cycle-accurate instruction-level sensor network simulator, is used for estimating the computation energy required for encoding/decoding operations in a Mica2 mote. AVRORA is designed explicitly for WSN simulation and can simulate the specified processors accurately [114]. The AVRORA is also compliant with IEEE 802.15.4 with an extension AVRORAZ [115]. The total energy spent by the processor in executing encoding and decoding operations is averaged out for the number of information bits to find the encoding energy per information bit (E_{enc}) and decoding energy per information bit (E_{dec}).

3.4.3 Total Energy

The total energy expenditure of the sensor node is contributed by radio and computation energy and can be obtained using the mathematical expression given below.

$$E_{radio} = \frac{(1+\alpha)P_{trans}T_{\text{ON}} + L(E_{enc}+E_{dec})\frac{N}{K}}{L}. \tag{3.17}$$

3.5 Simulation Parameters

The scheme is simulated for the Mica2 mote, a WSN platform. The radio unit in a Mica2 mote is CC1000 radio [107] which can operate at 315/433/868/916 MHz with a maximum data rate of

Table 3.1: Code Parameters

k_m : message length
k_2 : SYMBOL length
k_1 : $k_m - k_2$
S : no. of SYMBOLs in a codeword

76.8 kbps [100]. The modulation employed is NCBFSK. The noise figure of CC1000 is 12/13dB. The most energy-dominant component of the transceiver, PA, is characterized by its drain efficiency. A class-C amplifier with 75% efficiency is selected since the Mica2 node employs frequency shift keying, a constant envelope modulation scheme. A constant envelope modulation scheme doesn't call for a linear PA, and hence, a high-efficiency nonlinear PA can be used, which minimizes the peak current consumption.

The scheme is further evaluated in the context of the MicaZ mote, which employs CC2420 radio [106]. The CC2420 radio, which is compliant with the IEEE 802.15.4 standard, uses OQPSK modulation and a 2.4 GHz frequency with a maximum data rate of 250kbps. We consider a noise figure value of 7 dB, as this information is not available with the CC2420 datasheet and the receivers similar to CC2420 have values varied from 5-7 dB [116]. The constant envelope modulation scheme OQPSK permits to use relatively nonlinear PA [117]. We consider here a 60% efficient class AB PA which has better efficiency and less distortion [118].

We use a specific notation for the proposed scheme, as described here. The code characterization is done by M1 $\{S,\ k_m,\ k_1,\ k_2\}$, where, S denotes the number of SYMBOLs in a codeword, k_m defines the length of each message block, k_2 gives the number of bits in a SYMBOL and $k_1 = k_m - k_2$.

Simulations are performed rigorously for various values of code parameters and channel parameters. The code parameters are shown in Table 3.1 and channel parameters are shown in Table 3.2, and Table 3.3. The results obtained by changing the code parameters indicate the effect of the same in CG, compression, and energy efficiency. By changing the channel parameters in simulation, we can study the code's usefulness and potential under different channel conditions. The rectangular code parameters are selected considering the required protection for LABEL and the LABEL length. For

Table 3.2: Channel Parameters - with Mica2 platform

$B = 38.4$kHz	$P_e = 10^{-5}$
$f_c = 915$MHz	G_t,G_r=1
$NF = 13dB$	$k = 1.38064852 \times 10^{-23}$
α=0.3333	$T = 290$

Table 3.3: Channel Parameters - with MicaZ platform

$B = 1$MHz	$P_e = 10^{-5}$
$f_c = 2.4$GHz	G_t,G_r=1
$NF = 7dB$	$k = 1.38064852 \times 10^{-23}$
α=0.6667	$T = 290$

instance, for a particular characterization of M1 {S, 7, 1, 6} and 1-bit error protection to LABEL, the nearest possible rectangular code, rectangular (11, 6) code, and for M1 {S, 6, 1, 5} and 1-bit error protection to LABEL, the nearest possible rectangular code, rectangular (8, 4) code, [103] have been chosen.

The code is simulated under various conditions, as characterized by the following sets,

$$\mathscr{R}_{k_m k_1 k_2} := [\{5,7,2,5\},\ \{10,7,2,5\},\{30,7,2,5\}]$$
$$\mathscr{R}_{Sk_2} := [\{10,6,1,5\},\ \{10,7,2,5\},\{10,8,3,5\}]$$
$$\mathscr{R}_{Sk_m} := [\{10,8,1,7\},\ \{10,8,2,6\},\{10,8,3,5\}]$$
$$\mathscr{R}_{Sk_1} := [\{10,6,1,5\},\ \{10,7,1,6\},\{10,8,1,7\}]$$

where, $\mathscr{R}_{k_m k_1 k_2}$ denote the cases considered for simulation purposes with fixed k_2, k_m, and k_1 and varying S, and $\mathscr{R}_{Sk_2}$, $\mathscr{R}_{Sk_m}$, and $\mathscr{R}_{Sk_1}$ denote the cases considered for simulation purposes with fixed $S = 10$ and, k_2, k_m, and k_1 fixed, respectively.

For energy efficiency analysis, we use the simulator AVRORA to find the encoding and decoding

energies. The transmit energy is calculated analytically using the expressions in Section 3.4.1 and estimated by simulation using AVRORA. The obtained total energy expenditure for various coding schemes can be utilized to arrive at the most energy-efficient methodology.

3.6 Results and Discussions

3.6.1 Mica2 Platform

The scheme in the Mica2 platform with NCBFSK modulation is analyzed in this section. The BER performance obtained by simulating the proposed scheme with various values of S, k_m, k_1, and k_2 is presented. The CG can be deduced from the curve plotted. The difference in the number of input bits and encoded bits divided by the number of input bits and multiplied by 100 gives the percentage compression achieved. Energy expenditure per information bit is analytically calculated and estimated using AVRORA.

3.6.1.1 BER Performance and Compression

The performance of our scheme in the Mica2 platform for varying values of S is studied by keeping the values of k_2, k_m, and k_1 fixed. Fig. 3.9 shows this effect of S for $k_m = 7$, $k_1 = 2$, and $k_2 = 5$, i.e., the cases contained in $\mathscr{R}_{k_m k_1 k_2}$, and the performance of the uncoded transmission, Hamming (7, 4) code, and RS (31, 29) code. We observe that the CG increases as S increases. At a BER=10^{-5}, we achieve a CG of 2.88 dB for $S = 5$; 3.535 dB for $S = 10$; and 4.054 dB for $S = 30$, while the Hamming (7,4) code gives a negligible gain, and RS (31, 29) code provides a gain of 1.04 dB. Compression also increases as S increases. A compression of 23.81% is noted for $S = 30$ using the proposed scheme with the above parameters.

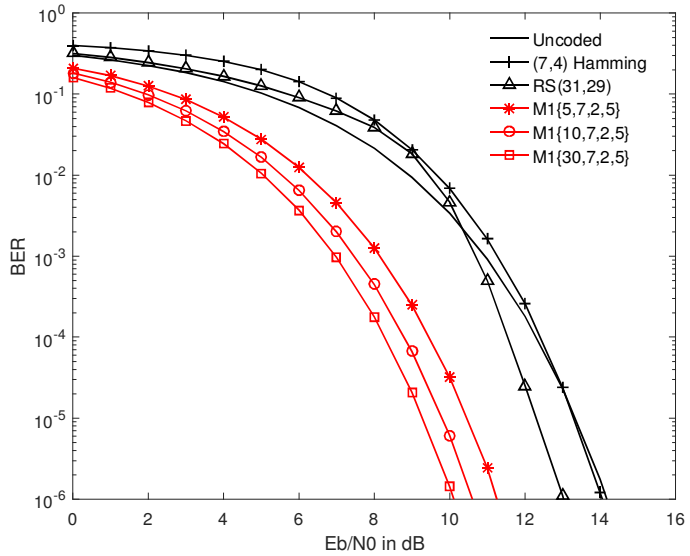

Figure 3.9: BER vs. E_b/N_0 performance of the uncoded, Hamming, RS, and Methodology 1 for $\{S,\ 7,\ 2,\ 5\}$ with $S = 5,\ 10,$ and 30 in Mica2.

Fig. 3.10 shows the theoretical and simulated BER performance. The theoretical plot is obtained using the equations (3.4), (3.5), and (3.7). It also plots the upper and lower bounds of the bit error probability, calculated using equations (3.8) and (3.9), respectively.

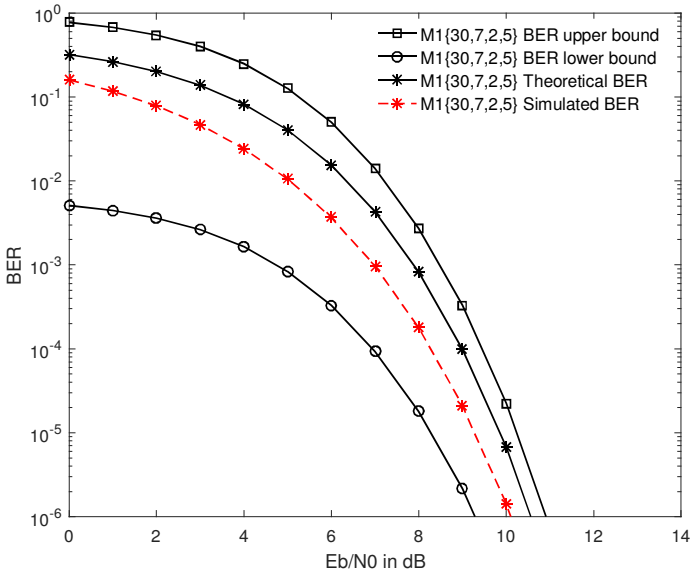

Figure 3.10: Theoretical, simulation, upper bound, and lower bound BER of Methodology 1 for $\{30,\ 7,\ 2,\ 5\}$ in Mica2.

The effect of increasing the k_m value, keeping k_2 fixed, as in the cases in $\mathscr{R}_{Sk_2}$, is shown in Fig.

3.11. The CG and compression are found increasing with k_m and k_1, as (2.97 dB, 3.33%), (3.535 dB, 14.2857%), and (4.086 dB, 23.75%). As k_m and k_1 increase with a fixed k_2, the grouping turns out to be better since more SYMBOLs can be associated with a LABEL. This is because more members are present in each group with the required d_{min}, which we term as grouping efficiency. As the number of SYMBOLs in a codeword increase, the error correction capability and compression achieved with the codeword increase.

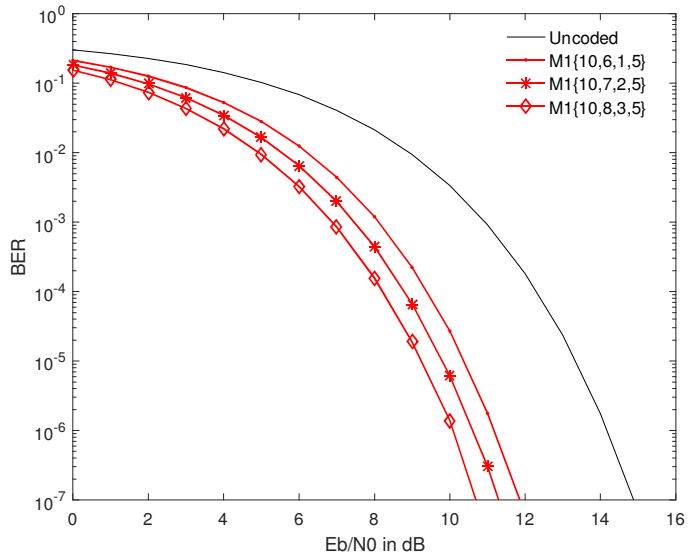

Figure 3.11: BER vs. E_b/N_0 performance of Methodology 1 for cases contained in $\mathscr{R}_{k_2}$ in Mica2.

When k_m is fixed, as in the cases of $\mathscr{R}_{Sk_m}$, a similar pattern can be observed from Fig. 3.12. As k_1 increases, better CG and compression are achieved since our grouping efficiency improves with more members in a group with minimum distance restriction. The CG, compression pair achieved in this case is (2.54 dB, 0%), (3.32 dB, 12.5%), and (4.086 dB, 23.75%).

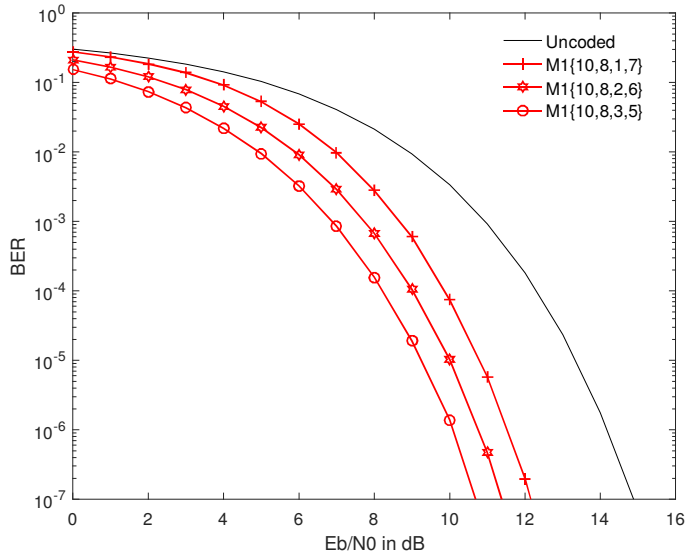

Figure 3.12: BER vs. E_b/N_0 performance of Methodology 1 for cases encompassed in $\mathscr{R}_{k_m}$ in Mica2.

However, when k_1 is fixed, as in $\mathscr{R}_{Sk_1}$, as k_m increases, k_2 also increases, thereby reducing the grouping efficiency. Hence, a marginal decrease in performance is obtained in this case. The CG and compression are evaluated as (2.97 dB, 3.33%), (2.86 dB, 2.8571%), and (2.54 dB, 0%), as k_m increases as found in Fig. 3.13

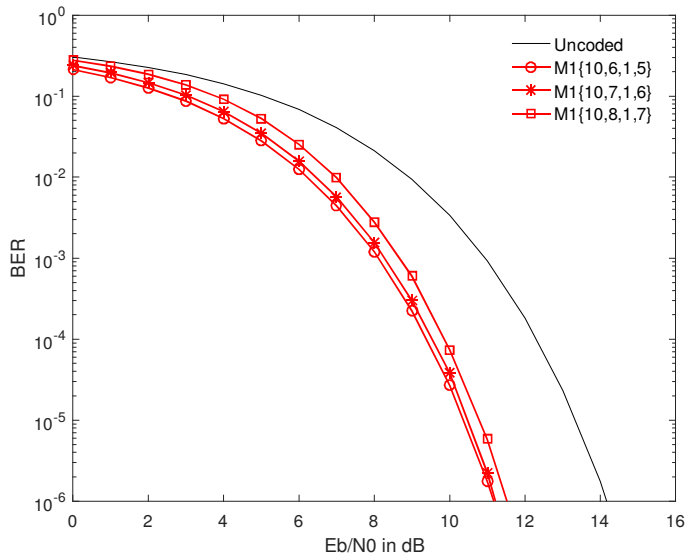

Figure 3.13: BER vs. E_b/N_0 performance of Methodology 1 for cases contained in $\mathscr{R}_{k_1}$ in Mica2.

3.6.1.2 Energy Efficiency

The radio energies and computation energies are plotted in this section. Radio energies comprise transmission energy and PA energy. Analytically calculated radio energies are used in theoretical plots, and radio energies estimated using AVRORA are used in the simulated plot. Computation energies comprise encoding energy and decoding energy, which are estimated using AVRORA.

Effect of various code parameters on Node Energy: For a fixed S, the effects of varying k_m, k_1, and k_2 values are presented in Fig. 3.14, for distance=40 meter, S=30, and n=5.5. The radio energies are calculated analytically, and the computation energy is obtained from AVRORA. It is found that at BER=10^{-5}, the scheme with characterizations {30, 6, 1, 5}, {30, 7, 2, 5},{30, 8, 2, 6}, and {30, 8, 3, 5} are energy efficient compared to uncoded, Hamming (7, 4) code, and RS (31, 29) code. Characterization {30, 7, 1, 6} is equally energy efficient to RS (31, 29) code. However, the BER performance of {30, 7, 1, 6} is higher than that of RS. Though the characterization {30, 8, 1, 7} is not better in energy efficiency compared to the standard schemes, its BER performance is better comparatively. Hence, it can be inferred that, by appropriately selecting the code parameters, higher CG, compression, and energy efficiency are achieved.

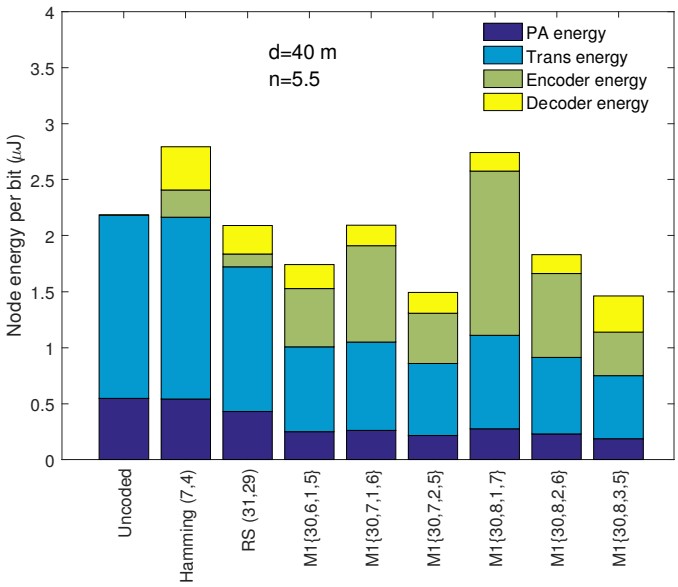

Figure 3.14: Comparison of energy expenditure of Methodology 1 with standard codes and uncoded in Mica2.

The scheme is further analyzed using radio values estimated from AVRORA with the same code

parameters used in Fig. 3.14. The simulated plot is shown in Fig. 3.15. A pattern similar to that of the theoretical plot can be observed here except for an increase in base energy, which occurs because of the additional transceiver components simulated in AVRORA compared to the components we have selected for theoretical analysis. In the theoretical analysis, we have only considered the most energy-hungry PA. However, AVRORA simulates all the components. We can also observe a higher rise in Hamming energy. This is due to the higher redundancy added to Hamming codes. When estimating the energy spent per information bit, instead of energy per transmitted bit, this redundancy value plays its role in increasing the energy.

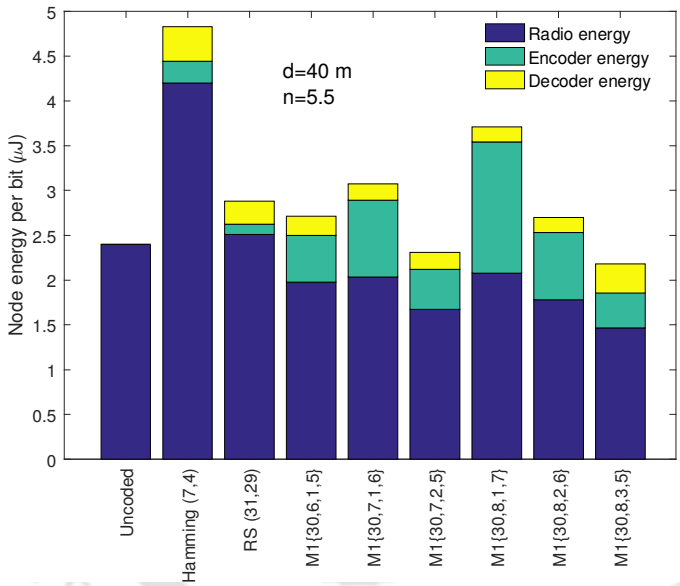

Figure 3.15: Comparison of simulated energy expenditure of Methodology 1 with standard codes and uncoded in Mica2.

The effect of varying S is studied in Fig. 3.16, for distance=40 meter, and n=5.5. As S increases, the energy efficiency also increases since more SYMBOLs are packed with a LABEL which increases CG, compression and decreases the number of calculations per bit.

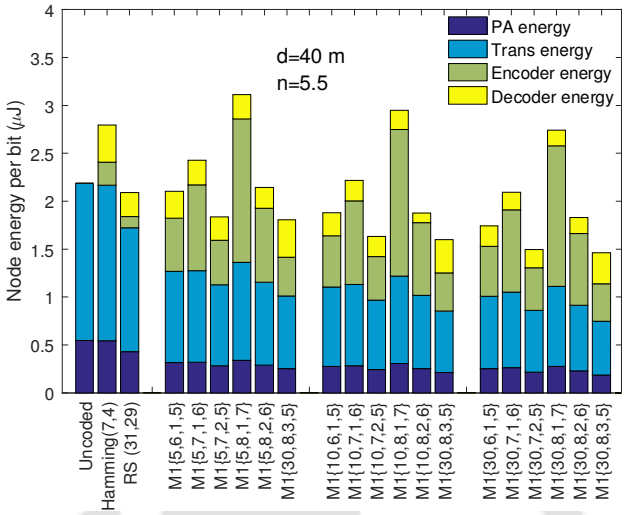

Figure 3.16: Effect of varying S in energy expenditure of Methodology 1 in Mica2.

Effect of various channel parameters on Node Energy: The energy efficiency of the scheme is studied for varying distances and path loss exponent in this section. The energy-saving is higher with longer distances, as evident from Fig. 3.17. The path loss exponent also plays an important role here. In a more cluttered environment, the advantage of FEC is more pronounced, as shown in Fig. 3.18.

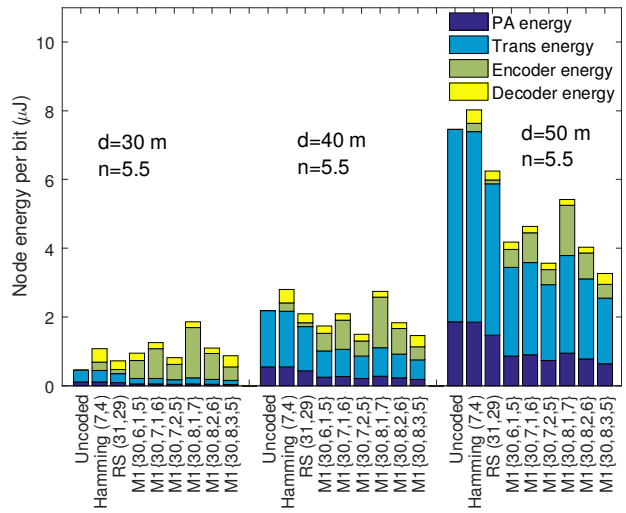

Figure 3.17: Energy comparison of Methodology 1 for different distances in Mica2.

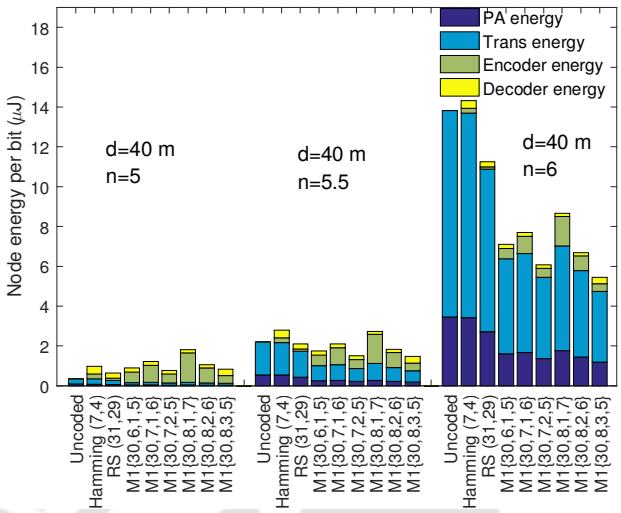

Figure 3.18: Energy comparison of Methodology 1 for different path loss exponent in Mica2.

3.6.2 MicaZ Platform

The scheme is further analyzed in the MicaZ platform with OQPSK modulation in this section. Again the channel considered here is AWGN. The results obtained by simulating Methodology 1 with various values of S, k_m, k_1, and k_2 are presented.

3.6.2.1 BER Performance and Compression

Fig. 3.19 plots the performance of our scheme for {5, 7, 2, 5}, {10, 7, 2, 5}, and {30, 7, 2, 5}; Hamming (7, 4) code; RS (31, 29) code, and uncoded transmission. We can observe that our proposed coding scheme gives a significant improvement in CG compared to the simple Hamming (7, 4) code and stronger RS (31, 29) code. It can also be observed that as the number of SYMBOLs in a codeword increase, CG also increases. The CG achieved at BER=10^{-5} is 2.832 dB for $S = 5$; 3.46 dB for $S = 10$; and 4.023 dB for $S = 30$, while the Hamming (7,4) code gives a negligible gain of 0.561 dB and RS (31, 29) code provides a gain of 1.068 dB. It is found that compression increases as S increases. Although the compression achieved for $S = 5$ is zero, yet a significant CG is attained. Both CG and compression are achieved simultaneously from $S > 5$. For $S = 10$, compression achieved is 14.2857% and that for $S = 30$, is 23.81%.

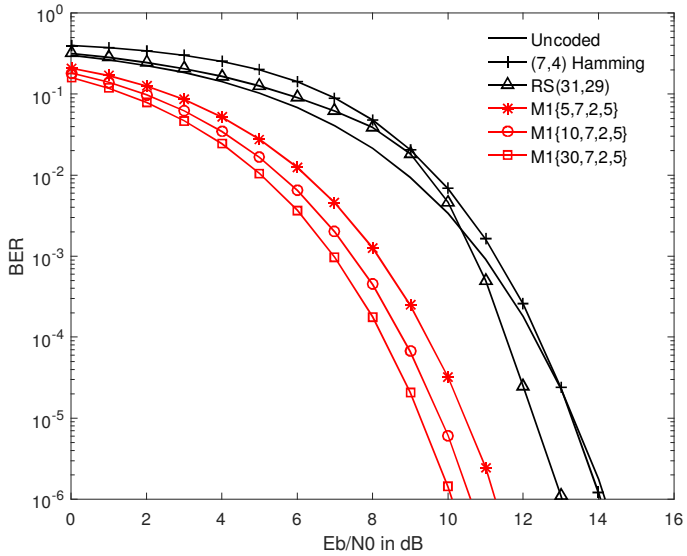

Figure 3.19: BER vs. E_b/N_0 performance of the uncoded, Hamming, RS, and Methodology 1 for $\{S,\ 7,\ 2,\ 5\}$ with $S = 5,\ 10,$ and 30 in MicaZ.

The theoretical and simulation results of the case $S = 10$, along with upper and lower bounds, are plotted in Fig. 3.20. The theoretical plot is obtained using the equations (3.4), (3.6), and (3.7). The upper and lower bounds of BER are calculated using (3.8) and (3.9), respectively. Theoretical and simulation BER performance curves fall well within the upper and lower bound curves.

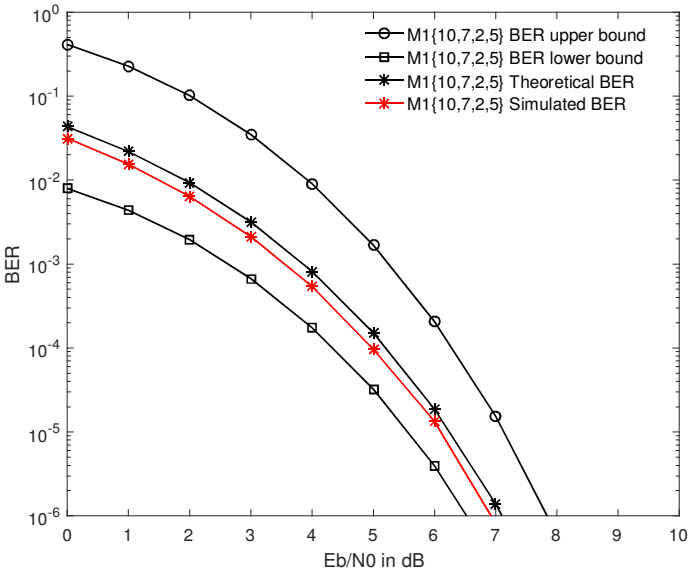

Figure 3.20: Theoretical, simulation, upper bound, and lower bound BER of Methodology 1 for $\{10,\ 7,\ 2,\ 5\}$ in MicaZ.

Fig. 3.21 shows the comparison of results for the cases contained in $\mathscr{R}_{k_2}$. An increment in the value of k_m and k_1 increases CG and compression. In each of the cases contained in $\mathscr{R}_{k_2}$, the achieved CG and compression are found as (3.045 dB, 3.33%), (3.46 dB, 14.2857%), and (3.962 dB, 23.75%).

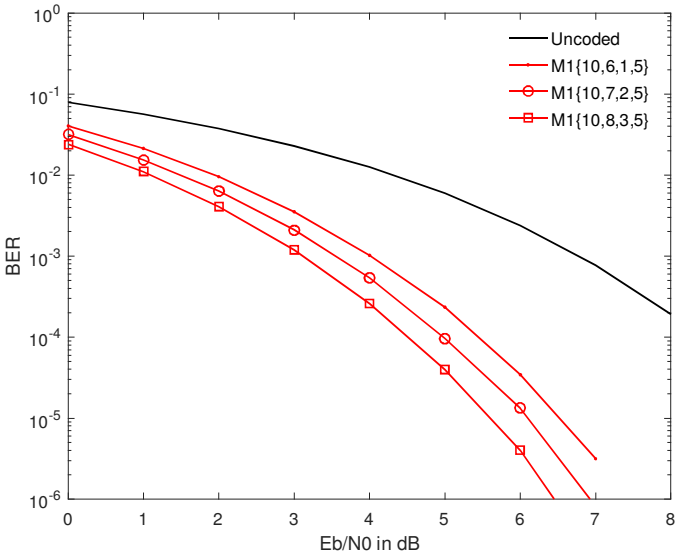

Figure 3.21: BER vs. E_b/N_0 performance of Methodology 1 for cases contained in $\mathscr{R}_{k_2}$ in MicaZ.

Further, results are illustrated for the cases in $\mathscr{R}_{k_m}$ in Fig. 3.22. As the value of k_1 increases, better CG is achieved in addition to compression, as depicted in Fig. 3.22. This is because as k_1 increases, our grouping improves with more members in a group with minimum distance restriction. Similarly for $\mathscr{R}_{k_m}$, the CG and compression are found as (2.796 dB, 0%), (3.393 dB, 12.5%), and (3.962 dB, 23.75%).

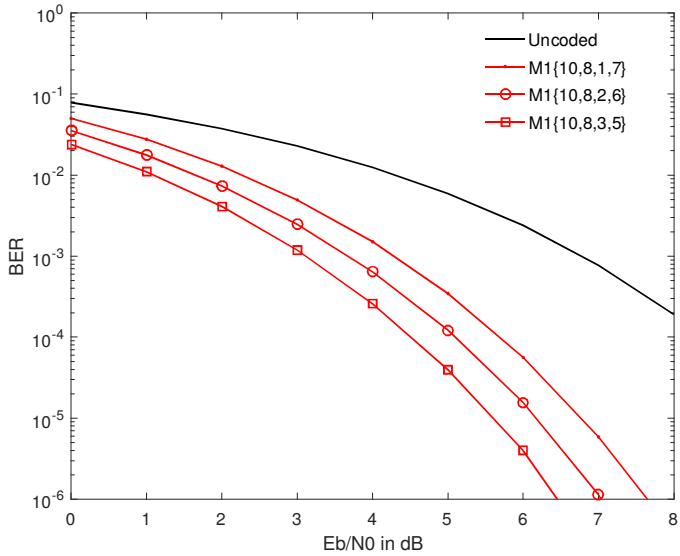

Figure 3.22: BER vs. E_b/N_0 performance of Methodology 1 for cases encompassed in $\mathscr{R}_{k_m}$ in MicaZ.

Withal, results for the cases encompassed in $\mathscr{R}_{k_1}$ are demonstrated in Fig. 3.23. It can be easily inferred that increasing the value of k_m leads to a marginal decrease in CG and compression. The performance degradation with increasing message length is due to the reducing effect of grouping. In the limiting case of $k_1 = 0$, there is no grouping at all. Therefore, for $\mathscr{R}_{k_1}$, CG and compression are evaluated as (3.045 dB, 3.33%), (2.996 dB, 2.8571%), and (2.796 dB, 0%).

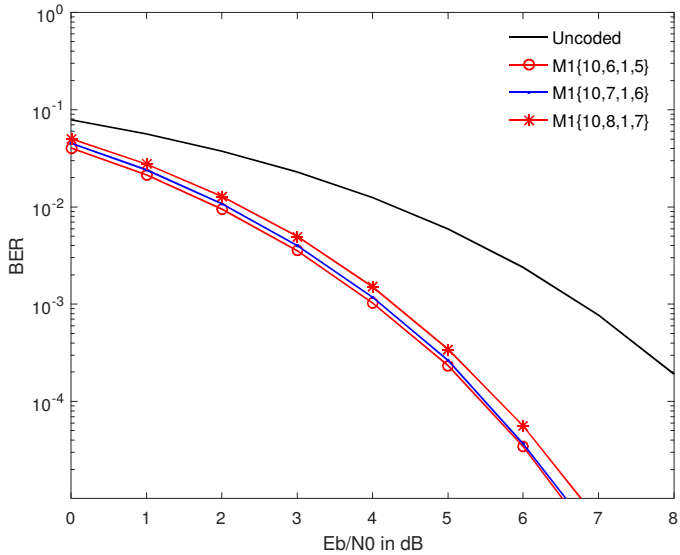

Figure 3.23: BER vs. E_b/N_0 performance of Methodology 1 for cases contained in $\mathscr{R}_{k_1}$ in MicaZ.

3.6.2.2 Energy Efficiency

The radio energies and computation energies of Methodology 1 for the MicaZ platform are plotted in this section. Again, radio energies are calculated analytically to be used in theoretical plots and estimated using AVRORA to be used in simulated plots. The computation energies are estimated using AVRORA.

Effect of various code parameters on Node Energy: The impact of varying k_m, k_1, and k_2 for a fixed S in energy expenditure of the proposed scheme in the MicaZ platform is presented in Fig. 3.24, for a distance=40 meter, S=30, and n=5.5. The analysis is performed at a BER of 10^{-5}. It is found that all characterizations of the scheme are energy efficient compared to uncoded and Hamming (7, 4) code. The characterizations except for {30, 8, 1, 7} are energy efficient compared to RS (31, 29) code too. The characterization {30, 8, 1, 7} is marginally higher in energy consumption compared to RS (31, 29) code, though its BER performance is significantly higher comparatively. It is learned here that we can more flexibly select the code parameters compared to the Mica2 platform. However, a clever selection is always better as we can see that the characterization {30, 8, 3, 5} is the most energy-efficient.

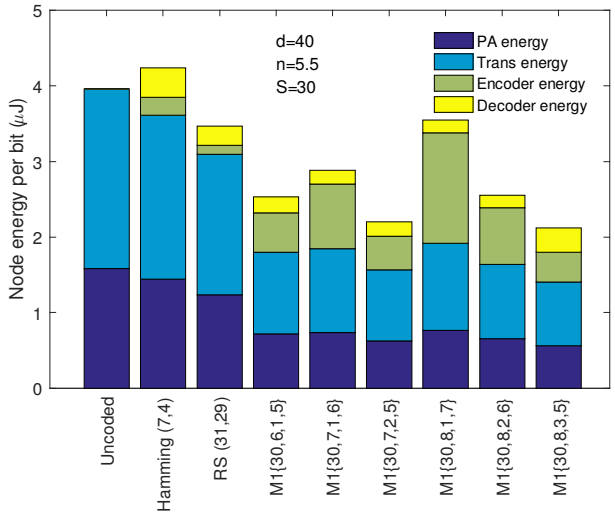

Figure 3.24: Comparison of energy expenditure of Methodology 1 with standard codes and uncoded in MicaZ.

From Fig. 3.25 in which the energy expenditure of each of the schemes along with uncoded, Hamming, and RS codes for distance=40 meter, and n=5.5, we can confirm that as S increases, the

energy efficiency also increases. As more SYMBOLs are packed with a LABEL, the energy spent per information bit decreases, which ends up in higher energy efficiency.

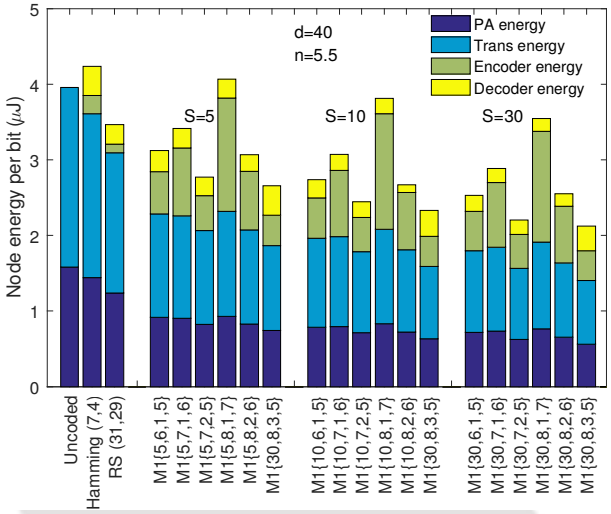

Figure 3.25: Effect of varying S in energy expenditure of Methodology 1 in MicaZ.

Effect of various channel parameters on Node Energy: It is again evident from Fig. 3.26 and 3.27 that the saving in energy is higher with increased distance and path loss exponent. In a more sophisticated environment, the saving in energy is better.

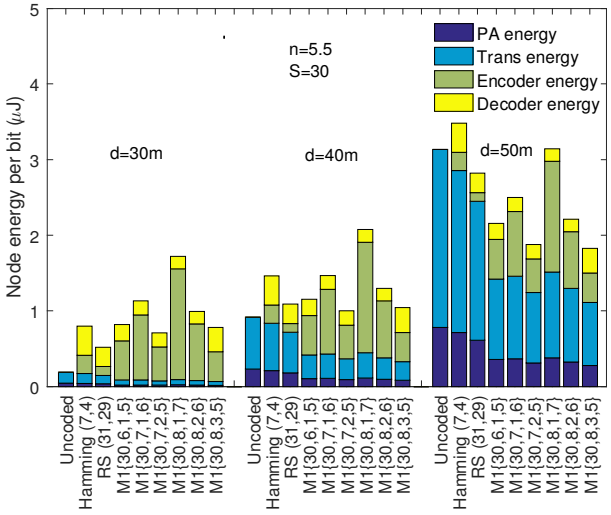

Figure 3.26: Energy comparison of Methodology 1 for different distances in MicaZ.

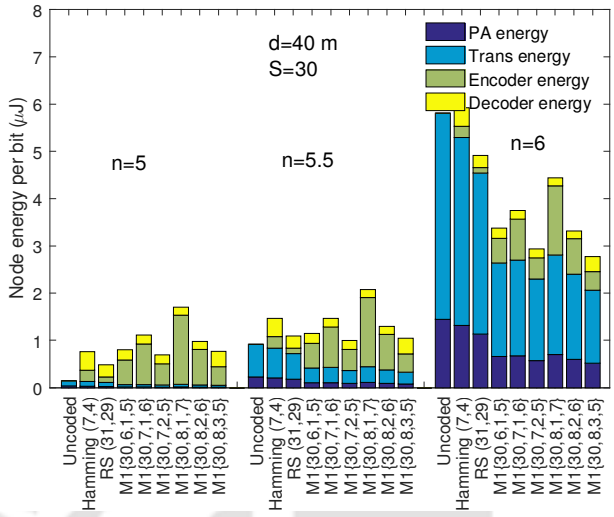

Figure 3.27: Energy comparison of Methodology 1 for different pathloss exponent in MicaZ.

3.6.3 Results for higher error protection for LABEL

It is evident that the overall performance of the Methodology 1 presented in this chapter is dependent on the error-correction capability of the LABEL even if that of the SYMBOL part of the codeword is improved (by taking a large d_{min} when grouping the SYMBOLs). Hence, increasing the d_{min} of the groups will not significantly improve the BER performance of the scheme. Alternately, enhancing the error-correction capability of the LABEL part can improve the BER performance of the scheme. The rectangular code is selected for the LABEL protection in the previous sections because it is a simple single-error correcting code (in line with each SYMBOL block's single error correction capability). However, better error protection is applied to the LABEL part in this section. The BCH (15,7) code is used to give a 2-bit error correction for LABEL. The resulting improvement in BER performance can be observed from Fig. 3.28. However, the energy efficiency is not appreciable in this case, as can be noted from Fig. 3.29, primarily because of the high decoding energy of the BCH code.

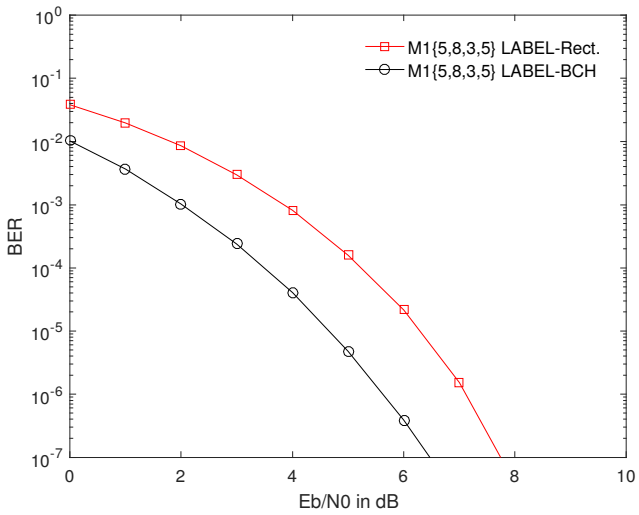

Figure 3.28: BER performance comparison of Methodology 1 for LABEL protected for 1-bit and 2-bit error-correction.

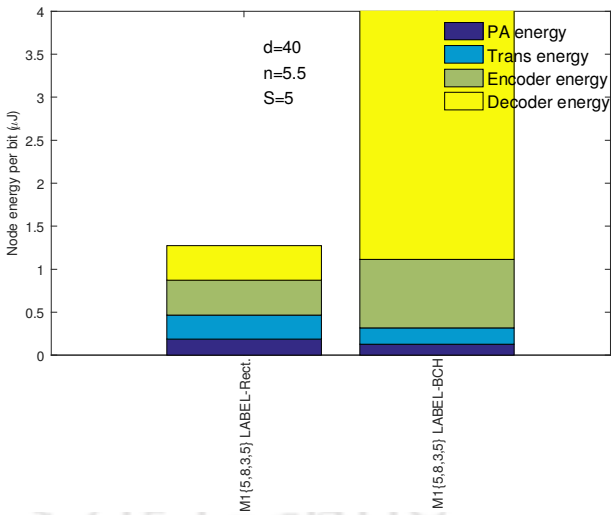

Figure 3.29: Energy consumption comparison of Methodology 1 for LABEL protected for 1-bit and 2-bit error-correction.

3.7 Conclusions

In the context of WSNs, reliable energy-efficient information transfer is studied, and a novel inter-dependent source-channel coding scheme is presented, which is referred to as Methodology 1. In this chapter, the error correction capability is analyzed and compared with standard schemes in terms of BER performance and CG. The bounds of BER performance have also been derived. As evident from the theoretical and simulation results, the proposed methodology provides a considerable amount of

compression in addition to good CG. A quantitative explanation of the energy efficiency of the proposed scheme is also provided. The redundant transmit energy and the encoding/decoding energies of channel coding are reduced by the intelligent design of the codeword, which provides both source coding and channel coding altogether. BER performance and energy comparisons are analyzed and plotted. Both theoretical and simulated values of radio energies are presented. It is concluded that a proper selection of the parameters of the proposed scheme yields high performance in terms of BER and energy efficiency with a fair amount of compression. The results are validated in the context of Mica2 and MicaZ platforms. For instance, our code with a characterization {30, 7, 2, 5} in the mica2 platform provides a CG of 4.054 dB and a compression of 23.81% while consuming significantly lesser energy compared to uncoded and Hamming (7, 4) and RS (31, 29) schemes. The scheme can also be employed conventionally after the source encoding procedure to attain additional compression.

The methodology is further enhanced in terms of coding gain, compression, and energy efficiency and is presented in the next chapter. The deterioration in energy efficiency found in Fig. 3.29 results from the effort to improve BER performance by providing extra protection to LABEL in the methodology presented in this chapter. This forms an additional motivation to a new methodology that doesn't rely on a single block, LABEL here, and not dependent on any other conventional schemes. Detailed analysis and evaluation are performed both analytically and by simulation with the help of an extensive performance evaluation framework.

4

Methodology II

Contents

4.1	Introduction	58
4.2	Description of Methodology 2	58
4.3	Performance Evaluation Framework	63
4.4	Simulation Parameters	65
4.5	Results and Discussions	66
4.6	Conclusions	84

4.1 Introduction

An enhanced methodology, superior in CG and compression, is proposed and presented in this chapter[1]. The methodology is termed Methodology 2 and abbreviated as M2. This intensified methodology for the energy-efficient Interdependent Source-Channel Coding scheme ensures robust communication with compression and reduced energy consumption. The scheme is studied and evaluated extensively for its BER performance and energy efficiency with the help of a mathematical framework and a simulated environment. An intensified CG, compression, and energy efficiency over previous methodology and standard error control codes are achieved. The methodology is studied, and BER performance and energy efficiency are validated in the context of the Mica2 and MicaZ sensor platforms in AWGN channel condition, analytically and by simulation. Our methodology for the characterization M2 $\{30,\ 7,\ 2,\ 5\}$ attains a 43% decrease in the total energy consumption, a CG of 4.33 dB, and compression of 26.2% compared to uncoded transmission. The scheme is further explored for enhanced grouping with higher error correction capability. Comparison with the conventional separated source and channel coding combinations is also performed to investigate the effectiveness of the proposed scheme.

4.2 Description of Methodology 2

The scheme is fundamentally based on an efficient grouping of data. A fraction of the input data is partitioned into groups with a minimum Hamming distance d_{min} restriction. The d_{min} maintained within each group ensures a degree of error correction capability within the groups. The data from the same group are sequenced together, with a label alongside for group identification, to form a codeword. The scheme is well suited for typical WSNs.

4.2.1 Encoding

Encoding comprises three steps, viz. group definition, alignment, and concatenation. The first step, Group definition, is done offline to reduce the computation required in real-time. The encoding

[1]The work reported in this chapter has been in part presented in the following conference:
N. Resmi and S. Chouhan, "Energy Efficient Communication with Interdependent Source-Channel Coding: An Enhanced Methodology," in Proc. IEEE SENSORS, 2018, pp. 1-4
and published in the following journal:
Resmi N.C. and S. Chouhan. An Enhanced Methodology for Energy-Efficient Interdependent Source-Channel Coding for Wireless Sensor Networks, IEEE Transactions on Green Communications and Networking, vol. 4, no. 4, pp. 1072-1080, Dec. 2020.

algorithm is summarized in Algorithm 4.1 in a nutshell.

Algorithm 4.1 Encoding algorithm

Group definition (offline)
1: Input d_{min}, input message length k_m, SYMBOL length k_2 ($k_2 >= d_{min}$)
2: $k_1 = k_m - k_2$
3: Divide all 2^{k_2} SYMBOLs into groups with minimum distance $d_{min} = 3$
4: Set a group label for each group
Alignment
5: Set least significant k_2 bits of input message as SYMBOL
6: Find the group of SYMBOL and pick its group label
7: Select LABEL from the groups defined matching the most significant k1 bits of input message.
Concatenation
8: **for** each LABEL **do**
9: codeword=[protected LABEL]
10: **for** each SYMBOL with the selected LABEL **do**
11: codeword=[codeword : SYMBOL]
12: **end for**
13: **end for**

4.2.1.1 Group Definition

The group definition is, in part, the same as in Methodology 1. To ensure the minimum distance d_{min} within each group, the number of members in each group is restricted by the term $A(k_2, d_{min})$, which is calculated using (3.1). The number of groups formed can be obtained from (3.2). However, Methodology 2 is different from Methodology 1 in LABEL formation. The 2^{k_1} labels per group, which will be explained in detail in Section 4.2.1.2, are also picked from the same group itself, where $k_1 = k_m - k_2$. Hence, the number of members in each group must be at least 2^{k_1}. Putting together both the conditions,

$$2^{k_1} \leq \text{No. of members per group} \leq A(k_2, d_{min}). \tag{4.1}$$

This poses an additional constraint in the characterization of Methodology 2. For instance, the characterization M1 $\{S,\ 8,\ 3,\ 5\}$ is not feasible in M2. This is because 2^{k_1}=8 labels are needed for this case, and the grouping of k_2=5 bit long SYMBOLs using (3.1) and (3.2) can not offer eight members per group. There can be only four members per group, according to the Eq. (4.1). Hence the code parameters for M2 should be selected accordingly.

For further understanding, an instance of $k_m = 7$, $k_2 = 5$, and $k_1 = 2$ is taken for Methodology 2 also. As the grouping part is the same in both the methodologies, the sample groups $group_A$ and $group_B$ are picked from Fig. 3.1 for example.

4.2.1.2 Alignment

The k_2 least significant bits of each input message of length k_m, termed as SYMBOL, equal with one of the members of any one group defined in the earlier step. The group is further examined to find a match between the most significant k_1 bits left from the input message and the least significant k_1 bits of the group members. This matching member is termed as LABEL, and the SYMBOL is appended with this LABEL to form a systematic code. If the no. of members per group is greater than 2^{k_1}, there may be more than one matching term. In such a scenario, the first matching member may be selected as the LABEL. The alignment process is depicted in Fig. 4.1. At this stage, there will be $k_2 - k_1$ redundant bits per input message, which will be compensated and overpowered with compression achieved in the concatenation stage.

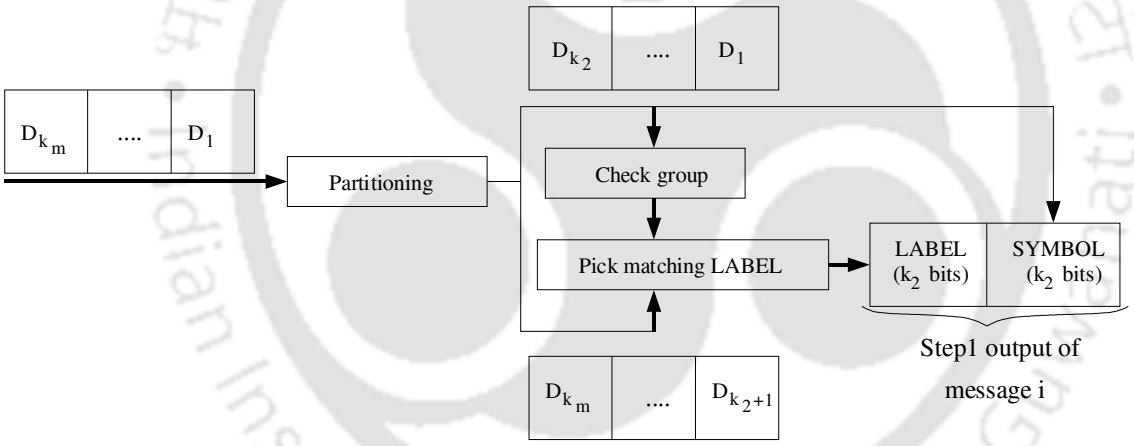

Figure 4.1: Methodology 2: Alignment of the input data as [LABEL: SYMBOL].

Returning to the instance taken in Section 4.2.1.1, the input messages are 7 bits long. Consider the same five input messages *Input* shown in Fig. 3.3, as an example. The first input message [1100000] on partitioning has the least significant five bits [00000], the SYMBOL, falls into $group_A$. Hence, the most significant two bits of the input message [11] are checked for a match in the same group, and the second member of the group, [00111], is found to have the same bits in the least significant position. This member is thus termed as the LABEL, and the output of the alignment process comes as [0011100000]. The alignment step output is obtained by processing the same way for all the five input messages, as shown in Fig. 4.2. The example messages are judiciously selected for having the same LABEL to show the concatenation process also. The LABEL may be any member of the group,

depending on the k_1 bits.

$$\text{Alignment step output} = \begin{bmatrix} 0 & 0 & 1 & 1 & 1 & 0 & 0 & 0 & 0 & 0 \\ 0 & 0 & 1 & 1 & 1 & 0 & 0 & 1 & 1 & 1 \\ 0 & 0 & 1 & 1 & 1 & 1 & 1 & 0 & 0 & 1 \\ 0 & 0 & 1 & 1 & 1 & 1 & 1 & 1 & 1 & 0 \\ 0 & 0 & 1 & 1 & 1 & 0 & 0 & 1 & 1 & 1 \end{bmatrix}$$

Figure 4.2: Alignment output as [LABEL: SYMBOL]

4.2.1.3 Concatenation

To comply with the delay tolerance of the application, desired compression rate, and the required error correction capability, the number of SYMBOLs S to be appended with each LABEL is determined. These SYMBOLs identified by the same LABEL are appended together alongside the LABEL itself. The concatenation process is the same as in M1, which is depicted in Fig. 3.6. The codeword structure, illustrated in Fig. 4.3 results in interdependent source-channel coding and is distinct from the codeword structure of M1, where protected LABEL forms a part of the codeword. Here, in M2, the protection bits for LABEL are not required, and hence additional compression is attained.

Figure 4.3: Methodology 2: codeword structure.

On considering $S = 5$ and as the LABEL for all five input messages are the same, one codeword is obtained with 5 SYMBOLs and a single LABEL alongside. The 35 bits in the input message of the example are reduced to 30 bits in the output. Compared to the same characterization in M1 as observed in Section 3.2.1.4, an additional saving of 5 redundant bits per codeword can be observed in M2.

$$\text{Codeword} = \begin{bmatrix} 0\,0\,1\,1\,1\,0\,0\,0\,0\,0\,0\,1\,1\,1\,1\,0\,0\,1\,1\,1\,1\,1\,0\,0\,0\,1\,1\,1 \end{bmatrix}$$

Figure 4.4: The output codeword

4.2.2 Decoding

The codeword with $S+1$ data-blocks (S SYMBOLs and 1 LABEL) from the same group has the defined error correction capability in each of the data blocks. For instance, if the minimum distance constraint within each group is $d_{min} = 3$, there will be a 1-bit error correction capability per data-block and thus a maximum of $S+1$ total error correction per codeword. This error correction is achieved, provided the group is determined correctly. The group of the maximum number of data blocks is used for decoding. The least significant k_1 bits of LABEL is adjoined with each of the SYMBOLs to retrieve the input messages associated with a codeword. The decoding algorithm is summarized in Algorithm 4.2.

Algorithm 4.2 Decoding algorithm

```
for each codeword do
    Find the group of each data block
    Select the group with highest count
    for each SYMBOL and LABEL in codeword do
        Match with the group members for error correction
        Input message=[k1 least significant bits from LABEL: SYMBOL]
    end for
end for
```

4.2.3 Enhancement over Methodology 1

The methodology presented in this chapter is superior to the previous methodology, Methodology 1, in the following aspects.

- ***Simplified operation:*** In the previous methodology, the LABEL was formed by clubbing the most significant k_1 bits of the input message with the fixed group label. This LABEL is further protected with rectangular coding. In the proposed methodology, the LABEL is implicitly protected being from the same group of SYMBOLs with a minimum Hamming distance constraint, and hence explicit protection is not needed.

- ***Increased compression:*** The implicit protection of LABEL in the current methodology saves the additional redundant bits required in the previous methodology for protection.

- ***Increased reliability:*** In the previous methodology, the reliability of the whole codeword was dependent on the correctness of the LABEL. The group was identified from the LABEL, and a wrong determination of LABEL made the entire codeword decoded incorrectly. However, in the

proposed methodology, the LABEL and SYMBOLs have equal importance, and the SYMBOLs' correction is not solely dependent on the LABEL correctness.

4.3 Performance Evaluation Framework

The proposed scheme is evaluated and compared for its energy efficiency and BER performance with the uncoded transmission, standard error correction schemes, Hamming (7, 4) and RS (31, 29), and Methodology 1. Performance evaluation is done in the context of MicaZ [105] mote and Mica2 [104] mote.

4.3.1 BER Performance

BER performance is obtained by both analytical and rigorous simulations using MATLAB. We choose an AWGN channel model. NCBFSK modulation is used in the Mica2 mote, which employs CC1000 radio. OQPSK modulation is used in the MicaZ mote, which employs CC2420 radio. The Methodology 2, Methodology 1, and the standard schemes Hamming (7, 4) code and RS (31, 29) are evaluated by rigorous simulations using MATLAB. The schemes are compared for their error correction capability using CG and BER performance curve. The SNR per bit obtained from this curve is used for the transmission energy calculation explained in the next section.

The block error probability of one data-block is calculated as

$$P_{DB} \leq \sum_{m=t+1}^{k_2} \binom{k_2}{m} p^m (1-p)^{k_2-m}, \tag{4.2}$$

where t number of bit errors per data-block can be corrected by the error correction scheme used [108]. The value of p used in (4.2) is obtained either from (3.5) or (3.6) depending on the sensor platform we are working with. The probability of a data-block in error with no error correction applied P_{DBNE} is calculated by putting $t = 0$ in (4.2). The probability of a wrong group determination can be found by calculating the probability of at least half of the data-blocks in error

$$P_{WGD} \leq \sum_{m=\left\lceil \frac{S+1}{2} \right\rceil}^{S+1} \binom{S+1}{m} P_{DBNE}^m (1-P_{DBNE})^{S+1-m}. \tag{4.3}$$

If the group determination is correct, t bits of errors can be corrected from each of the data-

blocks. Hence, the probability of an uncorrectable error in a data-block P_{DBUE}, provided the group determination is correct, can be calculated by putting appropriate value for t in (4.2). The probability of all possible uncorrectable errors in a codeword provided the group determination is correct P_{AUE}, is calculated by

$$P_{AUE} \leq \sum_{m=1}^{S+1} \binom{S+1}{m} P_{DBUE}^{m} (1 - P_{DBUE})^{S+1-m}. \tag{4.4}$$

The block error probability of the entire codeword is equal to the upper bit error probability of the codeword, calculated by

$$P_{CWberUP} = (1 - P_{WGD}) P_{AUE} + P_{WGD}, \tag{4.5}$$

where $1 - P_{WGD}$ gives the probability of correct group determination and P_{AUE} is the probability of uncorrectable errors, given that the group is correctly determined. When the group determined is wrong, the entire codeword is incorrectly decoded. The lower bit error probability is calculated by dividing the upper probability by the information bits in a codeword[110]

$$P_{CWberLOW} = \frac{P_{CWberUP}}{k_1 + Sk_2}. \tag{4.6}$$

The actual bit error probability is calculated using (4.2)-(4.5) with a little modification in (4.2) [109] and (4.4), as explained below. The bit error probability of one data-block is calculated as

$$P_{DBb} \leq \frac{1}{k_2} \sum_{m=t+1}^{k_2} (m+1) \binom{k_2}{m} p^m (1-p)^{k_2-m}. \tag{4.7}$$

The equation (4.7) is used to find the bit error probability of a data-block with no error correction applied P_{DBNEb} by putting $t = 0$. This probability is in turn used to find the bit error version of the probability of at least half of the data-blocks in error P_{WGDb} by substituting P_{DBNE} by P_{DBNEb} in equation (4.3). The bit probability of an uncorrectable error in a data-block P_{DBUEb}, provided the group determination is correct, can be calculated by putting appropriate value for t in (4.7). The bit probability of all possible uncorrectable errors in a codeword, provided the group determination is correct P_{AUEb}, is calculated by

$$P_{AUEb} \leq \frac{1}{S+1} \sum_{m=1}^{S+1} m \binom{S+1}{m} P_{DBUEb}^{m} (1 - P_{DBUEb})^{S+1-m}. \tag{4.8}$$

The bit error probability of the entire codeword is calculated by substituting P_{AUE} by P_{AUEb} and P_{WGD} by P_{WGDb} in (4.5).

4.3.2 Compression

The compression achieved by Methodology 2 is higher than that of Methodology 1. The omission of explicit LABEL protection improves the compression further, as the additional redundant bits for protection are not needed. Compared to standard schemes that need additional source coding techniques for compression, this saving is highly significant. Similar to Methodology 1, this compression is contributed by the concatenation stage in encoding. Beyond a certain number of SYMBOLs appended with a LABEL, the codeword length is lesser than the total information bits. The number of SYMBOLs needed in each codeword for achieving compression is less compared to that of Methodology 1. For instance, Methodology 1 required a minimum of 6 SYMBOLs in a codeword for the case, km = 7 and k1 = 2, to achieve compression. On the other hand, Methodology 2 requires only 3 SYMBOLs in a codeword for the same case for achieving compression. Compression calculation is performed by taking the ratio of the difference in the number of input and coded bits to the number of input bits.

4.3.3 Energy Efficiency

The energy efficiency is analyzed quantitatively by analytical and experimental methods. The energy efficiency comparison metric used here is the energy consumption per information bit required to achieve a specific value of BER. The node energy model, which comprises of Radio, Computation, and the Total Energies, is the same as in Chapter 3 and can be referred from Section 3.4.

4.4 Simulation Parameters

The code is characterized by M2 $\{S,\ k_m,\ k_1,\ k_2\}$, where, S indicates the count of SYMBOLs in a codeword, k_m is the input message length in bits, k_2 is the data-block length in bits, and $k_1 = k_m - k_2$. Rigorous simulations are carried out for diverse values of code parameters S, k_m, k_1, k_2, and $d_{min} = 3, 5$ within each group. The methodology is studied for the cases $\mathscr{R}_{k_m k_1 k_2} := [\{5,\ 7,\ 2,\ 5\},\ \{10,\ 7,\ 2,\ 5\}, \{30,\ 7,\ 2,\ 5\}]$, where the values of k_m, k_1, and k_2 are fixed, to find the effect of changing values of S on CG, compression, and energy efficiency. Further, keeping S fixed at 10 the results of varying k_m, k_1, and k_2, as characterized by $\mathscr{R}_S := [\{10,\ 6,\ 1,\ 5\},\ \{10,\ 7,\ 1,\ 6\}, \{10,\ 7,\ 2,\ 5\}, \{10,\ 8,\ 1,\ 7\}, \{10,\ 8,\ 2,\ 6\}]$, are studied. The methodology is compared with the previous methodol-

ogy further both in CC1000 and CC2420 radios. The code parameters and channel parameters used for this evaluation are listed in Table 3.1, 3.2, and 3.3.

4.5 Results and Discussions

In this section, we discuss the BER performance, compression, and energy efficiency of the proposed methodology. The results of the proposed scheme are compared with those of the previous scheme and standard codes such as Hamming and RS codes.

4.5.1 Mica2 Platform

4.5.1.1 BER Performance and Compression

Fig. 4.5 shows the effect of varying S values on BER performance of the proposed scheme with other code parameters fixed at $k_m = 7$, $k_1 = 2$, and $k_2 = 5$ in the Mica2 sensor platform. The figure also compares the scheme with the RS (31,29) code, Hamming (7,4) code, and the uncoded transmission. At a BER=10^{-5} Hamming (7,4) code achieves only a negligible CG and has a redundancy of 75%. RS (31,29) achieves 1.04 dB CG with redundancy of 6.9%. The proposed scheme achieves a CG and compression pair of (3.28 dB, 14.29%) for $S = 5$; (3.683 dB, 21.43%) for $S = 10$; and (3.956 dB, 26.19%) for $S = 30$. The CG and compression are found to increase as S increases.

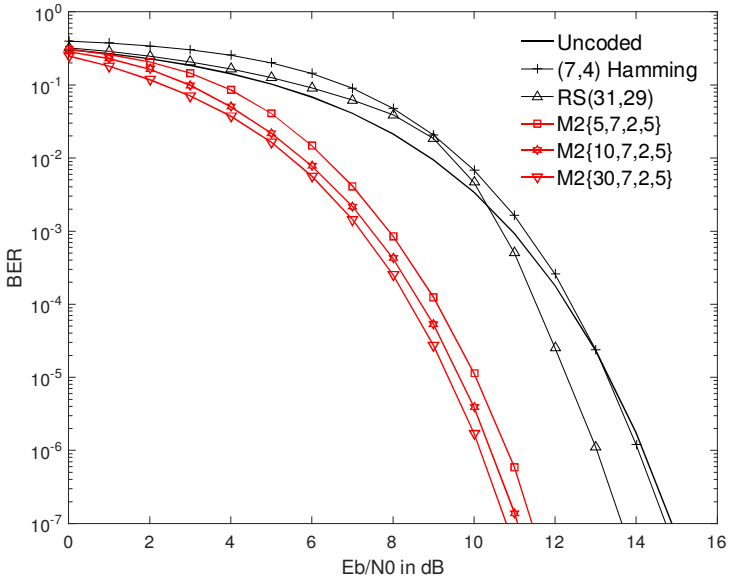

Figure 4.5: BER vs. E_b/N_0 performance of the uncoded, Hamming, RS, and M2 $\{S,\ 7,\ 2,\ 5\}$ with $S =$ 5, 10, and 30 in Mica2.

The BER performance for varying k_m, k_1, and k_2, and fixed S is studied in Fig. 4.6. The performance gets better with an increase in k_m and k_1 values, while k_2 is fixed due to improved grouping efficiency. Grouping efficiency enhances as there are more members in a group with a minimum distance constraint. This enhancement can be observed with the increase in k_1 as well, while k_m is fixed. However, the rise in k_2 and k_m reduces the grouping efficiency, and performance decreases marginally when k_1 is fixed. In a nutshell, it is better to increase k_m and k_1 while reducing k_2.

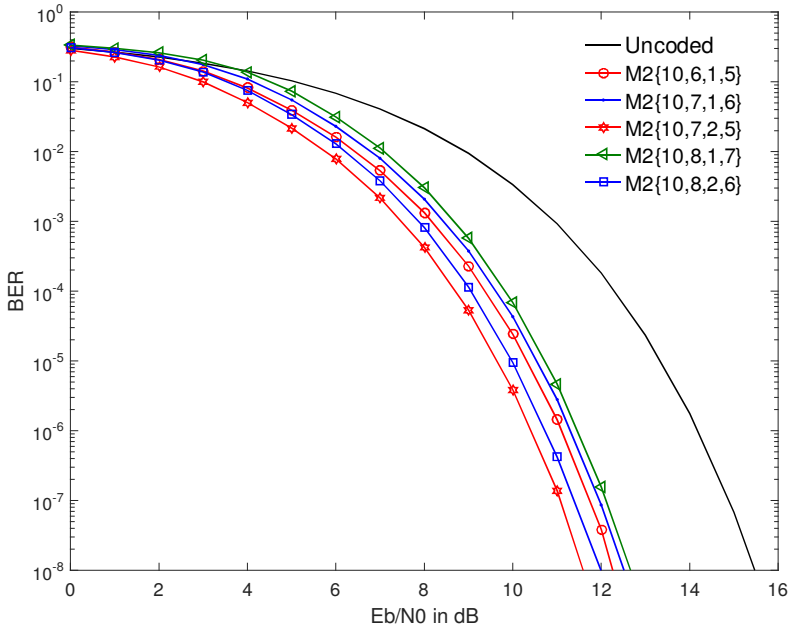

Figure 4.6: BER vs. E_b/N_0 performance of Methodology 2 for cases in $\mathscr{R}_S$ in Mica2.

Fig. 4.7 compares the theoretical and simulated BER performance. The equations described in Section 4.3.1 are used to obtain the upper bound, lower bound, and actual theoretical BER curves. The equivalence of the simulated and theoretical curves affirms the integrity of the scheme.

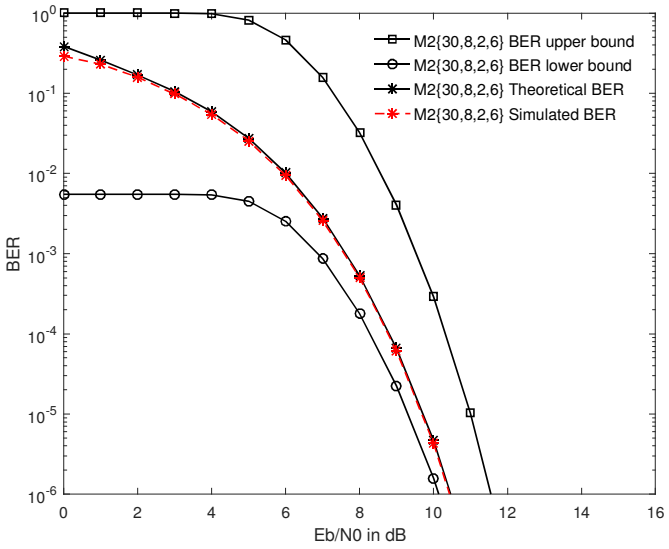

Figure 4.7: Theoretical, simulated, upper bound, and lower bound BER of M2 {30, 8, 2, 6} in Mica2.

4.5.1.2 Energy Efficiency

The coding schemes' energy efficiency is compared by plotting and comparing the radio and computation energies expended by one node. Radio energy constitutes transmission and PA energies, and the computation energy constitutes encoding and decoding energies. Radio energies in the AWGN channel can be calculated using the equations from Section 3.4.1 and estimated from the simulation. Computation energies are estimated using the simulator.

Effect of various code parameters on Node Energy: The total node energy per information bit is plotted in Fig. 4.8 of Methodology 2 with fixed S and changing k_m, k_1, and k_2 at distance=40 meter, $S = 30$, $n = 5.5$, and a required BER of 10^{-5}. The theoretically quantified radio energies and simulated computation energies sum up to give the total node energy. It is observed from the plot that Methodology 2 with characterizations {30, 6, 1, 5}, {30, 7, 1, 6}, {30, 7, 2, 5}, and {30, 8, 2, 6} expends less energy compared to Uncoded, Hamming (7, 4) code, and RS (31, 29) code. The percentage reduction of the characterizations compared to Uncoded is 28.96%, 13.59%, 50.73%, and 42.09%, respectively, while RS (31,29) saves about 4.35%, and Hamming (7,4) ends up spending more energy than Uncoded. The characterization {30, 8, 1, 7} though gives BER performance, spends more energy than RS (31,29).

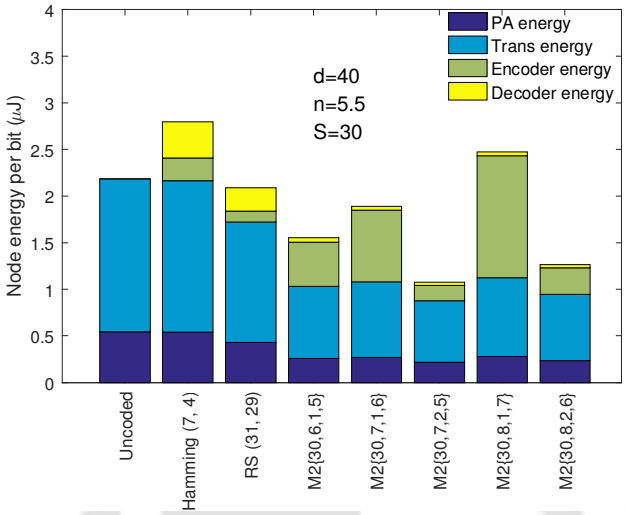

Figure 4.8: Comparison of energy expenditure of Methodology 2 with standard codes and uncoded in Mica2.

The validation is extended in Fig. 4.9 with both radio and computation energies estimated by simulation. Here, we can observe that the energy value is higher than the theoretical case, as the simulation calculates the energy spent on all the node components. In contrast, in the theoretical analysis, we considered only PA, the component which spends most of the energy. Though this difference is reflexed in the energy values, a similar pattern can be seen in the plot. Like the theoretical plot, characterizations $\{30,\ 7,\ 2,\ 5\}$ and $\{30,\ 8,\ 2,\ 6\}$ are the higher energy efficiency achievers.

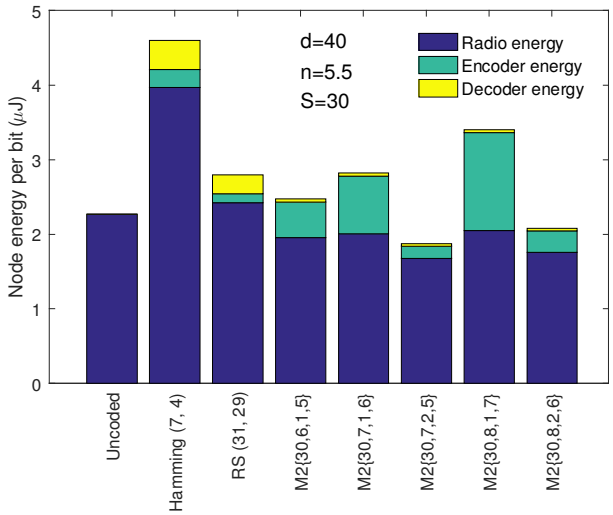

Figure 4.9: Comparison of simulated energy expenditure of Methodology 2 with standard codes and uncoded in Mica2.

Fig. 4.10 illustrates the energy consumption of the methodology with varying S, compared with standard schemes, for a distance of 40 meters, and a path loss exponent of 5.5. As it is intuitively explainable, the energy efficiency is better with increasing S value. For instance, the savings in energy consumption of the characterization $\{S,\ 7,\ 2,\ 5\}$ is 31.66%, 37.05%, and 50.73% respectively for $S = 5$, $S = 10$, and $S = 30$.

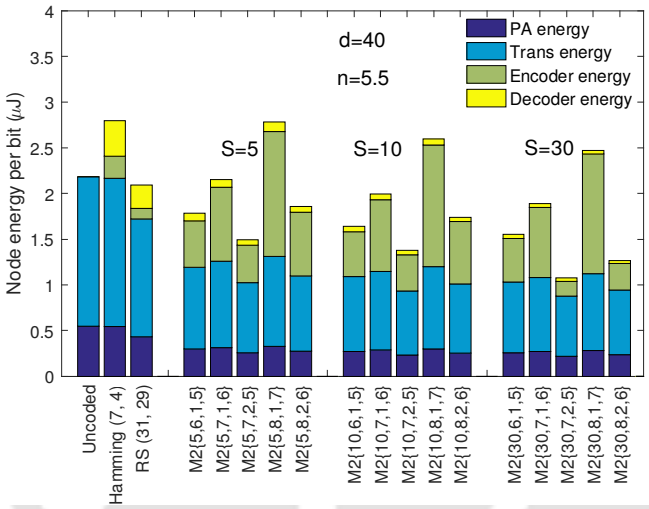

Figure 4.10: Effect of varying S in energy expenditure of Methodology 2 in Mica2.

Effect of various channel parameters on Node Energy: The channel parameters distance and path loss exponent are varied to study the effect in Fig. 4.11 and 4.12, respectively. As the transmitter and receiver are more distant from each other or there exists a more cluttered environment between them, the errors increase, and the use of a channel coding scheme is more important. This is reflected in both figures. The scheme gives better performance as the environment is harsher.

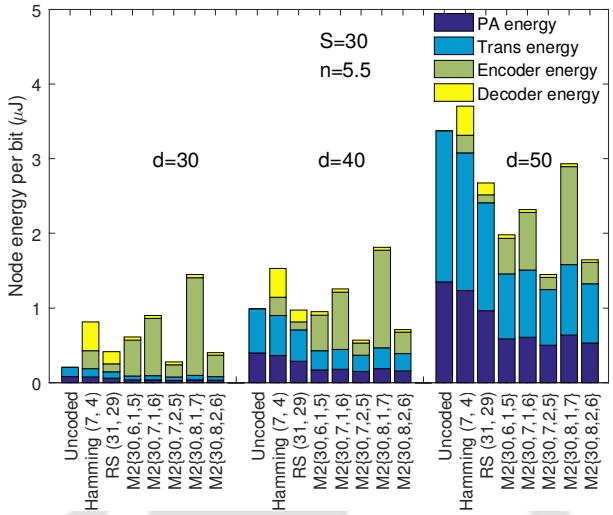

Figure 4.11: Energy comparison of Methodology 2 for different distances in Mica2.

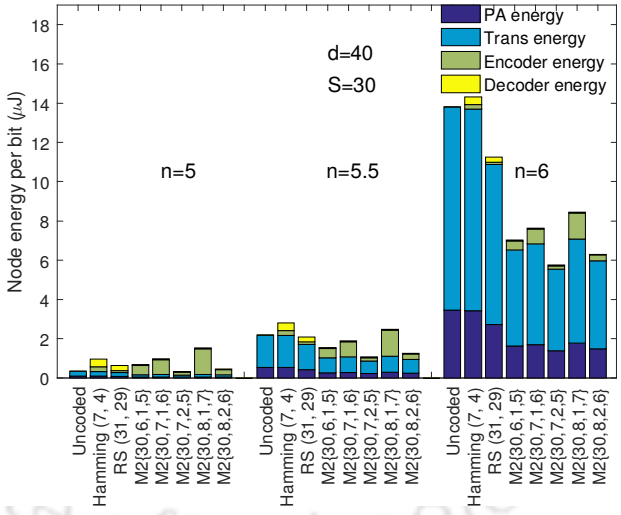

Figure 4.12: Energy comparison of Methodology 2 for different pathloss exponent in Mica2.

4.5.1.3 Comparison with Methodology 1:

The proposed methodology M2 is compared with the previous methodology M1 for the cases $\{5,\ 6,\ 1,\ 5\}$ and $\{5,\ 7,\ 2,\ 5\}$ in Fig. 4.13. The error correction is dependent on the correctness of group selection, and group selection is performed based on the number of correct data blocks in the received codeword. Moreover, the LABEL part is not exclusively protected, as in the previous methodology. Hence, the proposed scheme is found performing better for E_b/N_0 values greater than 7 dB. However, the compression achieved is significantly higher. While M1$\{5,\ 7,\ 2,\ 5\}$ has zero

compression/redundancy M2{5, 7, 2, 5} achieves 14.29% of compression. The 10% redundancy in M1{5, 6, 1, 5} is outperformed by M2{5, 6, 1, 5} with no redundancy.

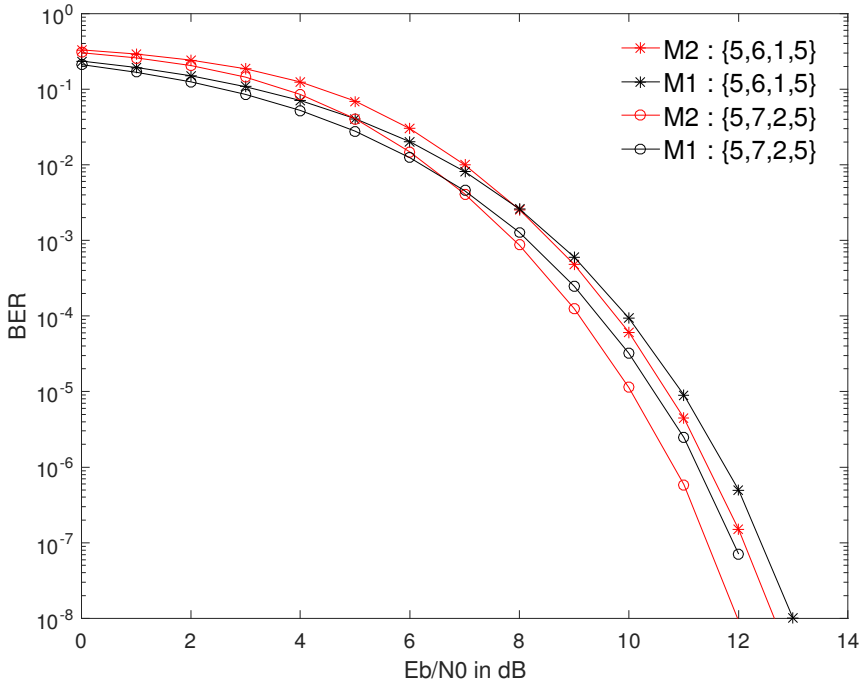

Figure 4.13: BER vs. E_b/N_0 performance comparison of the Methodology 1 with Methodology 2 in Mica2.

The energy efficiency is higher in Methodology 2 compared to Methodology 1 for all code characterizations, as can be inferred from Fig. 4.14. This reduced energy consumption is due to the simplified operations and improved compression, making the energy values per information bit less. The characterizations M2{30, 7, 2, 5} and M2{30, 8, 2, 6} have 17.55% and 22.09% energy reduction respectively compared to M1{30, 7, 2, 5} and M1{30, 8, 2, 6}, while M2{30, 6, 1, 5}, M2{30, 7, 1, 6}, and M2{30, 8, 1, 7} have about 7.78%, 7.54%, and 7.55% energy reduction compared to their M1 counterparts.

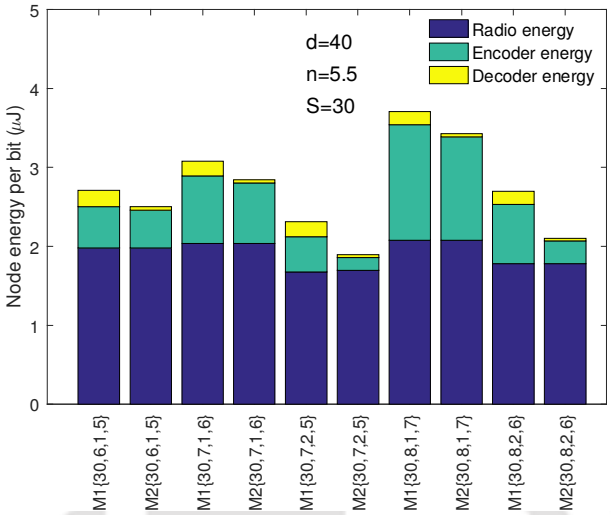

Figure 4.14: Energy comparison of Methodology 2 and Methodology 1 in Mica2.

4.5.2 MicaZ Platform

4.5.2.1 BER Performance and Compression

The BER performance achieved is depicted, and compression achieved is calculated in this section in the micaZ platform and AWGN channel condition. The presented methodology with $d_{min} = 3$ within each group is studied, and the performance is compared with the uncoded transmission, standard error correction schemes, Hamming (7, 4) and RS (31, 29), and the Methodology 1.

The methodology is studied, and the results are shown in Fig. 4.15 for the cases $\mathscr{R}_{k_m k_1 k_2} := [\{5,\ 7,\ 2,\ 5\},\ \{10,\ 7,\ 2,\ 5\}, \{30,\ 7,\ 2,\ 5\}]$, where k_m, k_1, and k_2 values are fixed at 7, 2, and 5, respectively, to observe the consequence of variation in S on BER and compression. The results are also compared with the uncoded transmission, Hamming (7, 4) code, and RS (31, 29) code, in the same circumstances. At a BER=10^{-5}, the CG achieved by Hamming (7,4) is 0.561 dB, with a redundancy of 75%. RS (31, 29) code posses a CG of 1.068 dB and redundancy of 6.9%. However, our code achieves compression in place of redundancy. The CG and compression pair attained by the proposed scheme is (3.739 dB, 14.29%) for $S = 5$; (4.181 dB, 21.43%) for $S = 10$; and (4.328 dB, 26.19%) for $S = 30$. An increase in S raises the CG and compression while other parameters are fixed.

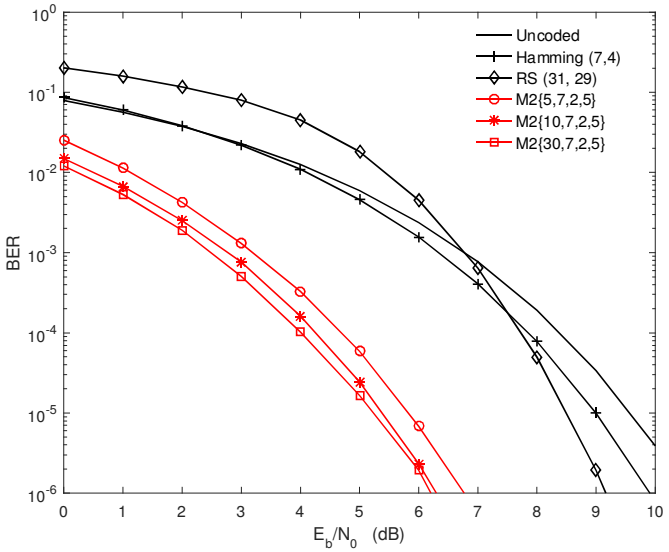

Figure 4.15: BER vs. E_b/N_0 performance of the Methodology 2 for $\mathscr{R}_{k_m k_1 k_2}$, uncoded, Hamming, and RS in MicaZ.

The effect of varying code parameters other than S, fixed at 10, for the cases in $\mathscr{R}_S := [\{10,\ 6,\ 1,\ 5\}, \{10,\ 7,\ 1,\ 6\}, \{10,\ 7,\ 2,\ 5\}, \{10,\ 8,\ 1,\ 7\}, \{10,\ 8,\ 2,\ 6\}]$ is studied and plotted in Fig. 4.16. The improvement in grouping efficiency with an increase in k_m and k_1 values and fixed k_2 brings better BER performance. The same effect can be noticed when k_m is fixed and k_1 increases. Nevertheless, an increase in k_2 with fixed k_m reduces the grouping efficiency and hence, brings the performance down marginally.

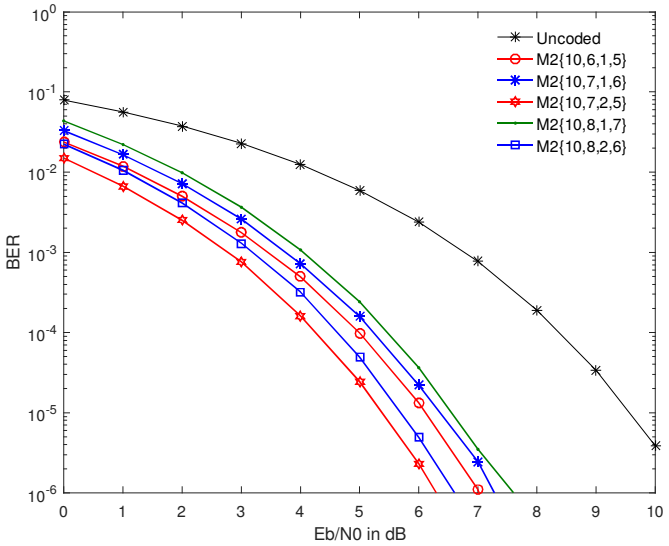

Figure 4.16: BER vs. E_b/N_0 performance of the Methodology 2 for the instances of $\mathscr{R}_S$ in MicaZ.

Fig. 4.17 compares the theoretical and simulated BER performance. The equations described in Section 4.3.1 are used to obtain the upper bound, lower bound, and actual theoretical BER curves. The equivalence of the simulated and theoretical curves affirms the integrity of the scheme.

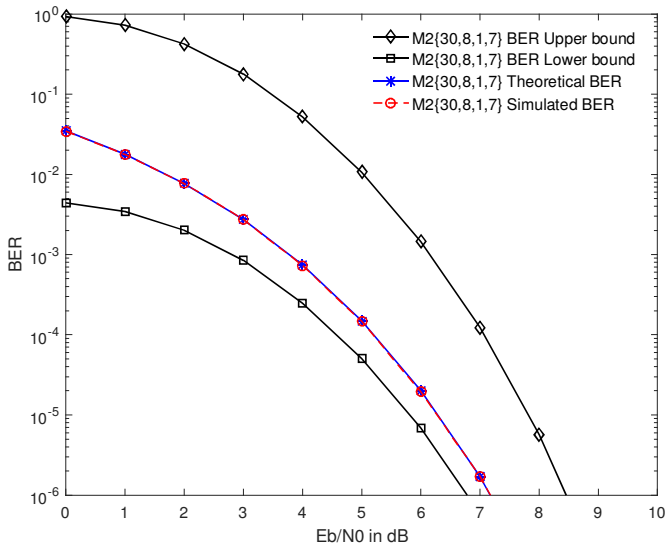

Figure 4.17: Theoretical, simulated, upper bound, and lower bound BER of M2 {30, 8, 1, 7} in AWGN channel and MicaZ platform.

4.5.2.2 Energy Efficiency

Effect of various code parameters on Node Energy: The node energies for a fixed S and changing k_m, k_1, and k_2 are plotted in Fig. 4.18 and Fig. 4.19, for achieving a BER of 10^{-5}, at distance=40 meter, $S = 30$, and $n = 5.5$. The radio energies are analytically quantified, and the computation energy is estimated by simulation in the former figure. All energies are obtained through simulation using AVRORA in the latter figure. The slight decrease in the theoretical values accounts for the approximation we have done while calculating the transceiver circuit power. It is inferred from Fig. 4.18 and Fig. 4.19 that the proposed methodology with characterizations {30, 6, 1, 5}, {30, 7, 2, 5}, and {30, 8, 2, 6} outperforms Hamming (7, 4) code and RS (31, 29) code in energy efficiency. For instance, from Fig. 4.18 a decrease of 4%, 42.92%, and 28.24% in total energy consumption is visualized for M2{30, 6, 1, 5}, M2{30, 7, 2, 5}, and M2{30, 8, 2, 6}, respectively in comparison with uncoded transmission, while Hamming (7,4) and RS (31, 29) codes expend 54.76% and 15.64% more energy compared with the uncoded transmission. The characterization {30, 7, 1, 6} and {30, 8, 1, 7} falls behind the standard schemes in energy efficiency, though it is better in BER

performance. Thus it is deduced that an appropriate choice of code parameters can deliver higher energy efficiency, CG, and compression.

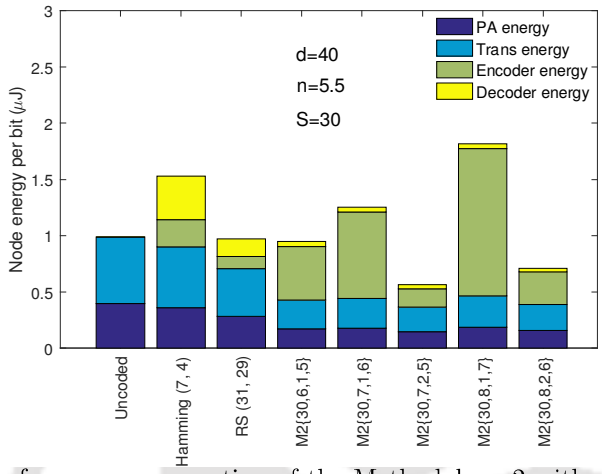

Figure 4.18: Comparison of energy consumption of the Methodology 2 with standard codes and uncoded in MicaZ, Radio energy computed theoretically.

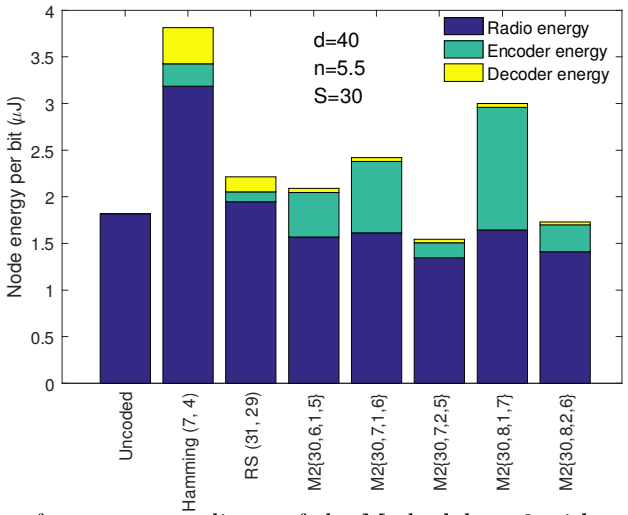

Figure 4.19: Comparison of energy expenditure of the Methodology 2 with standard codes and uncoded in MicaZ.

The result of using different S values in energy efficiency is plotted in Fig. 4.20, for a distance of 40 meters, and a path loss exponent of 5.5. The energy efficiency keeps increasing with increasing S value, as a higher number of data-blocks in a codeword raises CG and compression and reduces the computations per bit. The characterization $\{S,\ 7,\ 2,\ 5\}$ achieves 10.29% saving in total energy consumption when $S = 5$, 17.17% saving when $S = 10$, and 42.92% saving when $S = 30$.

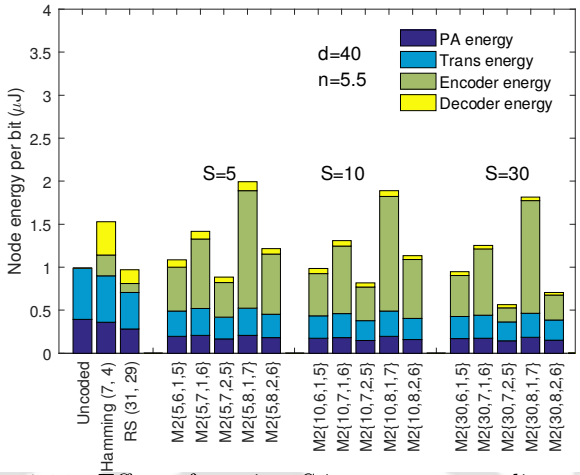

Figure 4.20: Effect of varying S in energy expenditure in MicaZ.

The energy efficiency is increasing with S, and to collect data for larger S will have increased latency, especially for real-time data transfer. In case of all combinations equiprobable (which is the worst case in terms of latency), it will take $T_c = (k_m S\text{number of groups})/\text{data rate}$. In addition, there would be some time to run the algorithm (T_a), but as most of the tasks, like checking to which group it belongs to, etc., are lookup table based it will not consume significant time. This can be estimated using the simulator AVRORA. In the case of a very large S, the latency will be dominated by T_c. The T_a and T_c are estimated in Table 4.1 for the particular case of M2 $\{S,\ 7,\ 2,\ 5\}$.

Table 4.1: Latency Estimate

S	T_c (for data rate=20kbps)	T_c (for data rate=250kbps)	T_a (for encoding operation)	T_a (for decoding operation)
5	0.0140	0.0011	0.020019124348958	0.003133680555555
10	0.0280	0.0022	0.038855929904513	0.004717881944444
30	0.0840	0.0067	0.047989637586805	0.0110546875
100	0.2800	0.0224	0.37796875	0.034798177083333

Effect of various channel parameters on Node Energy: The consequence of different channel parameters on the energy efficiency of the scheme is studied in this section. With longer distances, the bit error increases, and a channel coding scheme comes to be more significant. As a result, the energy-saving by the coding scheme becomes more significant, as shown in Fig. 4.21. The same is the

case with the path loss exponent. The less clear the environment more the need for an error correction scheme and the higher the energy-saving, as depicted in Fig. 4.22.

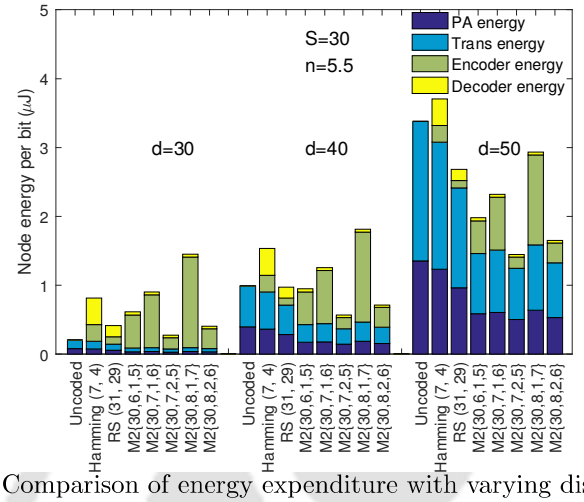

Figure 4.21: Comparison of energy expenditure with varying distances in MicaZ.

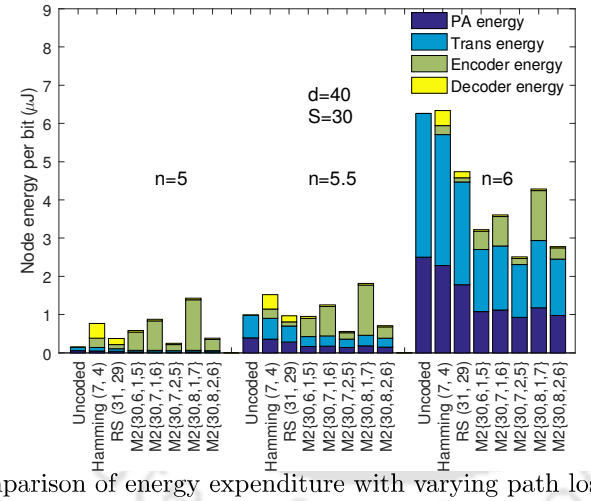

Figure 4.22: Comparison of energy expenditure with varying path loss exponent in MicaZ.

4.5.2.3 Comparison with Methodology 1:

The BER performance comparison of the proposed methodology M2 with the previous methodology M1 in the {5, 7, 2, 5} and {30, 7, 2, 5} cases are studied and graphed in Fig. 4.23 in AWGN channel condition. It can be inferred from the figure that M2 excels M1 in BER performance. M2 also outperforms M1 in compression, specifically 14.29% of compression is achieved by M2{5, 7, 2, 5}, while zero compression/redundancy is achieved by M1{5, 7, 2, 5}.

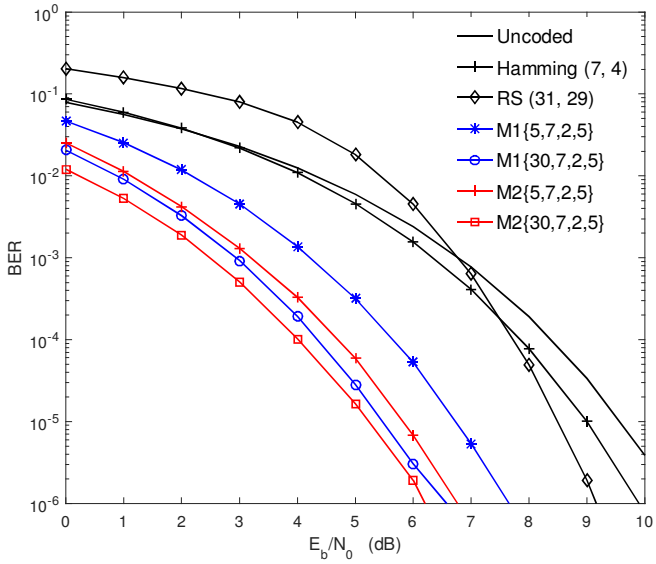

Figure 4.23: BER vs. E_b/N_0 performance comparison of Methodology 1 and 2 in MicaZ platform and AWGN channel.

The energy efficiency of the proposed methodology is found to be improved compared with that of the previous methodology in Fig. 4.24. The node energy expended per bit is less in the case of M2 compared to the case of M1 for each of the characterizations. As a representative case, M2{30, 8, 2, 6} has 46.46% saving in energy compared to M1{30, 8, 2, 6}. The freedom from exclusive LABEL decoding and its influence in SYMBOL decoding have played a major role in reducing energy consumption.

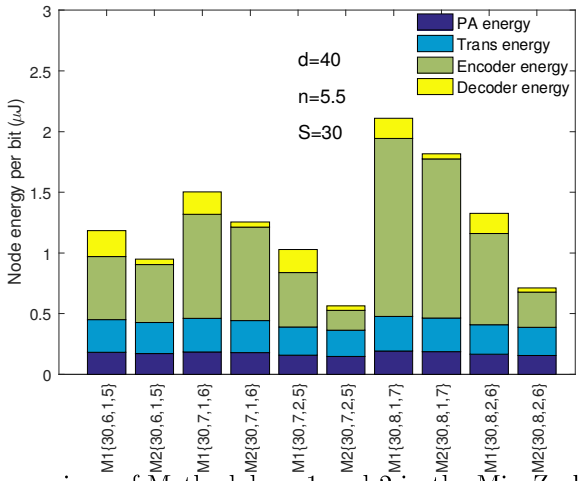

Figure 4.24: Energy comparison of Methodology 1 and 2 in the MicaZ platform and AWGN channel.

4.5.3 Results for Higher d_{min} among Group Members

The scheme expanded to have a $d_{min} = 5$ within each group is also designed and evaluated in the context of MicaZ and Mica2 motes. The BER performance of $\{S,\ 6,\ 1,\ 5\}$ with $d_{min} = 5$ for various S values are compared with the uncoded and RS (31, 27) scheme in Fig. 4.25. This comparison is exercised because RS (31, 27) also has a minimum distance of 5, which results in two symbols of error correction per codeword.

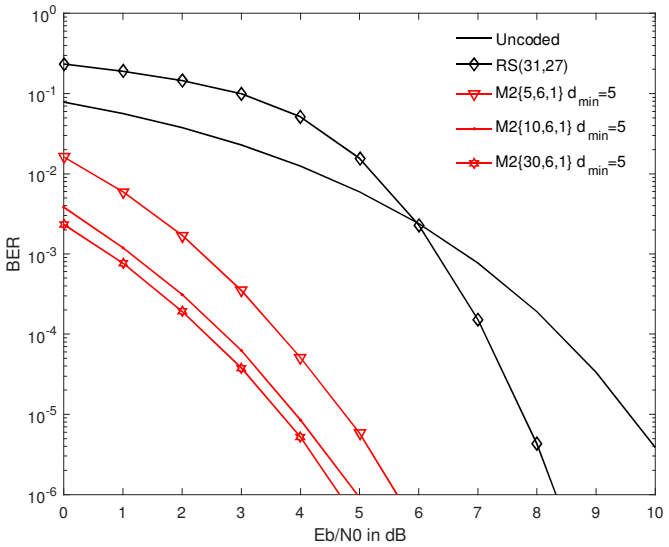

Figure 4.25: BER vs. E_b/N_0 performance of the Methodology 2 with $d_{min} = 5$, uncoded, and RS in MicaZ.

The results of Methodology 2 redesigned and studied for 2-bit error correction per data block scenario are compared with those of 1-bit error correction per data block scenario and are found improved, as shown in Fig. 4.26. The results affirm that the scheme can be refined with varying parameters to enhance the performance.

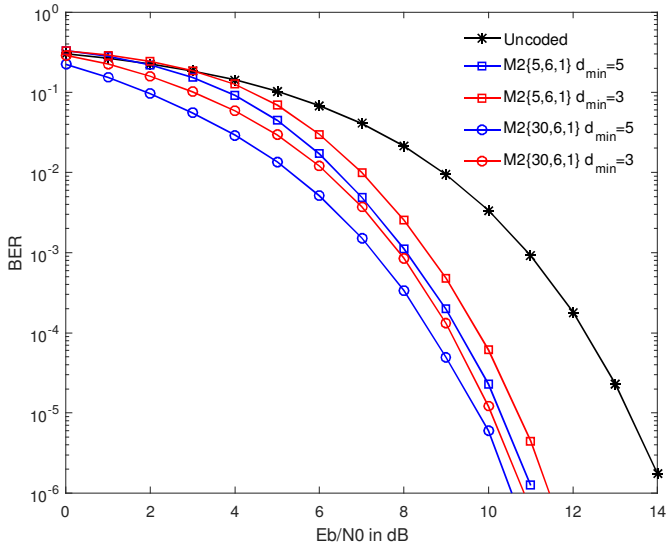

Figure 4.26: BER vs. E_b/N_0 performance comparison of the Methodology 2 with $d_{min} = 3$ and $d_{min} = 5$ in Mica2.

The energy efficiency of the expanded scheme for $\{S,\ 6,\ 1,\ 5\}$ with $d_{min} = 5$ for various S values is studied in the same platforms and compared with uncoded and RS (31, 27) scheme in Fig 4.27. It is observed that the scheme is energy efficient compared to uncoded and RS (31, 27). RS (31, 27) is selected here for comparison, as its d_{min} is also 5.

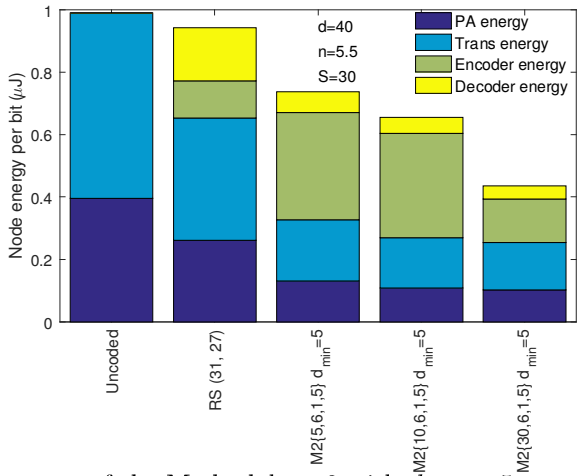

Figure 4.27: Energy performance of the Methodology 2 with $d_{min} = 5$ compared with uncoded and RS (31, 27) in MicaZ.

The 2-bit error correction per block scheme is more energy efficient compared to its 1-bit error counterpart, besides its improvement in BER performance, as is evident from Fig. 4.28. Hence, it is

deduced that the methodology performs better with higher d_{min} value.

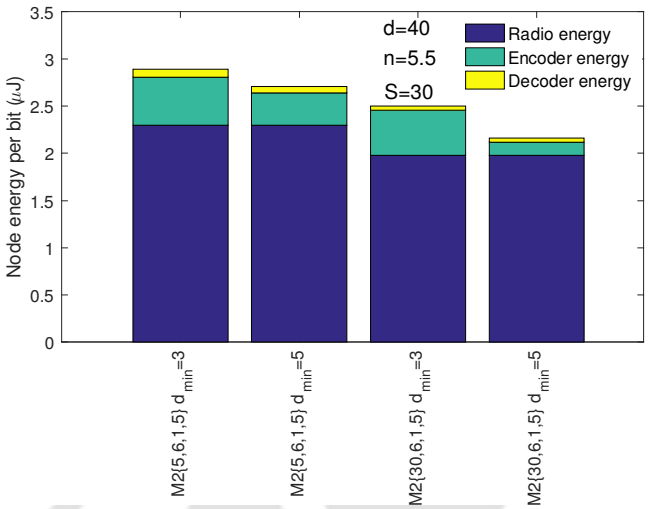

Figure 4.28: Energy comparison 2-bit and 1-bit error correction per block schemes of Methodology 2 in Mica2

4.5.4 Comparison with Conventional Source plus Channel Encoding Schemes

To compare the performance of the scheme with the combined effect of conventional source and channel encoding, two lossless source encoding schemes in combination with RS (31, 29) are considered; Huffman encoding and Run-length encoding (RLE). Huffman being the optimal encoding and RLE being the simplest one. The proposed methodology is compared with Huffman +RS, RLE +RS schemes in Fig. 4.29 and Fig. 4.30. From the figures, it can be observed that the proposed scheme is further better performing in terms of energy efficiency because of the additional energy expended for source encoding. Here, it should be noted that source decoder (decompression) energy has not been plotted, which will be an additional energy overhead. It is evident that in Huffman encoding compression achieved is more, hence the reduced radio energy, but the encoding energy consumption is more compared to RLE. It is also inferred from the plots that compression in data is achieved at the expense of computation energy in the case of standard compression techniques. In contrast, the compression is achieved in the proposed scheme with no additional energy requirement.

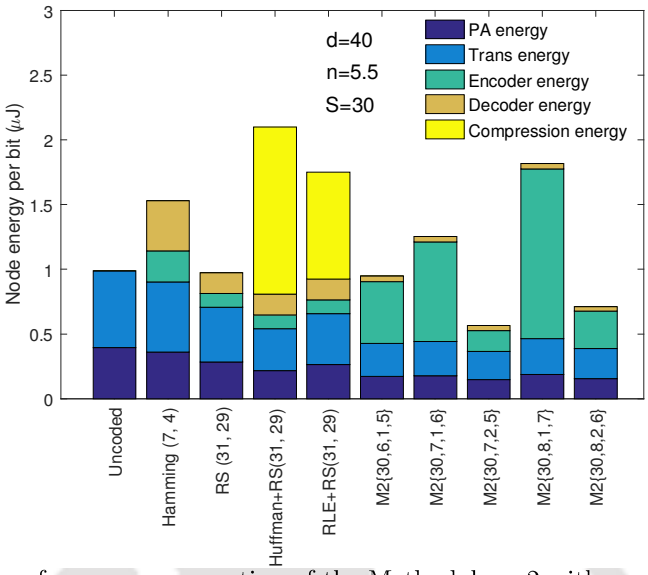

Figure 4.29: Comparison of energy consumption of the Methodology 2 with conventional source and channel codes combined and uncoded, Radio energy computed theoretically.

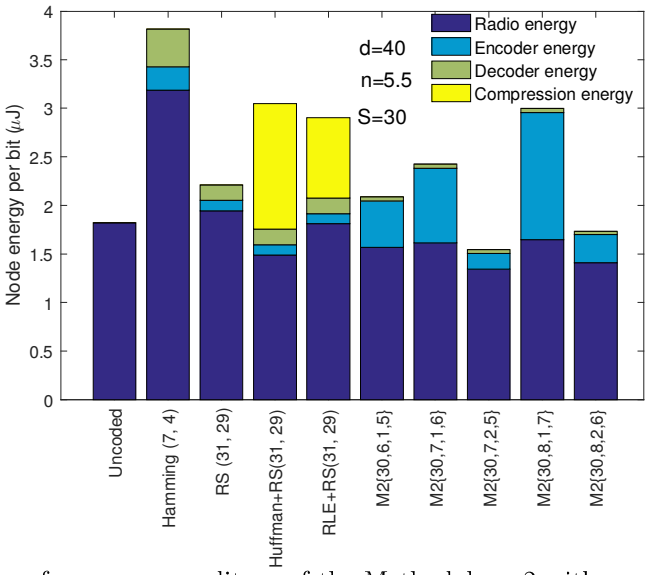

Figure 4.30: Comparison of energy expenditure of the Methodology 2 with conventional source and channel codes combined and uncoded.

In addition, our proposed scheme is orthogonal to the source compression scheme. Similar to the source encoding + RS/Hamming, we can apply source encoding + proposed scheme as well. And the relative difference in energy consumption will remain unchanged.

4.6 Conclusions

Methodology 1 from Chapter 3 is reinforced with a new methodology, Methodology 2, which provides better CG, compression, and energy efficiency in this chapter. The new methodology is studied and simulated for various simulation parameters and further compared with Methodology 1. A noteworthy raise in compression from 14.29% for M1 {10, 7, 2, 5} to 21.42% for M2{10, 7, 2, 5} and a significant increase in CG from 3.46 dB to 4.18 dB at BER of 10^{-5} can be observed in AWGN channel and Mica2 platform. Energy efficiency is also higher for Methodology 2. The method is compared with standard codes such as RS (31, 29) and Hamming (7, 4), and significantly higher performance is noted. Enhancing grouping with a higher d_{min} further improved the scheme with increased CG and better energy efficiency. The methodology is also compared with the conventional source and channel encoding schemes combined to find a more pronounced gain in energy efficiency.

In the next chapter, the scheme's effectiveness in a more realistic environment is investigated. A Rayleigh fading channel is considered, and both methodologies of the scheme are evaluated for the environment.

5

Methodology I and II in Rayleigh Channel

Contents

5.1	Introduction	86
5.2	Performance Evaluation Framework	86
5.3	Simulation Parameters	87
5.4	Performance Analysis of Methodology 1 in Rayleigh Channel	87
5.5	Performance Analysis of Methodology 2 in Rayleigh Channel	93
5.6	Performance Comparison of Methodology 1 and 2 in Rayleigh Channel	99
5.7	Conclusions	100

5.1 Introduction

The analysis of any communication scheme calls for the modeling of the channel used. The wireless channels are complex, and hence some stochastic models are usually used. In the previous chapters, we used the simplest model, the AWGN model, for the analysis of Methodology 1 and Methodology 2. The reason is to lighten the theoretical analysis. However, this model is not befitting for time-varying channels like fading channels. The WSNs use a small transmission power [119], which implies a short-range, and we can assume a changing environment and immobile nodes. Hence, the RMS delay spread is very low compared to symbol durations. Also, the data rates are not high. Then the channels can be assumed to be frequency nonselective fading channels [68]. For this reason, models specifically used for frequency-nonselective fading channels [120, 121] are appropriate for WSNs. Rayleigh fading model is one of the most popular models. In this chapter, we analyze the suitability of our scheme in the Rayleigh channel conditions. Both Methodology 1 and 2 are studied here rigorously.

5.2 Performance Evaluation Framework

Proposed methodologies are analyzed in the context of the Mica2 mote to study the performance in Rayleigh channel conditions.

5.2.1 BER Performance

Methodology 1: The channel transition probability p of Rayleigh channel when NCBFSK modulation is employed is given by the mathematical formula mentioned below [122]

$$p = \frac{1}{2 + \frac{E_b}{N_0}}. \tag{5.1}$$

The value of p is used in equations (3.3) and (3.4) to find the block and bit error probabilities of LABEL and SYMBOLs of a codeword. The error probability of codeword is determined by (3.7). The upper and lower limits of BER are calculated using equations (3.8) and (3.9).

Methodology 2: The channel transition probability equation (5.1) and the equations from Section 4.3.1 are being used to calculate the error probabilities, lower and upper limits of error probabilities of a Methodology 2 codeword.

5.2.2 Energy Efficiency

The theoretical and experimental analysis of energy efficiency is performed with the metric 'energy consumption per information bit required to achieve a specific value of BER'. The energy model used is the same as in the previous chapters and can be referred from Section 3.4.

5.3 Simulation Parameters

The methodologies are simulated for the Mica2 mote. The simulation is carried out for varying code and channel parameters. The code parameters are shown in Table 3.1, and channel parameters are shown in Table 3.2. The CG and energy efficiency are analyzed and compared for an error probability of 10^{-3}. The characterization simulated are shown in the following sets,

$$\mathscr{R}_{k_m k_1 k_2} := [\{5,7,2,5\},\ \{10,7,2,5\},\{30,7,2,5\}]$$

$$\mathscr{R}_{Sk_2} := [\{10,6,1,5\},\ \{10,7,2,5\},\{10,8,3,5\}]$$

$$\mathscr{R}_{Sk_m} := [\{10,8,1,7\},\ \{10,8,2,6\},\{10,8,3,5\}]$$

$$\mathscr{R}_{Sk_1} := [\{10,6,1,5\},\ \{10,7,1,6\},\{10,8,1,7\}]$$

where, $\mathscr{R}_{k_m k_1 k_2}$ denote the cases considered for simulation purposes with fixed k_2, k_m, and k_1 and varying S, and $\mathscr{R}_{Sk_2}$, $\mathscr{R}_{Sk_m}$, and $\mathscr{R}_{Sk_1}$ denote the cases considered for simulation purposes with fixed $S = 10$, and k_2, k_m, and k_1 fixed, respectively.

5.4 Performance Analysis of Methodology 1 in Rayleigh Channel

5.4.1 BER Performance and Compression

The performance of Methodology 1 in the Mica2 platform and Rayleigh channel for varying S values is studied by keeping the values of k_2, k_m, and k_1 fixed. Fig. 5.1 shows this effect of S for $k_m = 7$, $k_1 = 2$, and $k_2 = 5$, i.e., the cases contained in $\mathscr{R}_{k_m k_1 k_2}$, and the performance of the uncoded transmission, Hamming (7, 4) code, and RS (31, 29) code. It is observed that the CG increases as S increases. The CG achieved at a BER=10^{-3} is 10.66 dB for $S = 5$; 11.44 dB for $S = 10$; and 11.86 dB for $S = 30$. The CG of Hamming (7,4) and RS (31, 29) codes are 7.97 dB and 1.18 dB, respectively. The compression is calculated in Chapter 3; the values remain the same here.

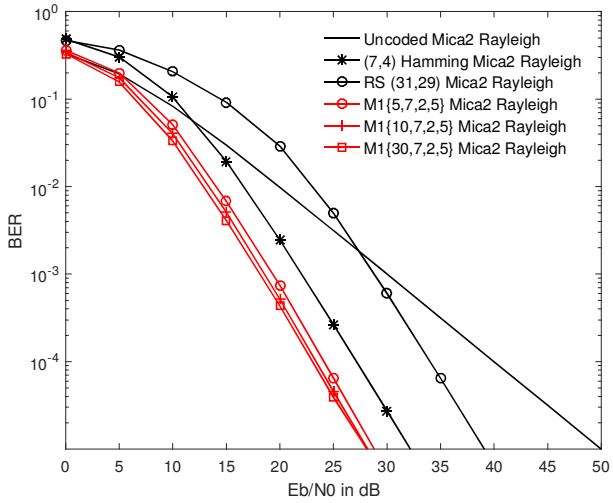

Figure 5.1: BER vs. E_b/N_0 performance of the uncoded, Hamming, RS, and M1 $\{S,\ 7,\ 2,\ 5\}$ with $S =$ 5, 10, and 30 in Mica2 platform and Rayleigh fading channel.

Fig. 5.2 compares the theoretical and simulated BER performance. The figure plots the upper and lower limits of theoretical error probability along with the simulated and theoretical bit error probability. The simulated plot is validated with the comparison with theoretical plots.

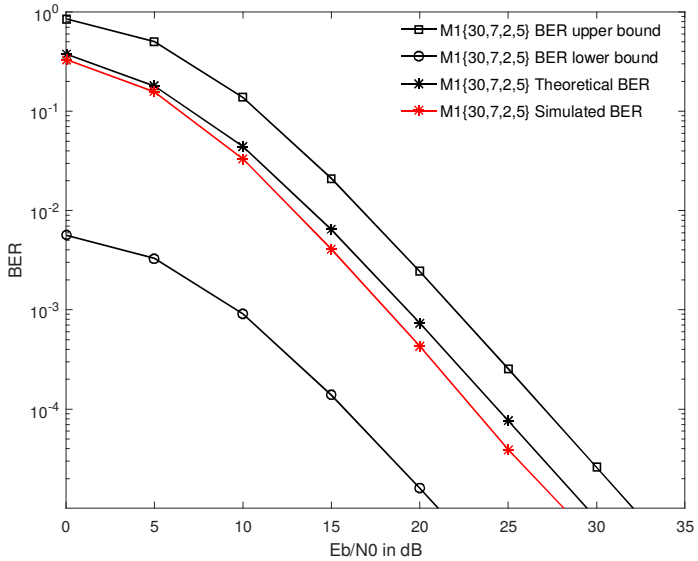

Figure 5.2: Theoretical, simulation, upper bound, and lower bound BER of M1 $\{30,\ 7,\ 2,\ 5\}$ in Mica2 platform and Rayleigh fading channel.

As expected from the result analysis in previous chapters, the CG and compression are found increasing with k_m and k_1, while k_2 is fixed in Fig 5.3. The cases considered are contained in $\mathscr{R}_{Sk_2}$.

The CG obtained for a fixed $k_2 = 5$, is 11.11 dB for $k_m = 6$, 11.44 dB for $k_m = 7$, and 11.68 dB for $k_m = 8$ and the compression achieved is 3.33%, 14.2857%, and 23.75% respectively. This improvement is caused by the betterment of grouping efficiency with increasing k_m and k_1 values.

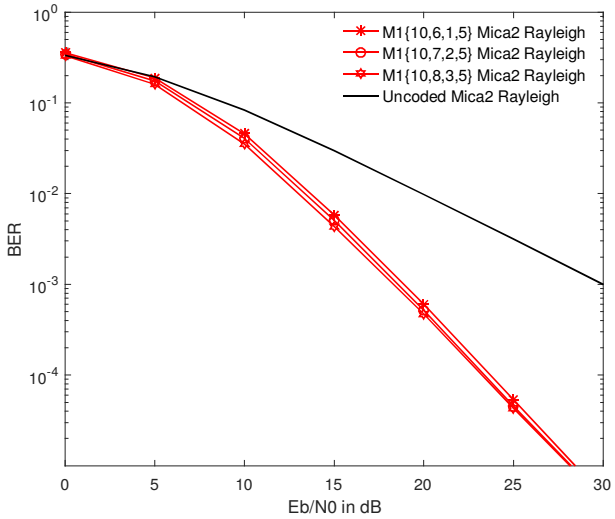

Figure 5.3: BER vs. E_b/N_0 performance of Methodology 1 for cases contained in $\mathscr{R}_{k_2}$ in Mica2 platform and Rayleigh fading channel.

A similar result can be found with fixed k_m and varying k_1 and k_2, as in the cases of $\mathscr{R}_{Sk_m}$, in Fig. 5.4. The CG and compression improves with increasing k_1 and fixed k_m. The CG, compression pair achieved is (10.53 dB, 0%) for $k_1 = 1$, (11.21 dB, 12.5%) for $k_1 = 2$, and (11.68 dB, 23.75%) for $k_1 = 3$.

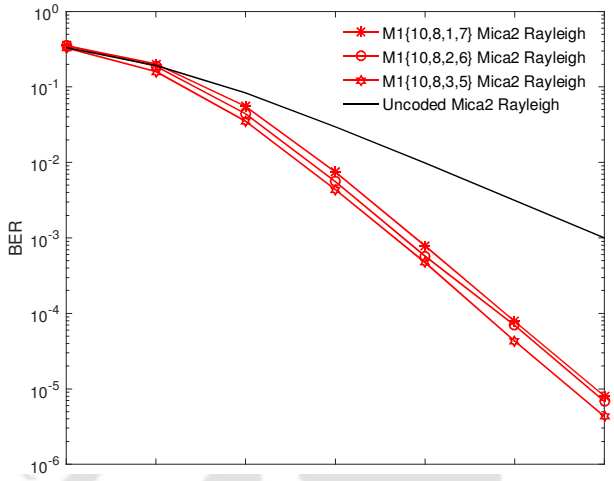

Figure 5.4: BER vs. E_b/N_0 performance of Methodology 1 for cases encompassed in $\mathscr{R}_{k_m}$ in Mica2 platform and Rayleigh fading channel.

The cases in $\mathscr{R}_{Sk_1}$, where k_1 is fixed, and k_m and k_2 are varying, shows reducing grouping efficiency with increasing k_m and k_2 values. The resulting plot is shown in Fig. 5.5. The CG obtained are 11.11 dB for $k_m = 6$, 10.82 dB for $k_m = 7$, and 10.53 dB for $k_m = 8$ and the compression gained are 3.33%, 2.8571%, and 0% respectively.

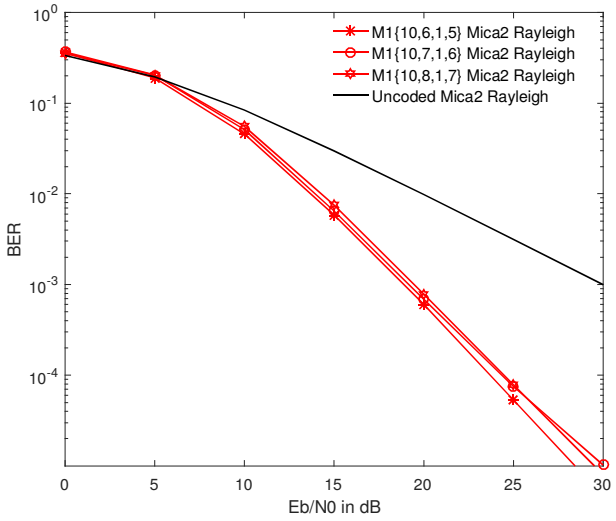

Figure 5.5: BER vs. E_b/N_0 performance of Methodology 1 for cases contained in $\mathscr{R}_{k_1}$ in Mica2 platform and Rayleigh fading channel.

5.4.2 Energy Efficiency

The radio and computation energies are plotted in this section for the energy efficiency comparison of the schemes.

Effect of various code parameters on Node Energy: Fig. 5.6 represents the effect of varying k_m, k_1, and k_2 values with a fixed S on energy efficiency. The channel parameters were set at distance=25 meter, S=30, and n=3.5. At a BER of 10^{-3}, Methodology 1 with characterizations {30, 6, 1, 5}, {30, 7, 2, 5}, and {30, 8, 3, 5} are energy efficient compared to uncoded, Hamming (7, 4) code, and RS (31, 29) code. All the schemes except M1{30, 8, 1, 7} are energy efficient compared to uncoded and RS (31, 29) code. Though the characterization M1 {30, 8, 1, 7} is not better in energy efficiency compared to the standard schemes, its BER performance is better comparatively. It is hence deduced that we can achieve higher CG, compression, and energy efficiency by the proper selection of code parameters. The percentage of energy efficiency improvement of the scheme M1{30, 7, 2, 5} is 41.45% compared to uncoded, 13.18% compared to Hamming (7, 4) code, and 44.96% compared to RS (31, 29) code.

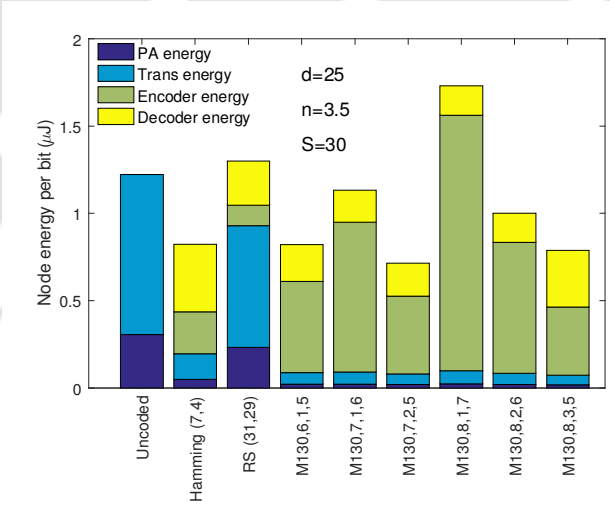

Figure 5.6: Comparison of energy expenditure of Methodology 1 with standard codes and uncoded in Mica2 platform and Rayleigh fading channel.

As anticipated, the energy efficiency is found to increase with increasing S in Fig. 5.7. The figure is plotted with channel parameters fixed at distance=25 meter and n=5. The reduced energy consumption is because of the increased number of SYMBOLs in each codeword, which improves CG and compression and decreases the number of calculations per information bit.

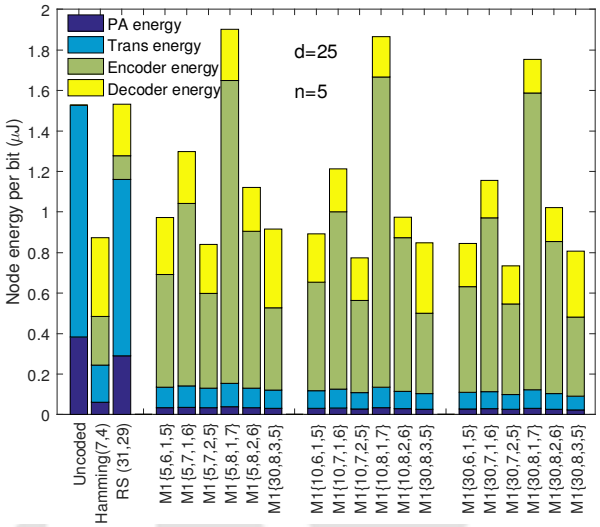

Figure 5.7: Effect of varying S in energy expenditure of Methodology 1 in Mica2 platform and Rayleigh fading channel.

Effect of various channel parameters on Node Energy: The channel parameters such as distance and path loss exponent are varied, and the impact of the same in energy efficiency is studied and plotted in Fig. 5.8 and Fig. 5.9 respectively. The amount of energy saved is higher for higher distance and path loss exponent, as is deducted from the figures.

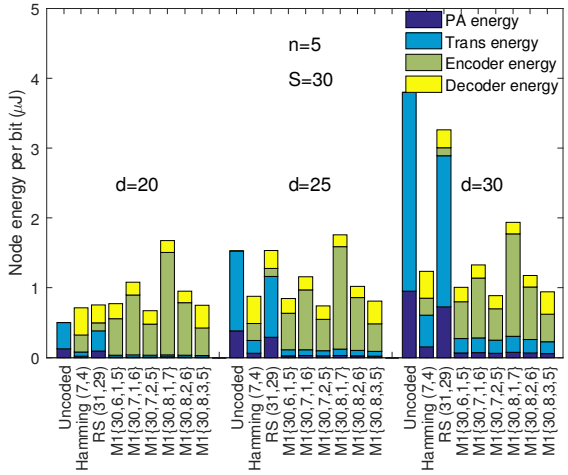

Figure 5.8: Energy comparison of Methodology 1 for different distances in Mica2 platform and Rayleigh fading channel.

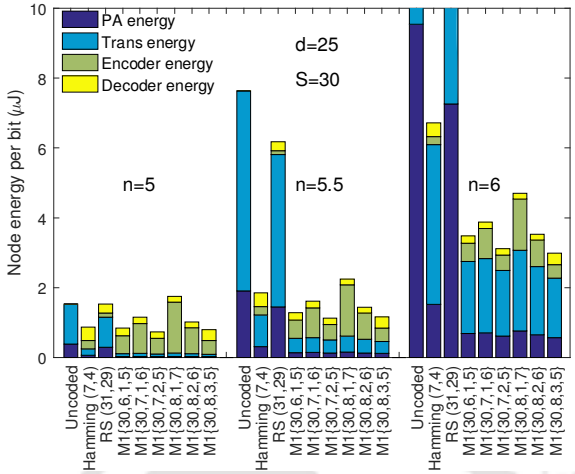

Figure 5.9: Energy comparison of Methodology 1 for different pathloss exponent in Mica2 platform and Rayleigh fading channel.

5.5 Performance Analysis of Methodology 2 in Rayleigh Channel

5.5.1 BER Performance and Compression

Fig. 5.10 shows the effect of varying S values on BER performance of the proposed scheme with other code parameters fixed at $k_m = 7$, $k_1 = 2$, and $k_2 = 5$ in the Mica2 sensor platform and Rayleigh channel. The figure also compares the scheme with the RS (31,29) code, Hamming (7,4) code, and uncoded transmission. The CG and compression achieved at a BER=10^{-3} is (12.46 dB, 14.29%) for $S = 5$; (12.95 dB, 21.43%) for $S = 10$; and (13.27 dB, 26.19%) for $S = 30$. The achievements are superior compared to the Hamming (7,4) code RS (31,29) code. The CG and compression are found to increase as S increases.

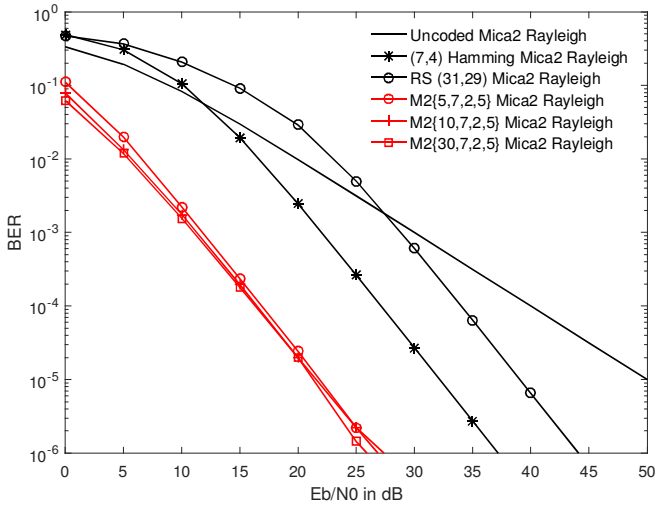

Figure 5.10: BER vs. E_b/N_0 performance of the uncoded, Hamming, RS, and M2 $\{S,\ 7,\ 2,\ 5\}$ with $S = 5,\ 10,$ and 30 in Mica2 platform and Rayleigh fading channel.

The BER performance of the scheme for varying k_m, k_1, and k_2 and fixed S is studied in Fig. 5.11, 5.12, and 5.13. The performance of the scheme with fixed k_2, gets better with an increase in k_m and k_1 values, as can be observed from Fig. 5.11, due to the improvement in grouping efficiency. Grouping efficiency enhances as there are more members in a group with a minimum distance constraint. When k_m is fixed, a similar increment can be observed with the increase in k_1 and decrease in k_2 as in Fig. 5.12. The increase in k_2 and k_m values with fixed k_1, however, reduces the grouping efficiency and hence performance.

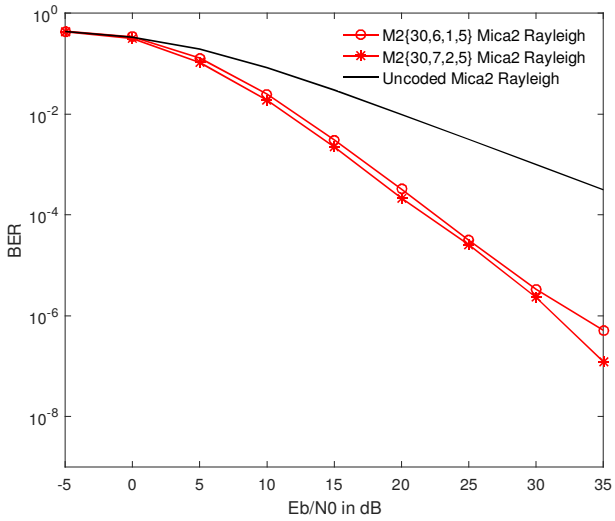

Figure 5.11: BER vs. E_b/N_0 performance of Methodology 2 for cases contained in $\mathscr{R}_{k_2}$ in Mica2 platform and Rayleigh fading channel.

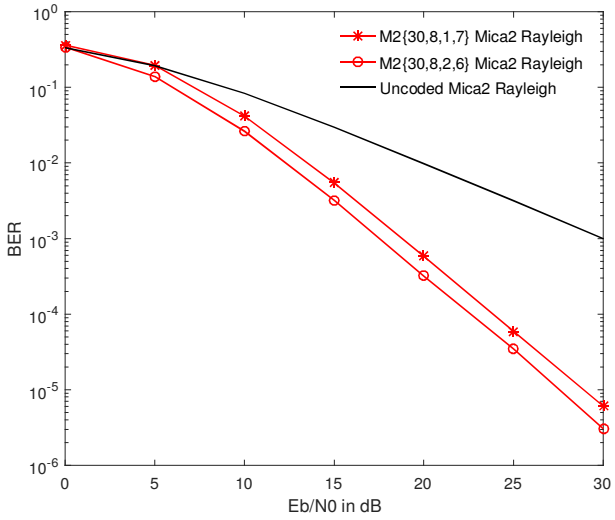

Figure 5.12: BER vs. E_b/N_0 performance of Methodology 2 for cases encompassed in $\mathscr{R}_{k_m}$ in Mica2 platform and Rayleigh fading channel.

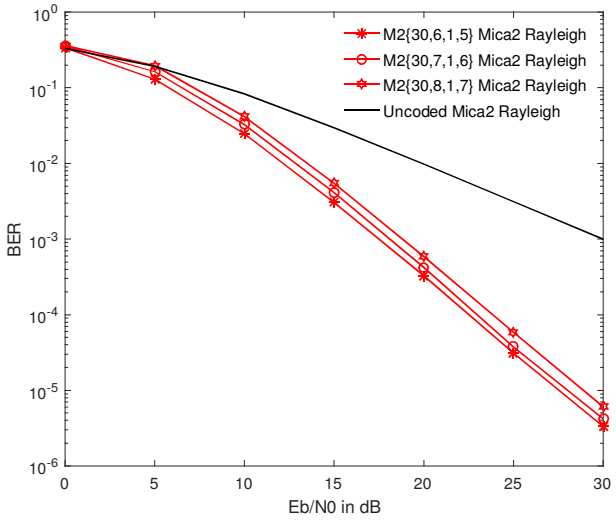

Figure 5.13: BER vs. E_b/N_0 performance of Methodology 2 for cases contained in $\mathscr{R}_{k_1}$ in Mica2 platform and Rayleigh fading channel.

The simulated BER performance is validated and compared with the theoretical plots in Fig. 5.14. The simulated graph well falls within the upper and lower limits and is analogous to the theoretical BER curve, hence proving the correctness of the scheme.

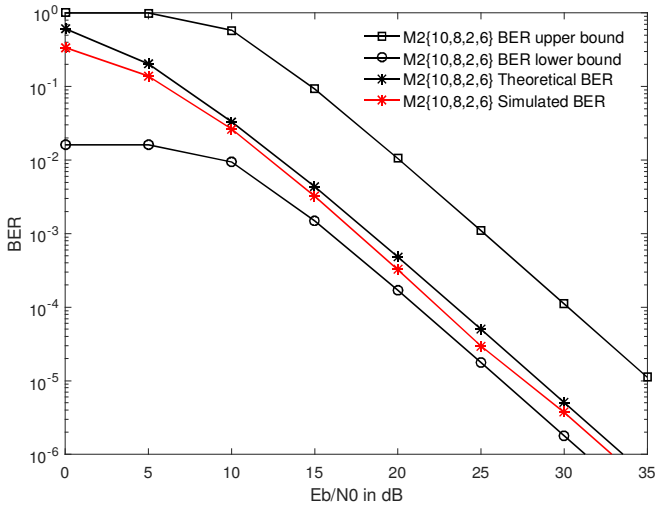

Figure 5.14: Theoretical, simulated, upper bound, and lower bound BER of M2 {10, 8, 2, 6} in Mica2 platform and Rayleigh fading channel.

5.5.2 Energy Efficiency

Effect of various code parameters on Node Energy: The energy analysis of the various characterization of Methodology 2 for distance=25 meter, $S = 30$, $n = 3.5$ is depicted in Fig. 5.15. The analysis is done at a BER of 10^{-3}. All characterizations except M2 $\{30,\ 8,\ 1,\ 7\}$ consume less energy compared to Uncoded, Hamming (7, 4) code, and RS (31, 29) code. The characterization M2 $\{30,\ 7,\ 2,\ 5\}$ is the best energy performer, which gives about 78.97% reduction in energy consumption compared to Uncoded, 68.81% reduction compared to Hamming (7,4), and 80.23% reduction compared to RS (31,29).

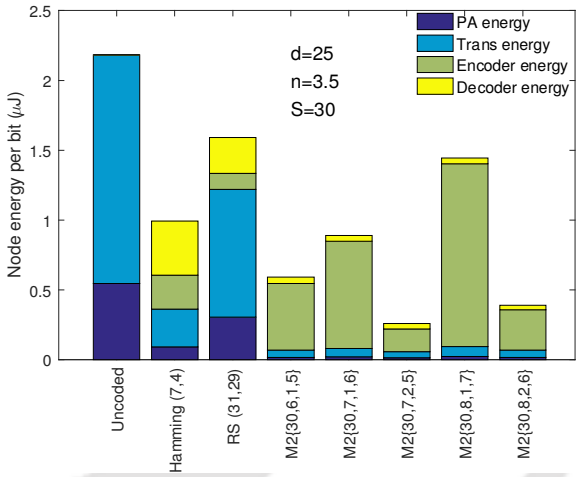

Figure 5.15: Comparison of energy expenditure of Methodology 2 with standard codes and uncoded in Mica2 platform and Rayleigh fading channel.

The energy consumption of the scheme for varying S values is depicted in Fig. 5.16 for a distance of 25 meters and a path loss exponent of 5. Energy efficiency improves with increasing S value. The characterization M2 $\{S,\ 7,\ 2,\ 5\}$ taken as an example gives energy saving in 63.62%, 66.03%, and 82.24% respectively for $S = 5$, $S = 10$, and $S = 30$.

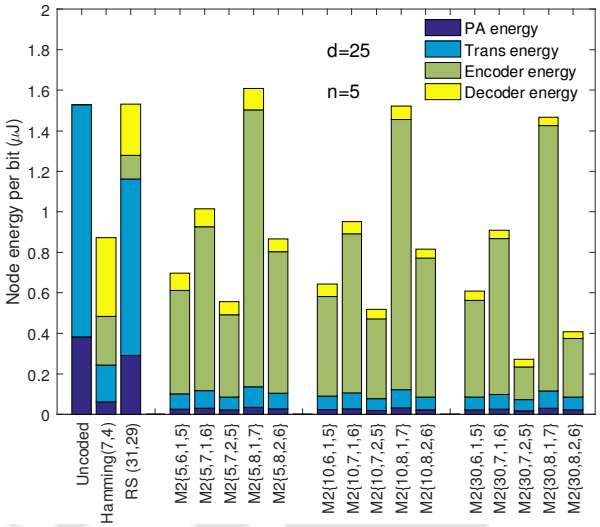

Figure 5.16: Effect of varying S in energy expenditure of Methodology 2 in Mica2 platform and Rayleigh fading channel.

Effect of various channel parameters on Node Energy: As the channel between transmitter and receiver becomes more difficult for communication, for instance, of higher distance or higher path loss exponent, the scheme's usage becomes more relevant, as is evident from Fig. 5.17 and 5.17.

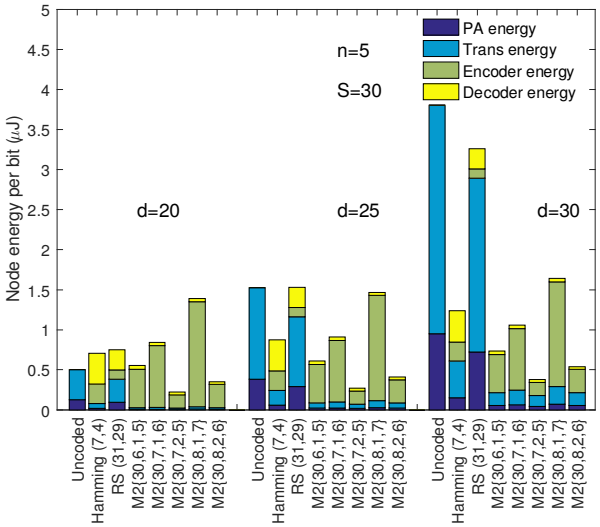

Figure 5.17: Energy comparison of Methodology 2 for different distances in Mica2 platform and Rayleigh fading channel.

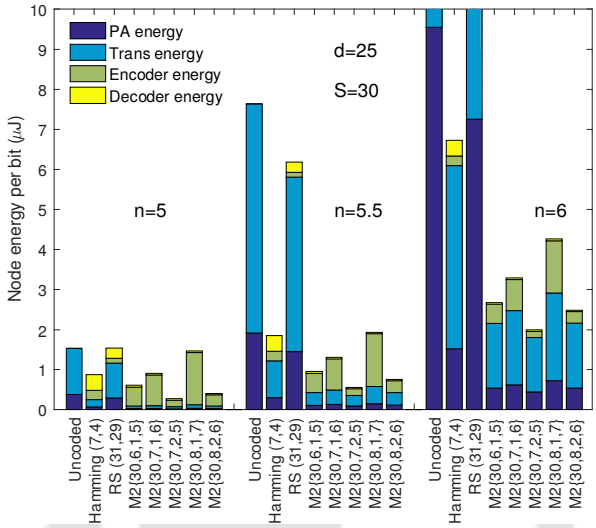

Figure 5.18: Energy comparison of Methodology 2 for different pathloss exponent in Mica2 platform and Rayleigh fading channel.

5.6 Performance Comparison of Methodology 1 and 2 in Rayleigh Channel

The two methodologies are compared in the context of the Rayleigh fading channel in this section, similar to the comparison in Chap. 4.6. The BER performance is compared in Fig. 5.19 and energy consumption is compared in Fig. 5.20. Analogous to the case of the AWGN channel, in the Rayleigh channel also Methodology 2 outperforms Methodology 1 in both BER performance and energy efficiency. Methodology 2 has 60.93% less energy expenditure compared to Methodology 1.

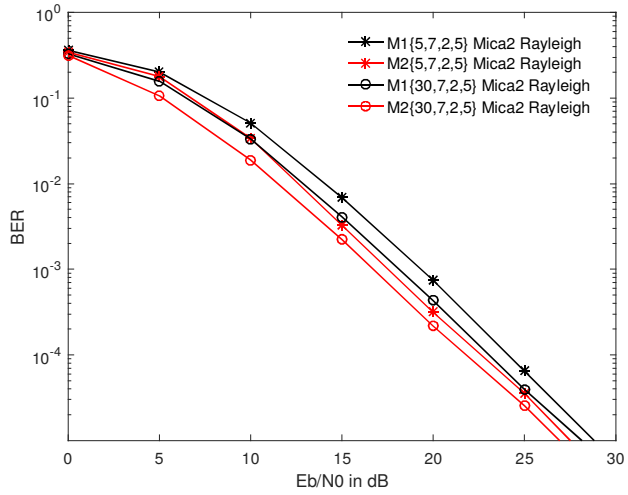

Figure 5.19: BER vs. E_b/N_0 performance comparison of Methodology 1 and 2 in Mica2 platform and Rayleigh channel.

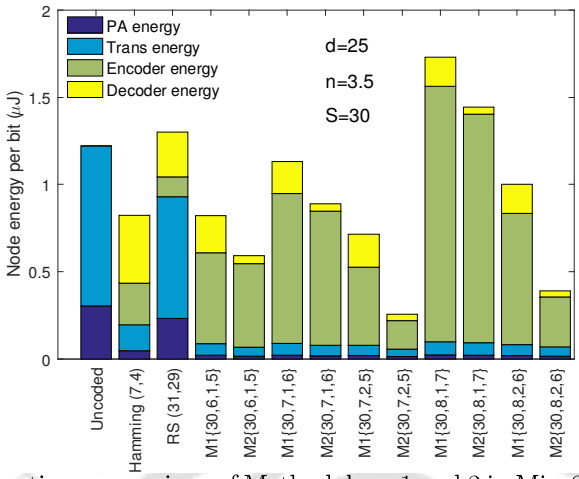

Figure 5.20: Energy consumption comparison of Methodology 1 and 2 in Mica2 platform and Rayleigh channel.

5.7 Conclusions

The methodologies proposed are analyzed and compared in Rayleigh channel conditions in order to study their usefulness in a fading environment. A fading channel is more realistic than the AWGN channel and hence needs to be studied. In line with the results obtained for the AWGN channel, methodologies perform better in CG and energy efficiency compared to uncoded and standard codes such as Hamming and RS. For instance, at a BER=10^{-3}, the characterization M1 {30, 7, 2, 5} achieves 11.86 dB CG and 23.81% compression and M2 {30, 7, 2, 5} achieves 13.27 dB CG and 26.19% compression . This achievement is compared with the 7.97 dB CG and 75% compression of Hamming (7,4) and 1.18 dB CG and 6.9% compression of RS (31, 29) codes. The improvement in energy efficiency of M1 {30, 7, 2, 5} is (41.45%, 13.18%, 44.96%) and of M2 {30, 7, 2, 5} is (78.97%, 68.81%, 80.23%) compared to uncoded, Hamming (7, 4) code, and RS (31, 29) code respectively. It is also inferred that M2 outperforms M1 in all aspects. M2 expends 60.93% less energy compared to M1.

The next chapter discusses the tradeoff of the scheme. An investigation is carried out for the methods to mitigate the scrambling that happens to the input data as a tradeoff to the pronounced achievements of the scheme.

6

Descrambling Methods

Contents

6.1	Introduction	102
6.2	Method 1: Delta Encoded Sequencing	102
6.3	Method 2: Successor Label Identification	103
6.4	Method 3: Successor Group Identification	105
6.5	Method 4: Predecessor Group Identification and Successor Group Identification	106
6.6	Conclusions	107

6.1 Introduction

The methodologies presented in the previous chapters provide us with significant achievements in terms of coding gain, compression, and less energy consumption. The tradeoff of these is the disorder occurring with the input data. The scheme is suitable for typical applications and constraints of WSNs rather than conventional networks. Typical applications of the WSNs include monitoring and surveillance, where the data from a time frame is used for further processing. The typical constraints include the scarcity of memory and energy stored and long battery life requirements. In many WSN applications, this sequence disorder for a short period is not a major concern. E.g., is an application in which the temperature of a room is monitored, and the values in a time frame are averaged out (or the peak value is found) at the receiver. Here, a sequence disorder in the codeword is not going to harm the credibility of the monitoring system. However, there are applications in which this sequence disorder matters, and we in this chapter make an effort to address this concern.

6.2 Method 1: Delta Encoded Sequencing

The first and most apparent attempt made is to include sequence numbers of each input message along with its corresponding SYMBOL in the codeword. The sequence numbers for a fixed amount of data are used in this method. To reduce the redundancy incurred to an extend, these sequence numbers are delta encoded [123].

Delta encoding is a way of storing or transmitting data in the form of differences (deltas) between sequential data rather than absolute values. Delta indicates the change in a variable. The first sequence number is kept as it is in the delta encoded stream. The second and the following values are the difference (delta) between the values themselves and the previous value to that. This method reduces the number of bits needed to transmit the data. The technique is applicable when there is only a small change between adjacent values. This is very likely to happen when sequential numbers are grouped. The number of bits required to represent the sequence numbers depends on the number of codewords we select as a frame, which depends on the data rate and the manageable latency of the application. The delta encoding applied to this reduces the number of bits required for representing the sequence value.

The codeword generated will be in the form as shown in Fig. 6.1.

LABEL	SEQ. No. 1	SYMBOL 1	SEQ. No. 2	SYMBOL 2	•••••••••	SEQ. No. S	SYMBOL S

Figure 6.1: Structure of the codeword with delta coded sequence numbers.

The additional unprotected sequence bits cause extra redundancy in the data, which reduces the BER performance of the scheme. The result depicted in Fig. 6.2 is for M2{5, 6, 1, 5} with seven sequence bits delta encoded into six bits, added with each SYMBOL. An attempt to keep the decoded and corrected data back in sequence produces an inferior result. Hence, we need to find a better way of getting sequencing back.

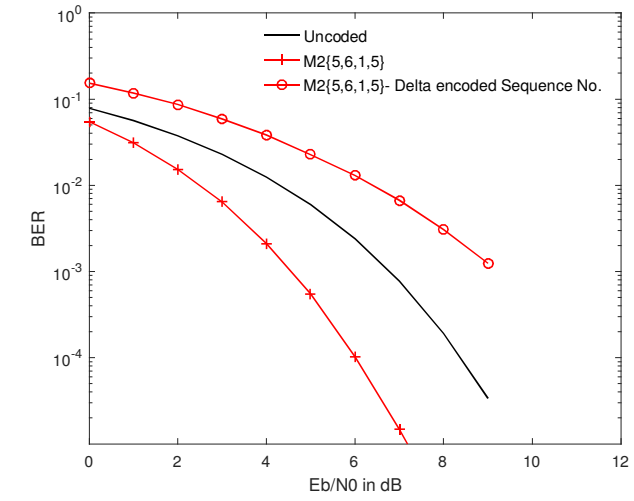

Figure 6.2: BER vs. E_b/N_0 performance of M2 {5, 6, 1, 5} with added sequence bits.

6.3 Method 2: Successor Label Identification

The second attempt made is to reduce the number of sequence bits needed for ordering the corrected data back in sequence. For achieving this, instead of using the sequence number as it is, we use some LABEL identification bits for the successor SYMBOL along with each SYMBOL. The number of bits needed for this LABEL ID is less than that required for sequence numbers. For instance, for the scheme M2{S, 7, 2, 5}, the number of bits needed for this LABEL ID is only four. The codeword generated will be in the form, as shown in Fig. 6.3.

LABEL	SYMBOL 1	SLI	SYMBOL 2	SLI	•••••••••	SYMBOL S	SLI

Figure 6.3: Structure of the codeword with Successor LABEL Identification.

The result of adding these SLI (Successor Label Identification) bits, as observed from Fig. 6.4, is the reduced coding gain and increased redundancy compared to the Methodology 2 without SLI bits. However, this still gives better performance compared to Hamming and RS codes. Method 2 gives improved performance compared to the sequencing method 1. Fig. 6.5 shows the performance of the scheme for various values of S in $\{S,\ 7,\ 2,\ 5\}$, which again affirms the functionality of the scheme.

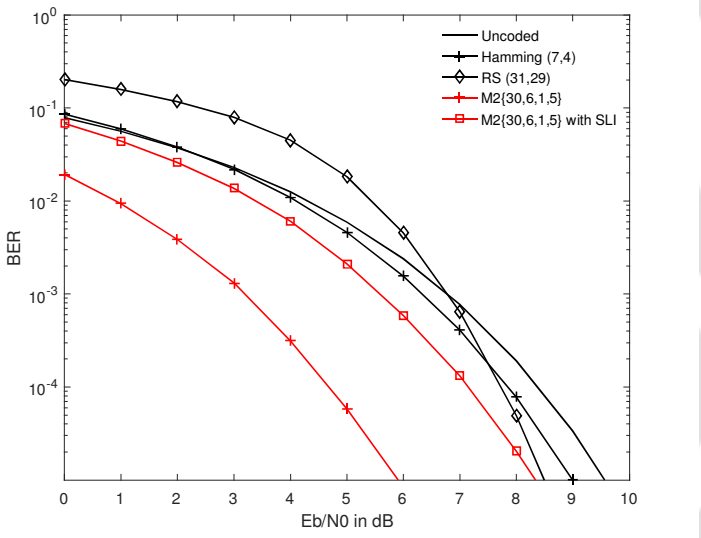

Figure 6.4: BER vs. E_b/N_0 performance of M2 for $\{30,\ 6,\ 1,\ 5\}$ with added Successor LABEL Identification.

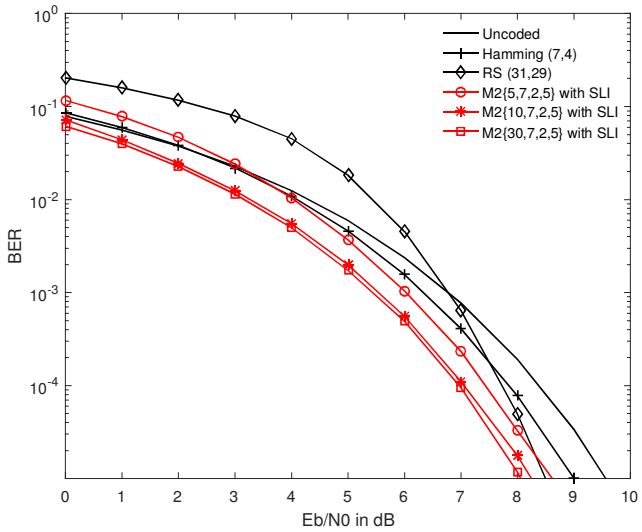

Figure 6.5: BER vs. E_b/N_0 performance of M2 for various S in $\{S,\ 7,\ 2,\ 5\}$ with added Successor LABEL Identification.

6.4 Method 3: Successor Group Identification

We can further reduce the number of bits needed for LABEL identification if the application gives values from a constrained set in a timeframe. For instance, let us take the case of $S,\ 6,\ 1,\ 5$ where input can take values ranging from zero to sixty-three; SLI requires four bits for the identification of the sixteen LABELs. Instead, if we consider transmitting a short timeframe of data, it can be assumed that the input ranges from zero to thirty-one (or thirty-two to sixty-three). We can then substitute SLI with SGI (Successor Group Identification), which requires only three bits. This reduces the unprotected redundant bits added. The codeword structure is depicted in Fig. 6.6.

LABEL	SYMBOL 1	SGI	SYMBOL 2	SGI	•••••••••	SYMBOL S	SGI

Figure 6.6: Structure of the codeword with Successor Group Identification.

The Fig. 6.7 shows the result of replacing SLI bits with SGI bits for LABEL identification. The redundancy is further reduced, and thus, the CG is increased compared to adding SLI bits.

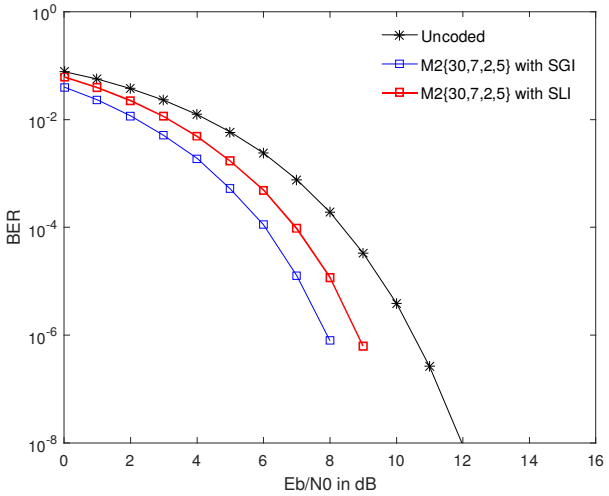

Figure 6.7: BER vs. E_b/N_0 performance of M2 for {30, 7, 2, 5} with added Successor Group Identification.

6.5 Method 4: Predecessor Group Identification and Successor Group Identification

In another attempt to ensure the decoded messages back in order, we identify the group the information block belongs to and embed this information in the data blocks. The Predecessor Group Identification (PGI) and SGI bits are appended at the beginning of the block. Now LABEL comprises of PGI, and SYMBOL comprises of SGI and information. The concatenation of SYMBOLs belonging to the same LABEL is done to form a codeword (Fig. 6.8). While decoding, based on the SYMBOLs, the group of the codewords is identified. Starting from the SGI of the first SYMBOL of the first received codeword, we identify a group of codewords belonging to the same group. One group among these codewords is selected based on the matching PGI in the LABEL with the group of the first codeword. The process repeats from the successor SYMBOLs.

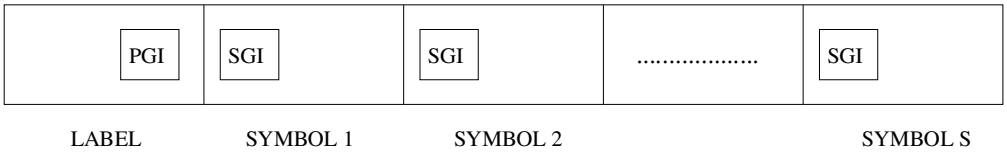

Figure 6.8: Structure of the codeword with PGI and SGI.

Adding PGI and SGI bits in this manner introduced an overhead of $S \log 2(\#Groups) + k_2$ bits. For instance, in the characterization M2 {30, 17, 3, 14} with PGI and SGI, the original input is of length 11 bits. Adding the PGI and SGI bits makes the code parameter k_m=17. When S=30, for

the original 330 bits of input, there is an overhead of $30 * 3 + 14 = 104$ bits with an error correction of 30 bits. For comparison, Hamming (15,11) with the same input of $30 * 11 = 330$ bits, overhead is $30 * 4 = 120$ bits, with the same error correction of 30 bits.

Fig. 6.9 shows the performance of the scheme for various configurations, with and without PGI-SGI. The overall impact is reduced performance as compared to the original proposal. However, still better performance is achieved compared to the Hamming and RS codes.

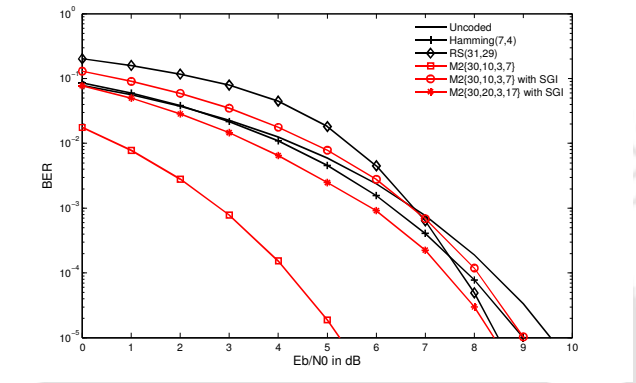

Figure 6.9: BER vs. E_b/N_0 performance of M2 with PGI and SGI.

6.6 Conclusions

The magnificent advantages achieved by the methodologies presented in the previous chapters, such as intensified CG, compression, and energy efficiency, comes with a tradeoff. The tradeoff is the disorder of the input data. This chapter attempted to mitigate this disadvantage. The first method being the simplest and most obvious, doesn't give a good result. However, the other three methods presented provided results better than the standard schemes, though the achievements are less compared to the schemes without the sequencing methods incorporated.

In some WSN applications, the sequence of information may not matter much, e.g., temperature or humidity measurements of a location taken between hourly or half-hourly intervals. Multiple measurements made between the prescribed duration may arrive out of order. In such cases, without the overheads for descrambling methods, we can save more energy. Furthermore, for applications with absolute sequence requirements, time-stamps are added with the measured data at the source and transmitted as the information. In such cases also, we do not need to include the overheads for descrambling. However, the descrambling methods can be used with the proposed methodologies

in the kind of applications where the order of the data stream is essential, and no time-stamps are present.

7

Conclusions and Future Work

Contents

7.1 Summary of the Present Work 110
7.2 Future Directions of the Research 111

The thesis proposes and presents two novel schemes for energy-efficient communication in WSNs. For the analysis of each methodology, we derive analytical expressions of BER and energy consumption per information bit and simulate the techniques. This chapter presents a summary of this thesis and suggests some possible future extensions of the present work. The main contributions of this thesis are summarized in Section 7.1, and possible future work is outlined in Section 7.2.

7.1 Summary of the Present Work

Chapter 3 presents our first novel methodology, Methodology 1, for energy-efficient, robust communication in WSNs. The methodology provides better error correction, implicit compression, and reduced complexity. The scheme is based on efficient grouping and placing of input data. A minimum Hamming distance restriction imposed in grouping offers error correction capability, and a significantly higher BER performance is achieved compared to standard coding schemes. The SYMBOL parts of the codeword are covered under the protection of the minimum distance groups. The LABEL part of the codeword is additionally protected with the help of rectangular codes. The particular structure of the codeword results in an implicit compression too, without the use of any standard compression techniques. The encoding and decoding operations are also simplified so that the computation energy per information bit is less compared to that of conventional schemes. Unlike some of the techniques in literature, which reduce the encoding complexity and hands over the complexity burden to the decoder in the assumption of energy abundant decoder, the proposed technique reduces decoder energy. This makes the schemes suitable for any topologies. The scheme is analyzed with both Mica2 and MicaZ platforms in the AWGN channel scenario.

In Chapter 4, an enhanced methodology, Methodology 2, to the one presented in Chapter 3, is presented. This methodology provides enhanced error correction, improved compression, and complexity further reduced. The grouping techniques remain the same. The encoding and decoding techniques are different from those of Methodology 1. Explicit use of rectangular coding is omitted in this methodology, which further reduces redundancy and computations. Both LABEL and SYMBOL parts of the codeword belong to the same group, covering them with implicit error protection. The technique excels in CG, compression, and energy efficiency compared to the first technique. The methodology is further enhanced with increased minimum distance value within each group, which proves its generality. Analysis of Methodology 2 also is performed with Mica2 and MicaZ platforms

in the AWGN channel scenario.

In Chapter 5, both the methodologies presented in the previous chapters are analyzed in a Rayleigh channel environment. An analysis of the scheme in different environments helps to affirm its usefulness in general. The Rayleigh channel is a more realistic channel than AWGN, posting the schemes suitable for fading channels as well. The comparison in this environment also proves Methodology 2 better than Methodology 1 and both methodologies better than standard schemes.

All the advantages of our schemes come with a tradeoff of sequence disorder, which is not a major concern in many types of WSN applications like temperature monitoring. However, for making the scheme suitable for those applications in which sequence order matters, in Chapter 6, the attempts to mitigate this disadvantage are presented. The sequence reordering does reduce the benefits of the scheme, though they still give better results compared to standard schemes.

7.2 Future Directions of the Research

The work reported in this thesis can be extended in the following directions.

- The schemes can be expanded with various code parameters further.
- A more advantageous method for sequencing can be introduced.
- Code-structure can be revised in ways so that sequence disorder doesn't occur.
- The schemes can be further compared with more standard schemes.

Bibliography

[1] I. F. Akyildiz, W. Su, Y. Sankarasubramaniam, and E. Cayirci, "Wireless sensor networks: a survey," *Comput. Netw.*, vol. 38, no. 4, pp. 393–422, March 2002.

[2] I. Stojmenovic, *Handbook of sensor networks: algorithms and architectures.* Hoboken, NJ, USA: John Wiley & Sons, Inc., 2005.

[3] K. Sohraby, D. Minoli, and T. Znati, *Wireless sensor networks: technology, protocols, and applications.* Hoboken, NJ, USA: John wiley & sons, 2007.

[4] J. Zheng and A. Jamalipour, *Wireless sensor networks: a networking perspective.* Hoboken, NJ, USA: John Wiley & Sons, 2009.

[5] I. F. Akyildiz and M. C. Vuran, *Wireless sensor networks.* Hoboken, NJ, USA: John Wiley & Sons, 2010.

[6] A. Hac, *Wireless sensor network designs.* Hoboken, NJ, USA: John Wiley & Sons Ltd, 2003.

[7] W. Dargie and C. Poellabauer, *Fundamentals of wireless sensor networks: theory and practice.* UK: John Wiley & Sons, 2010.

[8] J. Yick, B. Mukherjee, and D. Ghosal, "Wireless sensor network survey," *Comput. Netw.*, vol. 52, no. 12, pp. 2292–2330, April 2008.

[9] P. Rawat, K. D. Singh, H. Chaouchi, and J. M. Bonnin, "Wireless sensor networks: a survey on recent developments and potential synergies," *J supercomput.*, vol. 68, no. 1, pp. 1–48, April 2014.

[10] M. F. Othman and K. Shazali, "Wireless Sensor Network Applications: A Study in Environment Monitoring System," *Procedia Eng.*, vol. 41, pp. 1204–1210, 2012.

[11] I. F. Akyildiz, T. Melodia, and K. R. Chowdhury, "Wireless multimedia sensor networks: Applications and testbeds," *Proceedings of the IEEE*, vol. 96, no. 10, pp. 1588–1605, Oct. 2008.

[12] D. Puccinelli and M. Haenggi, "Wireless sensor networks: applications and challenges of ubiquitous sensing," *IEEE Circ. Syst. Mag.*, vol. 5, no. 3, pp. 19–31, Sept. 2005.

[13] B. Harjito and S. Han, "Wireless multimedia sensor networks applications and security challenges," in *Proc. Int. Conf. BWCCA*, 2010, pp. 842–846.

[14] J. Balen, D. Zagar, and G. Martinovic, "Quality of service in wireless sensor networks: A survey and related patents," *Recent Patents on Computer Science*, vol. 4, no. 3, pp. 188–202, Sept. 2011.

[15] D. Chen and P. K. Varshney, "QoS Support in Wireless Sensor Networks: A Survey," in *Proc. Int. Conf. Wirel. Netw.*, 2004, pp. 1–7.

[16] G. Anastasi, M. Conti, M. Di Francesco, and A. Passarella, "Energy conservation in wireless sensor networks: A survey," *Ad Hoc netw.*, vol. 7, no. 3, pp. 537–568, May 2009.

[17] M. C. Vuran and I. F. Akyildiz, "Cross-layer analysis of error control in wireless sensor networks," in *Proc. 3rd ann. IEEE SECON*, 2006, pp. 585–594.

[18] N. A. Pantazis and D. D. Vergados, "A survey on power control issues in wireless sensor networks," *IEEE Commun. Surv.*, vol. 9, no. 4, pp. 86–107, Fourth Quarter 2007.

[19] E. Callaway, P. Gorday, L. Hester, J. A. Gutierrez, M. Naeve, B. Heile, and V. Bahl, "Home networking with IEEE 802.15.4: a developing standard for low-rate wireless personal area networks," *IEEE Commun. Mag.*, vol. 40, no. 8, pp. 70–77, Aug. 2002.

[20] F. Marcelloni and M. Vecchio, "A simple algorithm for data compression in wireless sensor networks," *IEEE Commun. Lett.*, vol. 12, no. 6, pp. 411–413, June 2008.

[21] S. S. Pradhan, J. Kusuma, and K. Ramchandran, "Distributed compression in a dense microsensor network," *IEEE Signal Process. Mag.*, vol. 19, no. 2, pp. 51–60, March 2002.

[22] Z. Xiong, A. D. Liveris, and S. Cheng, "Distributed source coding for sensor networks," *IEEE Signal Process. Mag.*, vol. 21, no. 5, pp. 80–94, Sept. 2004.

[23] Y. Liang and Y. Li, "An efficient and robust data compression algorithm in wireless sensor networks," *IEEE Commun. Lett.*, vol. 18, no. 3, pp. 439–442, March 2014.

[24] C. M. Sadler and M. Martonosi, "Data compression algorithms for energy-constrained devices in delay tolerant networks," in *Proc. 4th Int. Conf. Embed. Netw. Sensor Sys.*, 2006, pp. 265–278.

[25] E. Fasolo, M. Rossi, J. Widmer, and M. Zorzi, "In-network aggregation techniques for wireless sensor networks: a survey," *IEEE Wirel. Commun.*, vol. 14, no. 2, pp. 70–87, April 2007.

[26] S. Croce, F. Marcelloni, and M. Vecchio, "Reducing power consumption in wireless sensor networks using a novel approach to data aggregation," *Comput. J.*, vol. 51, no. 2, pp. 227–239, March 2008.

[27] S. Yoon and C. Shahabi, "Exploiting spatial correlation towards an energy efficient clustered aggregation technique (cag)[wireless sensor network applications]," in *Proc. IEEE Int. Conf. Commun.*, 2005, pp. 3307–3313.

[28] V. Raghunathan, C. Schurgers, S. Park, and M. B. Srivastava, "Energy-aware wireless microsensor networks," *IEEE Signal Process. Mag.*, vol. 19, no. 2, pp. 40–50, Aug. 2002.

[29] G. Anastasi, M. Conti, M. Di Francesco, A. Passarella, M. Denko, and L. Yang, "How to prolong the lifetime of wireless sensor networks," *Mobile Ad Hoc and Pervasive Communications*, pp. 1–26, 2006.

[30] A. Bachir, M. Dohler, T. Watteyne, and K. K. Leung, "MAC essentials for wireless sensor networks," *IEEE Commun. Surv.*, vol. 12, no. 2, pp. 222–248, April 2010.

[31] V. Rajendran, J. Garcia-Luna-Aveces, and K. Obraczka, "Energy-efficient, application-aware medium access for sensor networks," in *Proc. IEEE Int. Conf. Mobile Adhoc and Sensor Sys.*, 2005.

[32] S. Yessad, F. Nait-Abdesselam, T. Taleb, and B. Bensaou, "R-MAC: Reservation medium access control protocol for wireless sensor networks," in *Proc. 32nd IEEE conf. Local Comp. Netw.*, 2007, pp. 719–724.

[33] M. Kohvakka, J. Suhonen, T. D. Hämäläinen, and M. Hännikäinen, "Energy-efficient reservation-based medium access control protocol for wireless sensor networks," *EURASIP J. Wirel. Comm.*, vol. 2010, no. 1, Aug. 2010.

[34] W. Ye, J. Heidemann, and D. Estrin, "Medium access control with coordinated adaptive sleeping for wireless sensor networks," *IEEE/ACM Trans. Netw.*, vol. 12, no. 3, pp. 493–506, June 2004.

[35] T. Van Dam and K. Langendoen, "An adaptive energy-efficient MAC protocol for wireless sensor networks," in *Proc. 1st Int. Conf. Embed. Netw. Sensor Sys.*, 2003, pp. 171–180.

[36] G. P. Halkes, T. Van Dam, and K. Langendoen, "Comparing energy-saving MAC protocols for wireless sensor networks," *Mobile Netw. Appl.*, vol. 10, no. 5, pp. 783–791, Oct. 2005.

[37] I. Rhee, A. Warrier, J. Min, and L. Xu, "DRAND: Distributed randomized TDMA scheduling for wireless ad hoc networks," *IEEE Trans. Mob. Comput.*, vol. 8, no. 10, pp. 1384–1396, March 2009.

[38] I. Rhee, A. Warrier, M. Aia, J. Min, and M. L. Sichitiu, "Z-MAC: a hybrid MAC for wireless sensor networks," *IEEE/ACM Trans. Netw.*, vol. 16, no. 3, pp. 511–524, June 2008.

[39] W.-Z. Song, R. Huang, B. Shirazi, and R. LaHusen, "TreeMAC: Localized TDMA MAC protocol for real-time high-data-rate sensor networks," *Pervasive Mob. Comput.*, vol. 5, no. 6, pp. 750–765, Dec. 2009.

[40] M. Cardei and J. Wu, "Energy-efficient coverage problems in wireless ad-hoc sensor networks," *Comput. commun.*, vol. 29, no. 4, pp. 413–420, Feb. 2006.

[41] S. Slijepcevic and M. Potkonjak, "Power efficient organization of wireless sensor networks," in *Conf. Rec. IEEE Int. Conf. Commun.*, 2001, pp. 472–476.

[42] D. Tian and N. D. Georganas, "A node scheduling scheme for energy conservation in large wireless sensor networks," *Wirel. Commun. Mob. Com.*, vol. 3, no. 2, pp. 271–290, March 2003.

[43] F. Ye, G. Zhong, S. Lu, and L. Zhang, "Energy efficient robust sensing coverage in large sensor networks," UCLA, LA, USA, Tech. Rep., Oct. 2002.

[44] H. Zhang, J. C. Hou *et al.*, "Maintaining sensing coverage and connectivity in large sensor networks," *Ad Hoc Sens. Wirel. Networks*, vol. 1, no. 1-2, pp. 89–124, March 2005.

[45] G. Xing, X. Wang, Y. Zhang, C. Lu, R. Pless, and C. Gill, "Integrated coverage and connectivity configuration for energy conservation in sensor networks," *ACM Trans. Sen. Netw.*, vol. 1, no. 1, pp. 36–72, Aug. 2005.

[46] J. Carle and D. Simplot-Ryl, "Energy-efficient area monitoring for sensor networks," *Computer*, vol. 37, no. 2, pp. 40–46, Feb. 2004.

[47] C. E. Shannon, "A mathematical theory of communication," *Bell system technical journal*, vol. 27, no. 3, pp. 379–423, July 1948.

[48] R. W. Hamming, "Error detecting and error correcting codes," *The Bell system technical journal*, vol. 29, no. 2, pp. 147–160, April 1950.

[49] G. Balakrishnan, M. Yang, Y. Jiang, and Y. Kim, "Performance analysis of error control codes for wireless sensor networks," in *Proc. 4th Int. Conf. Inf. Tech.*, 2007, pp. 876–879.

[50] S. Chouhan, R. Bose, and M. Balakrishnan, "Integrated energy analysis of error correcting codes and modulation for energy efficient wireless sensor nodes," *IEEE Trans. Wirel. Commun.*, vol. 8, no. 10, pp. 5348–5355, Oct. 2009.

[51] K. C. Barr and K. Asanović, "Energy-aware lossless data compression," *ACM Trans. Comput. Syst.*, vol. 24, no. 3, pp. 250–291, Aug. 2006.

[52] S. Xiao, T. Li, Y. Yan, and J. Zhuang, "Compressed sensing in wireless sensor networks under complex conditions of internet of things," *Cluster Comput.*, vol. 22, no. 6, pp. 14 145–14 155, 2019.

[53] T. A. ElBatt, S. V. Krishnamurthy, D. Connors, and S. Dao, "Power management for throughput enhancement in wireless ad-hoc networks," in *Conf. Rec. IEEE Int. Conf. Commun.*, 2000, pp. 1506–1513.

[54] M. C. Vuran and I. F. Akyildiz, "Error control in wireless sensor networks: a cross layer analysis," *IEEE/ACM Trans. Netw.*, vol. 17, no. 4, pp. 1186–1199, June 2009.

[55] S. Lin, F. Miao, J. Zhang, G. Zhou, L. Gu, T. He, J. A. Stankovic, S. Son, and G. J. Pappas, "ATPC: adaptive transmission power control for wireless sensor networks," *ACM Trans. Sen. Netw.*, vol. 12, no. 1, pp. 1–31, March 2016.

[56] H. Cotuk, K. Bicakci, B. Tavli, and E. Uzun, "The impact of transmission power control strategies on lifetime of wireless sensor networks," *IEEE Trans. Comput.*, vol. 63, no. 11, pp. 2866–2879, July 2013.

[57] S. Lin and D. J. Costello, *Error control coding.* NJ,USA: Prentice hall, 2001.

[58] H. Liu, H. Ma, M. El Zarki, and S. Gupta, "Error control schemes for networks: An overview," *Mob. Netw. Appl.*, vol. 2, no. 2, pp. 167–182, Sept. 1997.

[59] I. Chlamtac, C. Petrioli, and J. Redi, "Energy-conserving go-back-N ARQ protocols for wireless data networks," in *Proc. IEEE Int. Conf. Univ. Pers. Commun.*, 1998, pp. 1259–1263.

[60] ——, "Energy-conserving selective repeat ARQ protocols for wireless data networks," in *Proc. 9th IEEE Int. Symp. Pers., Indoor and Mobile Radio Commun.*, 1998, pp. 836–840.

[61] V. Nithya, B. Ramachandran, and V. Bhaskar, "Energy efficient coded communication for IEEE 802.15.4 compliant wireless sensor networks," *Wirel. Pers. Commun.*, vol. 77, no. 1, pp. 675–690, July 2014.

[62] J. H. Kleinschmidt, "Analyzing and improving the energy efficiency of IEEE 802.15.4 wireless sensor networks using retransmissions and custom coding," *Telecommun. Syst.*, vol. 53, no. 2, pp. 239–245, June 2013.

[63] Y. Sankarasubramaniam, I. F. Akyildiz, and S. McLaughlin, "Energy efficiency based packet size optimization in wireless sensor networks," in *Proc. 1st IEEE Int. Work. Sensor Netw. Protocols and Appl.*, 2003, pp. 1–8.

[64] Y. H. Yitbarek, K. Yu, J. Åkerberg, M. Gidlund, and M. Björkman, "Implementation and evaluation of error control schemes in industrial wireless sensor networks," in *Proc. IEEE Int. Conf. Ind. Tech.*, 2014, pp. 730–735.

[65] M. E. Pellenz, R. D. Souza, and M. S. P. Fonseca, "Error control coding in wireless sensor networks," *Telecommun. Syst.*, vol. 44, no. 1-2, pp. 61–68, June 2010.

[66] A. Neubauer, J. Freudenberger, and V. Kuhn, *Coding theory: algorithms, architectures and applications.* England: John Wiley & Sons, 2007.

[67] J. D. Gibson, *The mobile communications handbook.* Ohio, US: CRC press, 1999.

[68] E. Shih, S.-H. Cho, N. Ickes, R. Min, A. Sinha, A. Wang, and A. Chandrakasan, "Physical layer driven protocol and algorithm design for energy-efficient wireless sensor networks," in *Proc. 7th ann. Int. Conf. Mobile Comp. and Netw.*, 2001, pp. 272–287.

[69] G. J. Pottie and W. J. Kaiser, "Wireless integrated network sensors," *Commun. ACM*, vol. 43, no. 5, pp. 51–58, May 2000.

[70] S. Kasnavi, S. Kilambi, B. Crowley, K. Iniewski, and B. Kaminska, "Application of error control codes (ECC) in ultra-low power RF transceivers," in *Proc. IEEE Dallas/CAS Work. Arch., Circ. Implem. SOCs*, 2005, pp. 195–198.

[71] S. Chouhan, R. Bose, and M. Balakrishnan, "A framework for energy-consumption-based design space exploration for wireless sensor nodes," *IEEE Trans. Comput.-Aided Design Integr. Circuits Syst.*, vol. 28, no. 7, pp. 1017–1024, July 2009.

[72] N. A. Alrajeh, U. Marwat, B. Shams, and S. S. H. Shah, "Error correcting codes in wireless sensor networks: an energy perspective," *Appl. Math. Inform. Sci.*, vol. 9, no. 2, pp. 809–818, 2015.

[73] M. R. Islam, "Selection of error control/correction codes in wireless sensor network," in *Proc. Int. Conf. Elect. Comp. Eng.*, 2010, pp. 674–677.

[74] Y. Qassim and M. E. Magana, "Error-tolerant non-binary error correction code for low power wireless sensor networks," in *Proc. Int. Conf. Inf. Netw.*, 2014, pp. 23–27.

[75] M. Yigit, P. S. Boluk, and V. C. Gungor, "A new efficient error control algorithm for wireless sensor networks in smart grid," *Comput. stand. & inter.*, vol. 63, pp. 27–42, 2019.

[76] L. Li, R. G. Maunder, B. M. Al-Hashimi, and L. Hanzo, "A low-complexity turbo decoder architecture for energy-efficient wireless sensor networks," *IEEE Trans. Very Large Scale Integr. VLSI Syst.*, vol. 21, no. 1, pp. 14–22, Jan. 2013.

[77] M. Sartipi and F. Fekri, "Source and channel coding in wireless sensor networks using LDPC codes," in *Proc. 1st Ann. IEEE Commun. Soc. Conf. Sensor and Ad Hoc Commun. Netw.*, 2004, pp. 309–316.

[78] I. Ez-Zazi, M. Arioua, A. El Oualkadi, and P. Lorenz, "On the performance of adaptive coding schemes for energy efficient and reliable clustered wireless sensor networks," *Ad Hoc Netw.*, vol. 64, pp. 99–111, 2017.

[79] I. Ez-Zazi, M. Arioua, and A. El Oualkadi, "On the design of coding framework for energy efficient and reliable multi-hop sensor networks," *Procedia Comput. Sci.*, vol. 109, pp. 537–544, 2017.

[80] E. Arikan, "Channel polarization: A method for constructing capacity-achieving codes for symmetric binary-input memoryless channels," *IEEE Trans. Inf.*, vol. 55, no. 7, pp. 3051–3073, July 2009.

[81] Q. Wang, W. Zhou, S. Zhang, and S. Wang, "Performance Analysis of Polar Codes for Wireless Sensor Networks," in *Proc. IEEE 9th Int. Conf. Electr. Inf. Emerg. Commun.*, 2019, pp. 1–5.

[82] L. Li, Q. Wang, Y. Hu, and C. Zhang, "Energy consumption of polar codes for wireless sensor networks," in *Int. Wireless Internet Conf.* Springer, 2017, pp. 140–149.

[83] U. Datta, D. B. Kumar, A. K. Ball, and S. Kundu, "Performance of a Hybrid ARQ Scheme in CDMA Wireless Sensor Network," *Int. J. of Energy, Inf. and Comm.*, vol. 2, no. 3, pp. 59–74, Aug. 2011.

[84] S. M. Razali, K. Mamat, and N. S. K. Bashah, "Implementation of Hybrid ARQ (HARQ) error control algorithm for lifetime maximization and low overhead CDMA wireless sensor network (WSN)," in *Proc. IEEE Conf. Wirel. Sensors*, 2016, pp. 71–76.

[85] S. Vembu, S. Verdu, and Y. Steinberg, "The source-channel separation theorem revisited," *IEEE Trans. Inf. Theory*, vol. 41, no. 1, pp. 44–54, Jan. 1995.

[86] S. Z. Azami, P. Duhamel, and O. Rioul, "Joint source-channel coding: Panorama of methods," in *Proc. CNES workshop on Data Compression*, 1996, pp. 1232–1254.

[87] F. Hekland, "A review of joint source-channel coding," NTNU, Norway, Tech. Rep., July 2005.

[88] J. L. Massey, "Joint source and channel coding," MIT, MA, USA, Tech. Rep., Sept. 1977.

[89] C. Chen, L. Wang, and F. C. Lau, "Joint optimization of protograph LDPC code pair for joint source and channel coding," *IEEE Trans. Commun.*, vol. 66, no. 8, pp. 3255–3267, Aug. 2018.

[90] Q. Chen and L. Wang, "Design and Analysis of Joint Source Channel Coding Schemes Over Non-Standard Coding Channels," *IEEE Trans. Veh. Technol.*, vol. 69, no. 5, pp. 5369–5380, May 2020.

[91] N. Deligiannis, E. Zimos, D. M. Ofrim, Y. Andreopoulos, and A. Munteanu, "Distributed joint source-channel coding with copula-function-based correlation modeling for wireless sensors measuring temperature," *IEEE Sens. J.*, vol. 15, no. 8, pp. 4496–4507, Aug. 2015.

[92] Y. Zhao and J. Garcia-Frias, "Turbo compression/joint source–channel coding of correlated binary sources with hidden Markov correlation," *Signal Process.*, vol. 86, no. 11, pp. 3115–3122, Nov. 2006.

[93] C. Yaacoub and M. Sarkis, "Systematic polar codes for joint source-channel coding in wireless sensor networks and the Internet of Things," *Procedia Comput. Sci.*, vol. 110, pp. 266–273, 2017.

[94] L. Jin, P. Yang, and H. Yang, "Distributed joint source-channel decoding using systematic polar codes," *IEEE Commun. Lett.*, vol. 22, no. 1, pp. 49–52, 2017.

[95] J. Garcia-Frias, Y. Zhao, and W. Zhong, "Turbo-like codes for transmission of correlated sources over noisy channels," *IEEE Signal Process. Mag.*, vol. 24, no. 5, pp. 58–66, Sept. 2007.

[96] S. Tripathi, J. Jana, J. Samanta, and J. Bhaumik, "Fast and power efficient sec-ded and sec-ded-daec codes in iot based wireless sensor networks," in *IEEE Region 10 Conf.* IEEE, 2019, pp. 540–545.

[97] C. Yaacoub and M. Sarkis, "Joint source and channel coding with systematic polar codes for wireless sensor communication in next generation networks," *J. Ambient Intell. Humaniz. Comput.*, vol. 10, no. 12, pp. 4641–4649, 2019.

[98] C. Pielli, Č. Stefanović, P. Popovski, and M. Zorzi, "Joint compression, channel coding, and retransmission for data fidelity with energy harvesting," *IEEE Trans. Commun.*, vol. 66, no. 4, pp. 1425–1439, 2017.

[99] I. Ez-Zazi, M. Arioua, and A. El Oualkadi, "Adaptive joint lossy source-channel coding for multihop iot networks," *Wireless Communications and Mobile Computing*, vol. 2020, 2020.

[100] B. Dezfouli, M. Radi, S. A. Razak, T. Hwee-Pink, and K. A. Bakar, "Modeling low-power wireless communications," *J. Netw. Comput. Appl.*, vol. 51, pp. 102–126, May 2015.

[101] R. Hill *et al.*, *A first course in coding theory.* NY, USA: Oxford University Press, 1986.

[102] H. S. Warren, *Hacker's delight.* MA, USA: Addison-Wesley, 2013.

[103] B. Sklar *et al.*, *Digital communications: fundamentals and applications.* NJ, USA: Prentice Hall, 2001.

[104] "Mica2: Wireless Measurement System," Crossbow Technology, Inc. [Online]. Available: http://www.xbow.com/Products/Product_pdf_files/Wireless_pdf/MICA2_Datasheet.pdf

[105] "MicaZ: Wireless Measurement System," Crossbow Technology, Inc. [Online]. Available: http://www.xbow.com/Products/Product_pdf_files/Wireless_pdf/MICAz_Datasheet.pdf

[106] "2.4 GHz IEEE 802.15.4 / ZigBee-ready RF Transceiver," Texas Instruments. [Online]. Available: http://www.ti.com/lit/ds/symlink/cc2420.pdf

[107] "Single-Chip Very Low Power RF Transceiver datasheet (Rev. A)," Texas Instruments. [Online]. Available: http://www.ti.com/lit/ds/symlink/cc1000.pdf

[108] J. Proakis, *Digital communications.* Boston, USA: McGraw-Hill, 2001.

[109] T. Ha, *Theory and design of digital communication systems.* NY, USA: Cambridge University Press, 2011.

[110] R. Wells, *Applied coding and information theory for engineers.* NJ, USA: Prentice Hall, 1999.

[111] S. Chouhan, M. Balakrishnan, and R. Bose, "System-level design space exploration methodology for energy-efficient sensor node configurations: An experimental validation," *IEEE Trans. Comput.-Aided Design Integr. Circuits Syst.*, vol. 31, no. 4, pp. 586–596, April 2012.

[112] T. H. Lee, *The design of CMOS radio-frequency integrated circuits.* UK: Cambridge university press, 2003.

[113] B. L. Titzer, D. K. Lee, J. Palsberg, and O. Landsiedel. AVRORA: The AVR Simulation and Analysis Framework. [Online]. Available: http://compilers.cs.ucla.edu/avrora/

[114] B. L. Titzer, D. K. Lee, and J. Palsberg, "Avrora: Scalable sensor network simulation with precise timing," in *Proc. 4th Int. Symp. Inf. Proc. Sensor Netw*, 2005, pp. 477–482.

[115] R. de Paz Alberola and D. Pesch, "AvroraZ: extending Avrora with an IEEE 802.15.4 compliant radio chip model," in *Proc. 3rd ACM work. Performance Monitoring and Measurement of Heterogeneous Wireless and Wired Netw.*, 2008, pp. 43–50.

[116] H. R. Sharif and Y. S. Kavian, *Technological Breakthroughs in Modern Wireless Sensor Applications.* Hershey PA, USA: IGI Global, 2015.

[117] K. T. Le, "Designing a ZigBee-ready IEEE 802.15.4-compliant radio transceiver," *RF Design*, vol. 27, no. 11, pp. 42–50, Nov. 2004.

[118] L. Nashelsky and R. L. Boylestad, *Electronic devices and circuit theory.* India: Prentice Hall International, 1978.

[119] A. Wang, S. Cho, C. Sodini, and A. Chandrakasan, "Energy efficient modulation and MAC for asymmetric RF microsensor systems," in *Proc. Int. Symp. Low Power Electronics and Design*, 2001, pp. 106–111.

[120] E. Biglieri, J. Proakis, and S. Shamai, "Fading channels: Information-theoretic and communications aspects," *IEEE Trans. Inf. Theory*, vol. 44, no. 6, pp. 2619–2692, Oct. 1998.

[121] E. Biglieri, G. Caire, and G. Taricco, "Coding and modulation under power constraints," *IEEE Pers. Commun.*, vol. 5, no. 3, pp. 32–39, June 1998.

[122] K. D. Rao, *Channel coding techniques for wireless communications.* India: Springer, 2015.

[123] S. Smith, "The Scientist & Engineer's Guide to Digital Signal Processing," San Diego, CA, USA, 1997.

List of Publications

Journal Publications

1. N. C. Resmi and S. Chouhan, "An Enhanced Methodology for Energy-Efficient Interdependent Source-Channel Coding for Wireless Sensor Networks", in IEEE Transactions on Green Communications and Networking, vol. 4, no. 4, pp. 1072-1080, Dec. 2020, doi: 10.1109/TGCN.2020.3008079.
2. N. C. Resmi and S. Chouhan, "A Novel Interdependent Source-Channel Coding Technique for Enhanced Energy Efficiency in Communication over Wireless Sensor Networks", in Wireless Personal Communications, vol. 96, no. 3, pp. 3727-3743, Oct 2017, doi: 10.1007/s11277-017-4068-8.

International Conferences

1. N. C. Resmi and S. Chouhan, "Energy Efficient Communication with Interdependent Source-Channel Coding: An Enhanced Methodology", in Proc. IEEE SENSORS, New Delhi, 2018, pp. 1-4, doi: 10.1109/ICSENS.2018.8589643.
2. Resmi N C and S. Chouhan, "An Interdependent Source-Channel Coding for Energy Efficient Communication in WSNs", in18th International Symposium on Wireless Personal Multimedia Communications, Hyderabad, December 13-16, 2015.

1	Name:	Resmi N C
2	Date of Birth:	31-May-1984
3	Educational Qualification:	June-2005, B.Tech. in Electronics and Communication Engineering (60.1 %), Calicut University Institute of Engineering and Technology, Thenhipalam, Kerala, India June-2008, M.E. in Communication Systems (72.35 %), Sri Krishna College of Engineering and Technology, Coimbatore, Tamilnadu, India May-2021, Ph.D (Thesis Defended), Indian Institute of Technology Guwahati, Guwahati, Assam, India
4	Permanent Address:	Lakshmi(H) P.O.Kannikulangara Puthenchira District: Thrissur Kerala, India Pincode-680682